Variable Sampling Rate Control Charts for Monitoring Process Variance

Christopher S. Hughes

Dissertation submitted to the Faculty of the
Virginia Polytechnic Institute and State University
in partial fulfillment of the requirements for the degree of

Doctor of Philosophy
in
Statistics

Marion R. Reynolds, Jr., Co-Chair
Jesse C. Arnold, Co-Chair
Robert V. Foutz
Clint W. Coakley
Keying Ye

April 13, 1999
Blacksburg, Virginia

Keywords: Shewhart chart, CUSUM chart, EWMA chart, Integral Equation, Markov Chain

Variable Sampling Rate Control Charts for Monitoring Process Variance

Christopher S. Hughes

Abstract

Industrial processes are subject to changes that can adversely affect product quality. A change in the process that increases the variability of the output of the process causes the output to be less uniform and increases the probability that individual items will not meet specifications.

Statistical control charts for monitoring process variance can be used to detect an increase in the variability of the output of a process so that the situation can be repaired and product uniformity restored. Control charts that increase the sampling rate when there is evidence the variance has changed gather information more quickly and detect changes in the variance more quickly (on average) than fixed sampling rate procedures. Several variable sampling rate procedures for detecting increases in the process variance will be developed and compared with fixed sampling rate methods.

A control chart for the variance is usually used with a separate control chart for the mean so that changes in the average level of the process and the variability of the process can both be detected. A simple method for applying variable sampling rate techniques to dual monitoring of mean and variance will be developed. This control chart procedure increases the sampling rate when there is evidence the mean or variance has changed so that changes in either parameter that will negatively impact product quality will be detected quickly.

Dedication

To Grendel,
the best 'best friend' any person could have.

Acknowledgements

I would like to thank my wife, Lori Ann Hughes, for her encouragement and financial support throughout the past five years and for editing the final version of this dissertation. She provided many helpful suggestions that greatly improved this document.

My mother, Margie A. Norris, and grandmother, Georgia Queen, deserve a special thanks for supporting my education for these many years.

Dr. Jaimie Hebert converted me from a mathematician to an applied statistician. My interest in advanced statistics was originally due to Dr. Hebert.

I also wish to thank my co-advisors, Dr. Marion R. Reynolds, Jr., and Dr. Jesse C. Arnold, for directing my research. It has been an honor to share a small part of the insightful research careers of both men.

I have shared my experiences with many special friends while at Virginia Tech. It would be impossible to specifically mention every person by name, but I feel compelled to do my best. Susan Raught Luna, Jennifer Huffman, and Stephanie Saxby continually impressed me with with their work ethic and helped me strive to do my best. I learned much from their example. Daniel Eno introduced me to LaTeX and saved me from a horrible life as a Windows user. I also want to thank Greg Steeno for being a faithful weightlifting partner and a trusted friend. I also wish to specifically recognize Yew Haur Lee, Steven Kathman, David Burt, Tim Robinson, Jennifer Workinger, Peter Ammerman, Matt Rotelli, Robert Noble, and Lisa Chiaccherini.

The staff of the Statistics Department at Virginia Tech were my colleagues and my friends. Michelle Marini provided both statistical programming guidance and valuable horticultural advice. Linda Breeding always seemed genuinely happy to talk to me, even on the many occasions when I needed her expert assistance with office equipment. And Linda Seawell successfully guided me through the maze of university paperwork despite my forgetfulness and inattention to deadlines.

Finally, I owe an enormous debt to my ancestors, who carved a life out of the Appalachian wilderness of northwestern North Carolina. I will never forget your struggles and sacrifices. In the words of Fred Chappell, "I am one of you forever."

Contents

List of Figures

List of Tables

Chapter 1

Introduction

Control charts are widely employed in industry to monitor the output of processes and detect process changes that cause reductions in product quality. Samples are taken at various points in time to monitor some parameter of the quality variable of interest. A control chart is simply a plot of some statistic versus time or sample number. Control limits are set on the chart so that the probability that the plotted statistic will fall within the control limits is high when the process is operating in control. Thus the occurrence of a plotted statistic outside the control limits (a signal) indicates the process is no longer operating as desired. This information can be used to search for an assignable cause that has adversely impacted the process.

1.1 Variable Sampling Rate Control Charts

Traditional control charts use fixed sample sizes taken at uniformly spaced time points. This natural formulation is easy to understand and implement, but it is not necessarily the most efficient method for quickly detecting changes in a process. Methods that increase the sampling rate upon evidence of a change in a process allow the control chart to gather information more rapidly and perhaps signal earlier than a comparable chart with a fixed sampling rate. A control chart in which sampling rate depends on the observed data rather than being fixed in advance is known as a variable sampling rate (VSR) chart.

Two methods of increasing the sampling rate when there is evidence of a change in a process

parameter have been widely studied. Variable sample size (VSS) charts increase the sample size while variable sample interval (VSI) charts decrease the time interval between samples. The two methods can be combined to form a variable sample size-variable sample interval control chart (VSS-VSI) that increases the sample size and decreases the sample interval simultaneously. Either method or the combination of the two methods increases the rate at which observations are taken when the process goes out of control and leads to quicker detection of undesirable changes in the process output.

1.2 The Control Statistics

Let X be the quality variable that is being monitored. Throughout the rest of this dissertation, it is assumed that X has a normal distribution with mean μ and variance σ^2. Let $\underline{X}_k = X_1, X_2, \ldots, X_{n(k)}$ be the data observed at sampling time k where $n(k)$ is the sample size at sampling time k.

Assume μ_0 is the known target value for the mean and σ_0^2 is the known target value for the variance. In practice, the in-control parameter values will have to be estimated. We assume that a sufficiently large reference data set was obtained when the process was known to be operating in control and that these data are available to provide precise estimates so that assuming the parameter values are known has little effect.

We will first assume the mean is constant and consider control charts for detecting an increase in process variability. The procedures can be generalized to detect decreases in variability, but we will concentrate on methods for detecting increases in the process variance. An increase in the process variance is associated with a decrease in the uniformity of the output of the process and a decrease in product quality. A decrease in the process variance is associated with an increase in the quality of the output of the process. Detection of an improvement in the process might be of interest in some cases, but detecting increases in the variance (and the concurrent decrease in product quality) is a more immediate concern in most situations.

Since the mean is assumed to be a known constant (μ_0), the uniformly minimum variance unbiased estimator for the variance at sampling time k is

$$\hat{\sigma^2} = \frac{\sum_{i=1}^{n(k)} (X_{ki} - \mu_0)^2}{n}.$$

The control charts for monitoring variability considered in this dissertation will be based on the numerator of the statistic defined above. Let

$$T_k = \sum_{i=1}^{n(k)} (X_{ki} - \mu_0)^2 \tag{1.1}$$

be the statistic for monitoring the variance that is observed at sampling time k.

It may not be reasonable to assume the mean is constant in some situations when the variance alone is being monitored. Since the distribution of T_k depends on the true mean of the observations, the statistic

$$S_k = \sum_{i=1}^{n(k)} \left(X_{ki} - \bar{X}\right)^2 \tag{1.2}$$

should be used for the variance instead of T_k when the mean is not assumed to be constant. The distribution of S_k does not depend on the true mean of the observations. The conclusions in this dissertation can be applied in these cases if S_k is used as the observed statistic instead of T_k and all sample sizes are increased by one. Using T_k instead of S_k when the mean can be assumed to be constant gives the chart more power to detect changes in the variance, particularly when the sample size is small. If the mean is not constant, a change in the mean will affect the performance of a chart that is based on T_k. A chart that is based on S_k should be used when the mean cannot be assumed to be constant to eliminate the possibility that a change in the mean will be reflected in a control chart for the variance.

A control chart for the mean is used in conjunction with a control chart for the variance in most applications. The control chart for the variance will be based on S_k when the mean and variance are being monitored simultaneously.

Most traditional control charts for monitoring the mean use some function of the sample mean. Let $\bar{x}_k = \frac{\sum_{i=1}^{n(k)} X_{ki}}{n(k)}$ be the sample mean observed at time k. We will use the standardized sample mean

$$M_k = \frac{\sqrt{n\,(k)}\,(\bar{x}_k - \mu_0)}{\sigma_0} \tag{1.3}$$

as the statistic for the mean that is observed at sampling time k.

1.3 Objectives

The primary objective of this dissertation is to investigate VSR control charts for monitoring the process variance and for simultaneous monitoring of mean and variance when the observations come from a normal distribution. The specific goals of this dissertation include the following.

1. Control Charts for Monitoring Variability

   (a) Transformations: The density of T_k is not smooth and is not symmetric. The distribution of T_k depends on the sample size and the density of T_k is sharply discontinuous when the sample size is small. Evaluating the properties of cumulative sum (CUSUM) and exponentially weighted moving average (EWMA) charts based on T_k is difficult when the sample size is less than four. Chart design is also cumbersome since the control limits are different for each sample size. We will consider transformations of T_k to simplify calculations and control chart design. Fixed sample size and fixed sampling interval (FSS-FSI) CUSUM and EWMA charts based on the transformed statistics will be compared with FSS-FSI CUSUM and EWMA charts based on T_k. In particular, we will determine if the greater convenience of using a transformed statistic outweighs the expected loss in performance.

   (b) Variable Sample Size Charts: We will develop VSS Shewhart, CUSUM, and EWMA charts for detecting changes in process variability. Methods for evaluating the properties of these charts and general recommendations about the choice of sample sizes will also be given.

   (c) Variable Sampling Interval Charts: VSI Shewhart, CUSUM, and EWMA charts will be developed and compared with FSS-FSI and VSS charts. We will provide general recommendations for choosing the sampling intervals.

2. Control Charts for Simultaneous Monitoring of Mean and Variance

   (a) FSS-FSI Charts: We will investigate the joint properties of an EWMA chart for the mean and an EWMA chart for the variance.

   (b) VSR Charts: VSI and VSS EWMA charts for simultaneous monitoring of mean and variance will be developed. We will present methods for evaluating the properties of the VSR charts and give recommendations for the design of the charts.

Chapter 2

Literature Review

2.1 VSR Charts for Monitoring the Mean

The advantages of the VSS and VSI features have been thoroughly investigated when the process parameter of interest is the mean of a normal distribution. Reynolds et al. (1988) introduced a VSI Shewhart chart for monitoring the mean and showed that a VSI chart using two sampling intervals gives quicker detection of changes in the mean than a comparable fixed sampling interval (FSI) Shewhart chart. Runger and Pignatiello (1991) independently developed VSI Shewhart charts for the mean and reported extensive numerical results.

Reynolds et al. (1990) developed a VSI CUSUM chart for monitoring the mean and demonstrated that a VSI CUSUM chart detects changes in the mean quicker than a similar FSI CUSUM chart. A VSI EWMA chart for the mean was introduced by Saccucci et al. (1992). A VSI EWMA chart for the mean also detects changes quicker than a comparable FSI EWMA chart.

Costa (1994) considered Shewhart VSS charts and showed the VSS charts perform almost as well as VSI charts and have shorter detection times than fixed sample size-fixed sampling interval (FSS-FSI) Shewhart charts. Prabhu et al. (1994) defined a VSS-VSI Shewhart chart for the mean and showed that the VSS-VSI chart performs better than VSS or VSI charts.

VSI charts are sometimes considered too difficult to implement because the sampling times are random. Reynolds (see Reynolds (1996a) and Reynolds (1996b)) considered the effects of adding

samples at specific fixed times to reduce the administrative complexity of VSI charts. A VSI chart with sampling at additional fixed times (VSIFT chart) performs almost as well as an ordinary VSI chart.

The sequential probability ratio test (SPRT) chart (described in Stoumbos and Reynolds 1997a and 1997b) is an entirely new type of variable sampling rate control chart for monitoring the mean of a normal distribution. The SPRT chart utilizes a complete SPRT at each sample time. Observations are taken at each sample time until a decision is reached in the SPRT. The chart signals if the SPRT rejects the null hypothesis that the mean equals the target mean. Sampling terminates until the next scheduled sample time, and the process is deemed in control if the SPRT accepts the null hypothesis that the mean equals the target mean. The SPRT chart gives much quicker detection times than any traditional control chart method, but it may be difficult to implement in some settings.

Tagares (1998) gives a survey of variable sampling rate procedures. This recent article contains a thorough review of many variable sampling rate methods.

2.2 Control Charts for Detecting Increases in Variability

Simple Shewhart charts that plot the sample range (R-chart) or sample standard deviation (S-chart) have long been used for monitoring process variability. These charts are easy for users to understand, but their performance in detecting changes in the variance is often disappointing or wholly inadequate. See Lowry et al. (1995) or Tuprah and Ncube (1987) for a comprehensive comparison of R charts and S charts. Lowry et al. (1995) showed that the runs rules suggested for these charts in the *Western Electric Handbook* (Western Electric Company (1956)) can produce much larger false alarm rates than expected.

Page (1963) used the sample range to define a CUSUM chart for monitoring variability. A CUSUM chart for the standard deviation was outlined in van Dobben de Bruyn (1968). Further development of these procedures seemed to lag for an extended period of time. Howell (1987) illustrated a CUSUM procedure based on the sample variance and gave extensive tables for designing CUSUM charts. Hawkins and Olwell (1998) defined a similar CUSUM chart that uses the sample

variance. Hawkins and Olwell (1998) also gave results for a CUSUM chart based on the statistic T_k that was defined earlier.

Hawkins (1981) presented a CUSUM chart for a scale parameter that is based on the application of the widely known CUSUM chart for the mean to a transformed statistic. Hawkins showed that $\left|\frac{X_k}{\sigma}\right|^{\frac{1}{2}}$ is approximately standard normal if X_k is normally distributed with zero mean. The CUSUM chart of transformed statistics can be evaluated using well known properties of the CUSUM chart for the mean of a normal distribution. This method is obviously applicable to single observation samples. Quesenberrry (1995) transformed the sample variance to an exact standard normal distribution and formed Shewhart charts and CUSUM charts using the transformed statistics.

Crowder and Hamilton (1992) designed a one-sided EWMA chart for detecting increases in the variance that uses $\ln\left(s_k^2\right)$ as the observed statistic at time k. The statistic $\ln\left(s_k^2\right)$ has a smooth density function that simplifies calculations. Chang and Gan (1994) generalized the one-sided EWMA chart of Crowder and Hamilton by allowing the lower boundary of the chart to be a value other than zero. The EWMA chart presented by Chang and Gan performs slightly better than the EWMA chart of Crowder and Hamilton, but designing the chart is more difficult. MacGregor and Harris (1993) presented exponentially weighted control schemes for the variance that could be used with single observations and correlated data.

Lowry et al. (1995) presented a survey of procedures for monitoring variability. They found that all of the CUSUM procedures and the EWMA chart of Crowder and Hamilton are far superior to the S-chart and R-chart. Little difference was found between the CUSUM chart based on the sample standard deviation and the CUSUM chart based on the sample variance. Both were found to be significantly better than a CUSUM chart of the sample ranges.

2.3 Control Charts for Detecting Decreases in Variability

Methods for detecting a decrease in the process variance have received little attention from researchers. Nelson (1990) gave a set of runs rules for the Shewhart R-chart to improve detection of decreases in variability. Gan (1989) gave guidelines for designing a two-sided combined CUSUM-Shewhart chart based on the sample variance that can be used to detect variance decreases. A

CUSUM chart based on the range was suggested by Acosta-Mejia (1998) for monitoring reductions in variability. Acosta-Mejia showed that the range CUSUM chart and the sample variance CUSUM chart have similar performance.

2.4 Control Charts for Simultaneous Monitoring of Mean and Variance

The problem of simultaneous monitoring of the mean and variance of a normal random variable is significantly more difficult than monitoring the variance alone. The simplest method is, of course, the maintenance of two separate charts, but the joint behavior of the two charts in any given application is often unknown.

Hawkins (1987) suggested the use of four specially defined separate CUSUM charts. Simulation was used to evaluate the joint performance of the charts.

Domangue and Patch (1991) introduced a so-called omnibus EWMA scheme for simultaneous monitoring. The omnibus EWMA chart is based on the statistic $\left|\frac{X_k}{\sigma}\right|^{\alpha}$ and this single EWMA chart is shown to be sensitive to changes in the mean and variance. The omnibus EWMA chart performs similarly to the CUSUM charts suggested by Hawkins (1987).

Gan (1995) considered dual monitoring procedures that use EWMA or CUSUM charts for the mean and separate EWMA or CUSUM charts based on the natural log of the sample variance for the variance. Gan (1997) presented a joint monitoring scheme utilizing two EWMA charts and an elliptical acceptance region. Gan also showed that the omnibus EWMA chart of Domangue and Patch (1991) performs poorly when the variance decreases and the mean simultaneously increases.

Chengular-Smith et al. (1989) developed variable sampling rate Shewhart charts for joint monitoring of the mean and variance.

2.5 VSR Charts for Monitoring Variability

The application of variable sampling rate enhancements to control charts for monitoring variability has not been previously considered in any detail. The properties of variable sampling rate charts

for monitoring variability alone or for simultaneous monitoring of mean and variance are not well known.

Chapter 3

Types of Control Charts and Measures of Control Chart Performance

Some commonly used performance measures for control charts are defined in the first section of this chapter. General definitions for the types of control charts considered in the rest of this dissertation are given in the later sections.

3.1 Measures of Control Chart Performance

3.1.1 General Definitions

An effective control chart should signal very rarely when the process parameter being monitored is at the target value but should signal quickly if the parameter of interest changes to a new value. Define the average number of samples until a signal (ANSS) to be the expected value of the number of samples until a signal. The ANSS should be large when the process is in control (few false alarms) but small when the process is not in control (quick detection).

Let the time to signal be the time interval between the initiation of the chart and the first signal by the chart. Define the average time to signal (ATS) as the expected value of the time to signal.

If the length of time between samples is d time units, $ATS = d \cdot ANSS$.

Define the average number of observations until a signal (ANOS) to be the expected value of the number of sample items observed until the first signal. The ANOS and ANSS are clearly related. If the sample size is constant (say n) at all sample times, then $ANOS = nANSS$.

3.1.2 Steady State Behavior

The ANSS, ATS, and ANOS as defined above are calculated by assuming that the parameter of interest is at some specific value when the control chart procedure begins and that the parameter remains at that value until the chart signals. This assumption may be reasonable at the start of a new process since the process parameter may not be at the target value initially and the condition will not be corrected until the chart signals.

In other situations, the process is known to be in statistical control at some particular time and then goes out of control at some unknown time. For example, consider an FSS CUSUM chart for detecting an increase in variability. Suppose the process is in control initially ($\sigma^2 = \sigma_0^2$ at time $t = 0$), but the variance increases to σ_1^2 at some arbitrary time $t > 0$. The value of the chart statistic at the sample time immediately before time t is random and the statistic may be anywhere between 0 and the upper control limit h. The time to signal after the shift obviously depends on the value of the chart statistic at the previous sample time. If the statistic is near the upper control limit h, then the time to signal would likely be quite small, but the time to signal would probably be much greater if the chart statistic were near zero.

Suppose the process operates for a long (theoretically infinite) period of time in control with no signals by the chart. The steady state distribution of the chart statistic is the distribution of the chart statistic over its region of possible values during the period with no signals.

When calculating steady state properties of a control chart, we will assume the process has operated in control without a signal for a sufficiently long period of time so that the distribution of the chart statistic at the time of a change in the process can be approximated by the steady state distribution of the chart statistic.

When the change in a process parameter occurs at some random time, the average number of

samples between the change in the process parameter and the first signal by the chart should be calculated using the distribution of the chart statistic at the time of the change. The steady state ANSS (SSANSS) is the average number of samples between the change in the parameter and the first signal by the chart when the ANSS is calculated using the steady state distribution of the chart statistic. Similarly, the steady state ATS (SSATS) is the expected time between the change in the parameter and the first signal by the chart when the ATS is calculated using the steady state distribution of the chart statistic. The steady state ANOS (SSANOS) is the expected number of individual items between the time of the change and the first signal by the chart when the ANOS is adjusted for the steady state distribution of the chart statistic.

Suppose the process operates in control for some long period of time and then shifts to the out-of-control state. The shift may occur at a sample time or between samples. Suppose the shift occurs at some time t between sample k and sample $[k+1]$. Let t_k be the time that sample k is taken and let t_{k+1} be the time that sample $k+1$ is taken. We will assume that the distribution of the time of the shift is uniform on the interval $[t_k, t_{k+1}]$. Then the expected value of t is $t_k + \frac{t_{k+1}-t_k}{2}$.

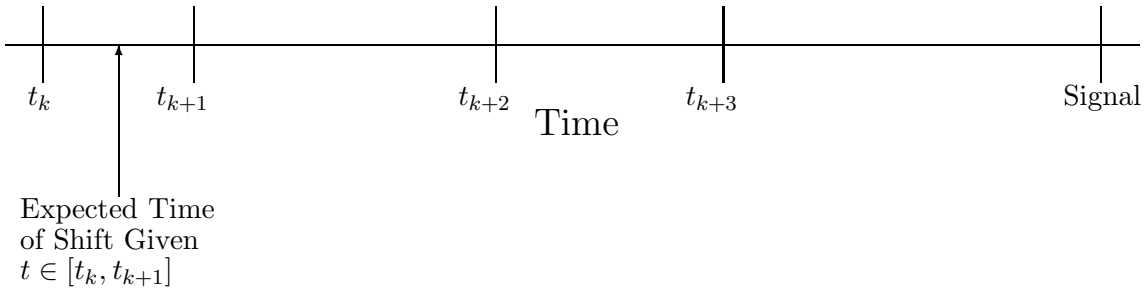

Figure 3.1: Relationship Between ATS and Steady State ATS

Figure 3.1 illustrates the relationship between the ATS and the SSATS of a control chart. The SSATS is the expected time between the change in the parameter and the first sample after the change plus the ATS from the time of the first sample after the change.

3.2 Shewhart Charts

3.2.1 General Shewhart Charts

The Shewhart chart for monitoring a process parameter is the simplest and perhaps the most commonly employed control chart. We will first define the chart in terms of an arbitrary parameter θ before considering Shewhart charts for monitoring the variance of a normal distribution. Suppose θ_0 is the known target value for θ. A Shewhart chart is a plot of some sample statistic $Q_k\left(\underline{X}_k\right)$ observed at sampling time k versus time or sample number. Since it is usually understood that the statistic at time k is a function of the data observed at time k, we will drop the argument $\underline{X}_k$ and use the simpler notation Q_k for the statistic observed at time k.

A two-sided Shewhart chart for detecting changes in a process parameter θ can be viewed as a sequence of hypothesis tests of the form $H_0 : \theta = \theta_0$ versus $H_1 : \theta \neq \theta_0$. A signal at time k is equivalent to a rejection of the null hypothesis. The Shewhart chart signals a change in θ if $S_k > c_U$ or $Q_k < c_L$ where c_L is the lower control limit and c_U is the upper control limit for the chart or, equivalently, c_L and c_U are the critical values of the hypothesis test. If the distribution of Q_k is symmetric about θ_0, it is customary to take $c_L = \theta_0 - c$ and $c_U = \theta_0 + c$ for some constant c so that the chart is equally effective for detecting increases and decreases in θ.

The control limits c_L and c_u can be found from the distribution of Q_k if an acceptable false alarm rate is specified. This is the preferred method of design from a statistical perspective since the false alarm rate is specified in advance. However, the control limits have traditionally been set at $\theta_0 \pm 3\sigma_{Q_k}$ without regard for the true false alarm rate. This method is obviously simpler but the true performance of the chart may not be as expected.

The probability of a signal is equivalent to the power of the hypothesis test. Let $\beta(\theta)$ be the power function of the associated hypothesis test when θ is the true value of the parameter. If we assume that the samples are independent, the number of samples to signal is a geometric random variable with parameter $\beta(\theta)$ and the expected number of samples to signal is $\frac{1}{\beta(\theta)}$. When the process is in control, $\theta = \theta_0$ and $\beta(\theta) = \beta(\theta_0) = \alpha$ where α is the significance level of the hypothesis tests. The ANSS of the chart when the process is in control is $\frac{1}{\alpha}$.

If the process parameter is at some other value θ_1 at the start of the process and remains at

that value until the chart signals and corrective action is taken, then the ANSS is $\frac{1}{\beta(\theta_1)}$.

For an FSS-FSI Shewhart chart with samples of size n taken d time units apart, it is clear that the ATS is $d \cdot ANSS = \frac{d}{\beta(\theta)}$ and the ANOS is $n \cdot ANSS = \frac{n}{\beta(\theta)}$.

Steady state calculations for an FSS-FSI Shewhart chart are very simple since the decision at time k depends only on the data observed at time k. If we assume the time of the change in the parameter is uniformly distributed over the sampling interval before the change, the steady state ATS is

$$\begin{aligned} SSATS &= \frac{d}{2} + ATS - 1 \\ &= ATS - \frac{d}{2} \\ &= d \cdot ANSS - \frac{d}{2}. \end{aligned}$$

Since the decision at sample time k does not depend on previously observed data, SSANOS=ANOS and SSANSS=ANSS.

The properties of VSR Shewhart charts can be derived by simplifying the Markov chain method of Brook and Evans (1972) to the case of a control statistic with a discrete number of states. Details of this method will be given in the individual applications. Steady state calculations are based on the steady state behavior of the Markov chain.

3.2.2 Shewhart Charts for Monitoring Process Variance

The ordinary FSS-FSI S-chart utilizes samples of size n taken d time units apart. The sample standard deviation at each time interval is plotted as the chart statistic. The lower control limit is frequently taken to be zero, so the the chart is designed only to detect increases in the process variance. A lower control limit of zero is sometimes a consequence of simply specifying the control limits as $\sigma_0 \pm 3\sigma_S$ where σ_S is the standard error of the sample standard deviation. Using this ad hoc method of specifying control limits can result in a negative lower control limit. In this case, the lower control limit is usually stated to be zero, but no effective lower control limit exists.

The R-chart is sometimes used to monitor variability. The sample range is the chart statistic.

The R-chart will sometimes have no effective lower control limit if the control limits are specified at $R_0 \pm 3\sigma_R$ where R_0 is the target value for the range and σ_R is the standard error of the sample range.

The R-chart and S-chart use well-known, easily calculated statistics. No assumptions about the mean of the distribution are necessary. The charts are easy for practitioners to understand and this probably accounts for their wide usage.

A one-sided Shewhart chart for detecting increases in the process variance can be viewed as a sequence of hypothesis tests of the form $H_0 : \sigma = \sigma_0$ versus $H_1 : \sigma > \sigma_0$. When the mean of X is known to be μ_0, it is well known that the most powerful test of this hypothesis rejects at sample time k when $T_k > C$ where $C > 0$ is a constant. Accordingly, a Shewhart chart for the variance should be based on T_k when the objective is quick detection of increases in the variance.

Example

The diameter of the output shaft of a lawn tractor transmission is a normally distributed random variable with mean $\mu_0 = 20$ mm and variance $\sigma_0^2 = 0.01$ mm^2. The manufacturer takes samples of size $n = 4$ every two hours. Data for twenty (simulated) samples is given below. The variance increases to $\sigma_0^2 = 0.0225$ mm^2 beginning with sample 16. Figure 3.2 is a Shewhart chart for these data. When the process is in control, the expected number of samples until a signal for this Shewhart chart (and for the CUSUM and EWMA charts considered later) is 500.

Table 3.1: Sample Data for Example

Sample	T_k	Sample	T_k	Sample	T_k	Sample	T_k
1	0.0022760	6	0.0065702	11	0.0107322	16	0.0202657
2	0.0028731	7	0.0067276	12	0.0134754	17	0.0264116
3	0.0060116	8	0.0070371	13	0.0142591	18	0.0321903
4	0.0061577	9	0.0077117	14	0.0145617	19	0.0342943
5	0.0062396	10	0.0094305	15	0.0156180	20	0.0350202

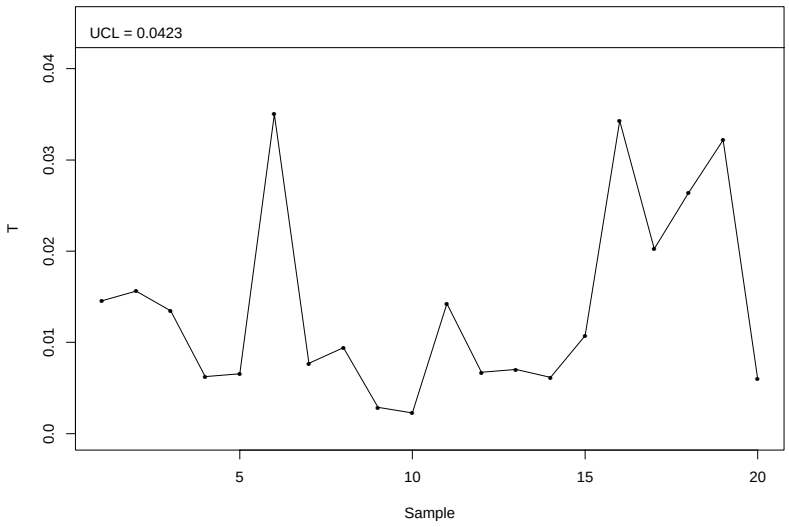

Figure 3.2: Sample Shewhart Chart for Detecting an Increase in the Variance

3.3 CUSUM Charts

3.3.1 General CUSUM Charts

Shewhart charts are generally not very effective for detecting small changes in a parameter. A very extreme value of the chart statistic from a single sample must be observed to cause a signal. The CUSUM chart accumulates information over several samples and is much more sensitive to small changes in a process parameter. See Hawkins and Olwell (1998) for an excellent description of general CUSUM procedures.

Define the one-sided CUSUM statistic at time $k \geq 1$ by

$$Y_k = max\{0, Y_{k-1}\} + z_k \tag{3.1}$$

where z_k is a function of the data, $\underline{X}_k$, observed at sampling time k. The initial value Y_0 is frequently taken to be zero, but Lucas and Crosier (1990) suggest taking $Y_0 > 0$ so the chart can more easily detect problems at the start of the process. The chart signals a change in θ at time k if $Y_k \geq h$ for some critical value h. In most applications, the value z_k is defined to be the log likelihood ratio

$$z_k = \ln\left(\frac{f\left(\underline{X}_k, \theta_1\right)}{f\left(\underline{X}_k, \theta_0\right)}\right) \tag{3.2}$$

where θ_1 is an unacceptable parameter value such that the chart should signal quickly if θ changes from the in control value θ_0 to the undesirable value θ_1. The choice of θ_1 should be made using practical knowledge of the process that is being monitored. For example, if a change from θ_0 to θ_1 for some particular value of θ_1 is thought to be likely (and important to detect) based on the history of the process, then that value θ_1 should be used in the design of the chart.

The CUSUM statistic Y_k as defined above is reset to zero at time $k+1$ if the actual value of Y_k is less than or equal to zero. The CUSUM chart statistic is sometimes defined as $Y_k = max\{0, Y_{k-1} + z_k\}$ (see, for example, Howell (1987)) so that a negative value of Y_k is reset to zero immediately at time k. The two definitions result in charts with identical properties when the

sample size and sampling interval are fixed. Our definition retains the actual value of Y_k from the previous sample time. This will sometimes be useful in VSS and VSI charts where the sample size for the next sample and/or the time of the next sample depend on the previously observed data.

A one sided CUSUM chart can be viewed as a sequence of Wald (1947) sequential probability ratio tests where each test is of the form $H_0 : \theta = \theta_0$ versus $H_1 : \theta > \theta_0$. The chart resets to zero and a new SPRT begins if the null hypothesis is accepted, and the chart signals if this hypothesis is rejected.

Reynolds (1995) developed a unified Markov chain-integral equation method for evaluating the properties of control charts that combines the accuracy of the integral equation method with the generality of the Markov chain method when the distribution of the chart statistic is continuous and has a smooth density function. Detailed descriptions of the application of this method to FSS-FSI CUSUM charts and VSR CUSUM charts are given in the appendices.

The unified Markov chain-integral equation method performs poorly if the density function of the chart statistic is not smooth. The Markov chain method of Brook and Evans (1972) can be used in these cases. Hawkins (1992) gave an algorithm that uses accelerated convergence techniques to increase the accuracy of the Markov chain method. Appendix D gives the mathematical details of the Markov chain method for the special case of one-sided VSI charts.

3.3.2 CUSUM Chart for Monitoring Process Variance

A brief summary of an FSS CUSUM chart for monitoring process variance is given here to facilitate the development of the VSS CUSUM chart. The CUSUM chart presented here is designed to detect an increase in the variance. A separate CUSUM chart would normally be used to detect decreases in variability if detection of a decrease in σ is of interest. See Howell (1987) or Hawkins and Olwell (1998) for more details on the FSS CUSUM chart for detecting increases in variability.

Suppose it is desirable to detect a shift in the process standard deviation from $\sigma = \sigma_0$ to $\sigma = \sigma_1 > \sigma_0$ (i.e., the chart should be optimized for detecting a change from σ_0 to σ_1). Then the logarithm of the likelihood ratio is

$$
\begin{aligned}
z_k &= \ln\left(\frac{f\left(\underline{X}_k, \mu_0, \sigma_1\right)}{f\left(\underline{X}_k, \mu_0, \sigma_0\right)}\right) \\
&= \ln\left(\frac{\left(\frac{1}{\sigma_1\sqrt{2\pi}}\right)^n \exp\left(\frac{1}{2\sigma_1^2}\sum_1^n \left(X_{ki}-\mu_0\right)^2\right)}{\left(\frac{1}{\sigma_0\sqrt{2\pi}}\right)^n \exp\left(\frac{1}{2\sigma_0^2}\sum_1^n \left(X_{ki}-\mu_0\right)^2\right)}\right) \\
&= n\ln\left(\frac{\sigma_0}{\sigma_1}\right) + \frac{1}{2}\left(\frac{1}{\sigma_0^2}-\frac{1}{\sigma_1^2}\right)T_k \qquad (3.3) \\
&= r_1 + r_2 T_k \qquad (3.4)
\end{aligned}
$$

where

$$
r_1 = n\log\left(\frac{\sigma_0}{\sigma_1}\right) \quad \text{and} \quad r_2 = \frac{1}{2}\left(\frac{1}{\sigma_0^2}-\frac{1}{\sigma_1^2}\right).
$$

Notice the log likelihood ratio in (3.4) is a multiple of T_k plus a constant. For consistency with the Shewhart chart, the CUSUM chart will be defined in terms of T_k. Define the CUSUM statistic at sample time k by

$$
Y_k = \begin{cases} Y_k = max\{0, Y_{k-1}\} + T_k - \gamma & k \geq 1 \\ T_1 - \gamma & k = 1 \end{cases} \qquad (3.5)
$$

where $\gamma = -\frac{r_1}{r_2}$. Let σ^2 be the true process variance. If we assume the mean is constant at the target value, $X_{ki} \sim N\left(\mu_0, \sigma^2\right)$ and it is easy to show that $T_k \sim \Gamma\left(\frac{n}{2}, 2\sigma^2\right)$. The density of T_k is

$$
f_{T_k}(t) = \frac{t^{-\frac{n}{2}} e^{-\frac{n}{2\sigma^2}t}}{\left(2\sigma^2\right)^{\frac{n}{2}}\Gamma\left(\frac{n}{2}\right)} \quad t > 0 \ .
$$

Figure 3.3 shows a CUSUM chart for the variance using the same data that is plotted in Figure 3.2. The observed data was rescaled by dividing by the target standard deviation of 0.1 mm to put the chart on a standard scale for data with unit standard deviation. The chart was designed using $\sigma_1 = 1.5\sigma_0 = 0.15\,\text{mm}$, and the upper control limit is $h = 14.688$. The chart signals an increase in the variance at sample 18.

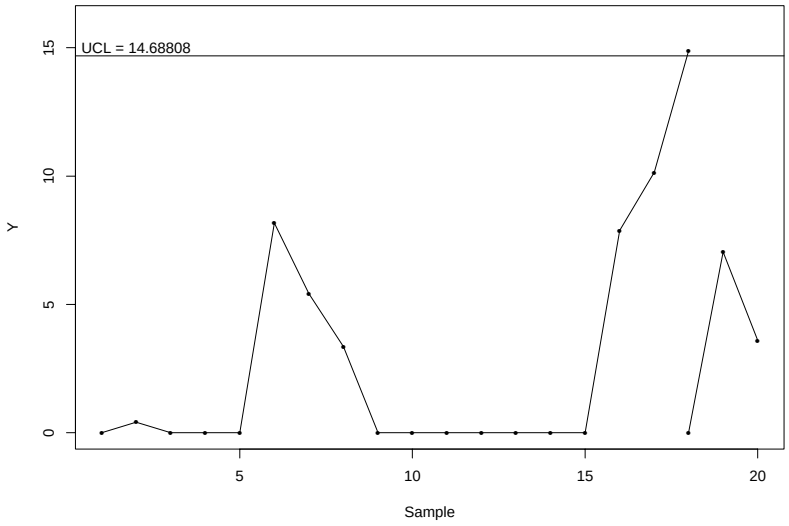

Figure 3.3: Sample CUSUM Chart for Detecting an Increase in the Variance

3.4 Exponentially Weighted Moving Average Charts

3.4.1 General EWMA Charts

The EWMA chart is an alternative to the CUSUM chart that offers similar performance (in terms of ATS) in most cases. Like the CUSUM chart, the EWMA chart combines information from the current sample with previously observed data. A two-sided EWMA chart for the detection of a change in a process parameter and a one-sided EWMA chart for detecting increases in a parameter will be defined here.

The chart parameter λ determines the amount of weight that is placed on the current sample versus the information in the accumulated statistic. Choosing λ near one makes the chart perform well for large changes in θ while small values of λ make the chart perform well for small changes in θ.

Define the two-sided EWMA statistic at time k by

$$Y_k = \begin{cases} \lambda Q_k + (1-\lambda)\, Y_{k-1} & k \geq 1 \\ \theta_0 & k = 0 \end{cases} . \tag{3.6}$$

The control limits for a two-sided EWMA chart are usually chosen at $\theta_0 \pm C \cdot \sigma_{Y_k}$ where σ_{Y_k} is the standard deviation of Y_k and C is a constant. The exact standard deviation of Y_k is a function of k but quickly approaches the asymptotic value $\frac{\lambda}{2-\lambda}\sigma_{Q_k}$ where σ_{Q_k} is the standard deviation of Q_k.

Define the upper one-sided EWMA statistic at sample time k by

$$U_k = \begin{cases} \lambda Q_k + max\{l, (1-\lambda)\, Y_{k-1}\} & k \geq 1 \\ \theta_0 & k = 0 \end{cases} . \tag{3.7}$$

The constant l is called the lower reflecting boundary of the chart. The lower reflecting boundary for a one-sided EWMA chart is usually the target value θ_0, but Chang and Gan (1994) showed that the performance of the chart can be improved slightly by adjusting the value of l in particular applications.

The control limit for a one-sided EWMA chart is usually determined using the asymptotic standard deviation of Q_k. The upper control limit is $\theta_0 + C \cdot \frac{\lambda}{2-\lambda}\sigma_{Q_k}$ where C is a constant.

The properties of EWMA charts can be evaluated using the methods of Reynolds (1995) when the density of the chart statistic is smooth. The Markov chain method of Brook and Evans (1972) can be used when the density is not smooth. Mathematical details of the evaluation methods are given in the appendices.

3.4.2 An EWMA Chart for Monitoring Process Variance

The EWMA procedure described by Crowder and Hamilton (1992) can easily be extended to the case in which the process mean is known. The observed statistic at time k is $T_k = \sum_{i=1}^{n(k)} (X_{ki} - \mu_0)^2$. Define the chart statistic at time k by $Y_k = \lambda \ln(T_k) + max\{\ln(\sigma_0^2), (1-\lambda) Y_{k-1}\}$ for $k \geq 1$ and let $Y_0 = \ln(\sigma_0^2)$. Since T_k has a gamma distribution, $\ln(T_k)$ has a log-gamma distribution. Crowder and Hamilton showed that an increase in the process variance causes an increase in the mean of $\ln(T_k)$, so the EWMA chart responds with an increase in level.

Figure 3.4 shows a one-sided EWMA chart for the variance for the data used in Figure 3.2. The observed data was rescaled by dividing by the target standard deviation of 0.1 mm to put the chart on a standard scale. The sample chart shows control limits drawn using the asymptotic approximation to the standard deviation of Y_k. The upper control limit is $h = 0.6007$ and $\lambda = 0.2$. These values were obtained from a table in Crowder and Hamilton (1992). The chart signals an increase in the variance at sample 19.

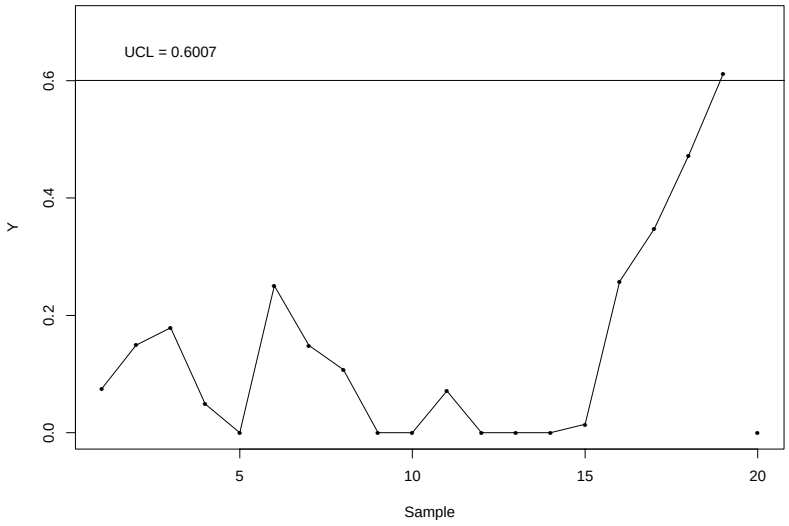

Figure 3.4: Sample EWMA Chart for Detecting an Increase in the Variance

Chapter 4

Transformations

Transformations are frequently used to obtain a statistic that simplifies the analysis. Statistics that have a normal distribution or an approximate normal distribution are appealing to most practitioners. Most users of control charts are familiar with the design and the properties of control charts for the mean of a normal distribution. A transformation that makes monitoring the variance of a normal distribution similar to monitoring the mean of a normal distribution would simplify the charting procedure for most users.

A chart that uses a transformed statistic will likely not be as efficient as a chart for the variance that uses T_k. A transformation that simplifies chart design and the evaluation of chart properties without a large loss in detection capability is desirable. We will investigate the performance of a natural log transformation of T_k and normal probability transformation of T_k in this chapter.

4.1 Single Observations Example

Evaluating the properties of CUSUM and EWMA charts for the variance can be difficult when the sample size n is small. Consider the case of single observations taken at equally spaced time intervals. Such a small sample size is clearly undesirable from a statistical viewpoint, but single observation samples are quite common due to time or expense considerations. When $n = 1$, $T_k \sim \Gamma\left(\frac{1}{2}, 2\sigma^2\right)$ and the density of T_k is

$$f_{T_k}(t) = \frac{t^{-\frac{1}{2}} e^{-\frac{1}{2\sigma^2}t}}{(2\sigma^2)^{\frac{1}{2}}\,\Gamma\left(\frac{1}{2}\right)} \quad t > 0\ .$$

Figure 4.1 is a plot of this density when $\sigma_0 = 1.0$. The sharp discontinuity at $t = 0$ causes the evaluation method in Appendix A to perform poorly. Evaluating the properties of a CUSUM chart or EWMA chart based on T_k is difficult or impossible for $n \leq 2$ using the methods of Appendix A. The Markov chain method can be used to approximate the ANSS and ANOS in this case, but achieving reasonable accuracy requires a large number of states in the transition matrix. The results for $n = 1$ reported later in this section were obtained using a Markov chain with 250 transient states.

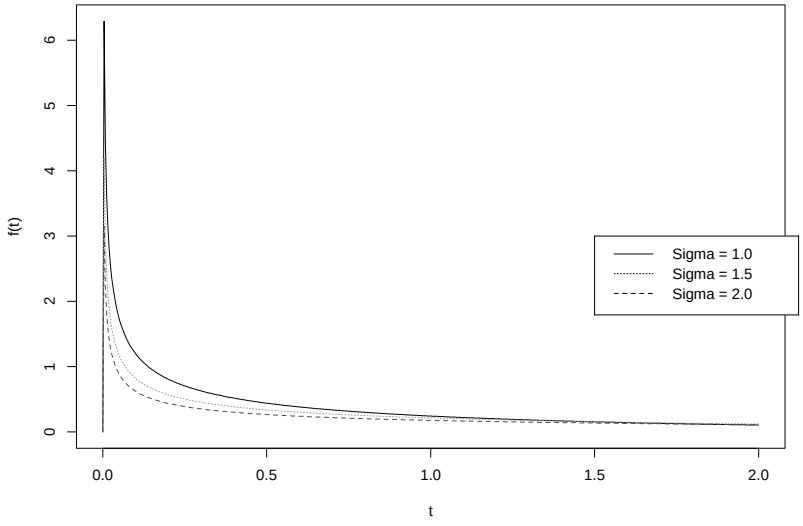

Figure 4.1: Density of T_k for $n = 1$

We will show the natural log and normal probability transformations eliminate the numerical difficulties. The performance of EWMA and CUSUM charts based on the transformed statistics will be compared with the performance of charts based on T_k to evaluate the performance penalty caused by the transformations.

4.2 Natural Log Transformation

Crowder and Hamilton (1992) suggested using the natural log of the sample variance in an EWMA chart for the variance. We will define EWMA and CUSUM charts based on $\ln(T_k)$.

Let $L_k = \ln(T_k)$. The statistic L_k has a log-gamma distribution with density

$$f_L(l) = \frac{\exp\left(\frac{1}{2\sigma^2}e^l + \frac{n(k)}{2}l\right)}{\Gamma\left(\frac{n(k)}{2}\right)(2\sigma^2)^{\frac{n(k)}{2}-1}} \quad -\infty < l < \infty\,. \tag{4.1}$$

The expected value of L_k (see Crowder and Hamilton (1992)) is

$$E(L_k) = \ln\left(2\sigma^2\right) + \Psi\left(\frac{n}{2}\right) \tag{4.2}$$

and the variance of L_k is

$$Var(L_k) = \Psi'\left(\frac{n}{2}\right) \tag{4.3}$$

where $\Psi(\cdot)$ is the digamma function and $\Psi'(\cdot)$ is the trigamma function. Notice the mean of L_k is an increasing function of σ^2 and the variance of L_k depends only on the sample size.

The density of L_k is a smooth function. Figure 4.2 is a plot of the density of L_k for several values of σ when $n = 1$.

Since the mean of L_k is an increasing function of the variance, the statistic L_k can be used to form EWMA and CUSUM charts that are sensitive to changes in variability.

4.3 Normal Transformation

We suggest a transformation of the T_k such that the observed statistic at time k has an exact normal distribution when the process is in control. The transformation eliminates the numerical difficulties of the gamma distribution. The design of the control chart is also greatly simplified

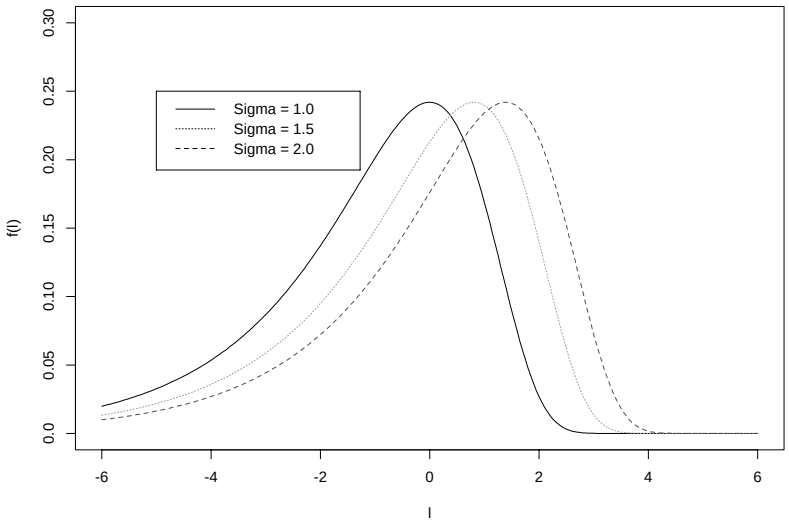

Figure 4.2: Density of L_k for $n = 1$

since the control limit can be obtained from existing tables of control limits for control charts for the mean of a normal distribution.

Let $M_{n(k)}$ = cumulative distribution function (cdf) of T_k when $\sigma^2 = \sigma_0^2$ and let Φ = the cdf of a standard normal random variable. Define the transformed statistic at time k by

$$Z_k = \Phi^{-1}\left(M_{n(k)}\left(T_k\right)\right). \tag{4.4}$$

Quesenberrry (1995) previously suggested a similar transformation for the sample variance in the Q chart for monitoring process variance when the target values are not assumed to be known.

The distribution of Z_k can be found by applying a change of variables method to T_k.

$$F_Z(z) = F_T\left(M_{n(k)}^{-1}\left(\Phi(z)\right)\right) \tag{4.5}$$

$$f_Z(z) = \frac{f_T\left(M_{n(k)}^{-1}\left(\Phi(z)\right)\right)\Phi'(z)}{M'_{n(k)}\left(M_{n(k)}^{-1}\left(\Phi(z)\right)\right)}. \tag{4.6}$$

Notice that Z_k has a standard normal distribution when the process is in control $\left(\sigma^2 = \sigma_0^2\right)$.

The distribution of Z_k will not be normal when $\sigma^2 \neq \sigma_0^2$, but the density of Z_k is a smooth function. A plot of the density of Z_k for several values of σ is given in Figure 4.3.

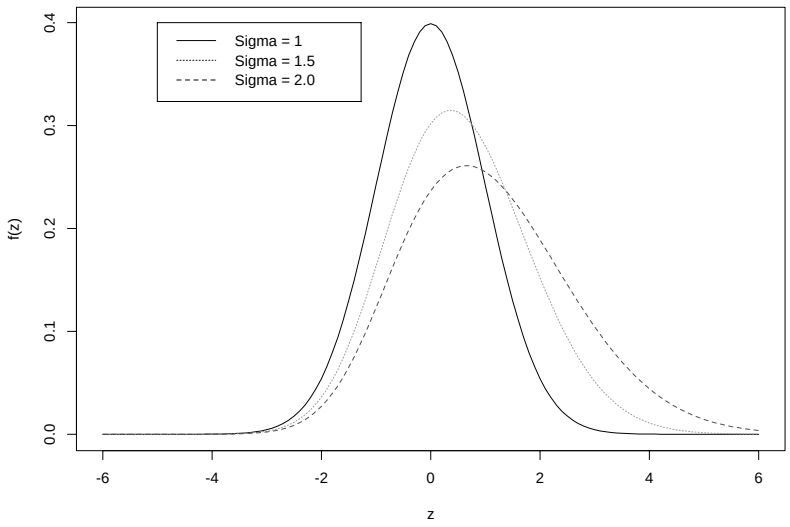

Figure 4.3: Density of Z_k for $n = 1$

An increase in the process standard deviation σ causes an increase in the mean of Z_k. The transformed statistics Z_k can be used to form CUSUM and EWMA charts that are sensitive to changes in σ.

4.4 CUSUM Charts for Monitoring Process Variance

Three one-sided CUSUM charts for detecting increases in process variability will be compared in this section.

1. The natural CUSUM statistic derived from the likelihood ratio uses T_k. The chart statistic is given in (3.5).

2. A CUSUM chart can also be constructed using the natural log transformation. The chart statistic is defined by substituting L_k for T_k in (3.5) and choosing a reference value γ. More

details on selecting an appropriate reference value for the chart that is based on L_k (and the chart based on Z_k that is defined below) are given later in this section.

3. A CUSUM chart based on Z_k will also be sensitive to changes in variability. The chart statistic is defined by substituting Z_k for T_k in (3.5) and choosing a reference value.

The properties of the CUSUM charts based on L_k and Z_k may easily be evaluated using the integral equation method. The density functions of L_k and Z_k are sufficiently smooth to eliminate all numerical difficulties in the calculations.

In a typical application of a CUSUM chart, the reference value is chosen to optimize the performance of the chart at some particular value of the parameter of interest. For the chart based on T_k, the optimal value of γ for detecting an increase in σ from σ_0 to σ_1 is

$$\gamma = -\frac{r_1}{r_2} = -\frac{n \log\left(\frac{\sigma_0}{\sigma_1}\right)}{\frac{1}{2}\left(\frac{1}{\sigma_0^2} - \frac{1}{\sigma_1^2}\right)}.$$

The reference value for the transformed charts can be chosen so the SSATS at some particular value of $\sigma_1 > \sigma_0$ is minimized by calculating the SSATS for a grid of possible reference values and simply choosing the value of γ that minimizes the SSATS at σ_1. We will use this grid search method to select the reference value when a CUSUM chart based on L_k or Z_k is to be compared with a CUSUM chart based on T_k.

It is possible that a chart that is optimized for some particular $\sigma_1 > \sigma_0$ could perform poorly for other values of σ. Fortunately, charts that are designed using the common value of $\sigma_1 = 1.5\sigma_0$ seem to perform well across a wide range of possible changes in σ.

The CUSUM charts based on the transformed statistics are competitive with the ordinary FSS CUSUM chart. Table 4.1 and Table 4.2 contain ATS and SSATS values at several values of σ for the three types of CUSUM charts with $n = 1$ and $n = 5$. The charts are all designed to detect a 50% increase in σ, and the ANSS is 500 when the process is in control. The ATS calculations were performed assuming the sampling interval is $d = 1$ time unit. The control limit and reference value for each chart are given in the table headings.

The ordinary chart and the transformed charts give similar performance for all values of σ when $n = 5$. The steady state ATS of the chart based on L_k is larger than the SSATS of the other two charts for all values of σ but the differences are very small. As expected, the chart based on T_k has the smallest SSATS for all values of σ. None of the differences among the three charts are likely to be significant in practice.

When $n = 1$, the SSATS for the chart based on T_k is smaller than the SSATS of the other two charts for all values of σ. The chart based on L_k performs worst when $\sigma < 1.8\sigma_0$, but the chart based on Z_k is worst for very large increases in σ. The natural logarithm transformation performs especially poorly when the increase in the variance is small. The steady state ATS of the chart based on Z_k is approximately 20% larger than the SSATS of the chart that uses T_k for most values of σ.

The simplicity of the natural logarithm chart comes with the cost of severely degraded performance when $n = 1$ and the increase in σ is small. The normal transformation performs much better than the natural logarithm transformation in those cases, but the ordinary chart is still significantly better. We recommend the CUSUM chart based on T_k for detecting increases in the process variance despite the increased difficulty in evaluating the properties of this chart. The properties need to be evaluated only once, but the chart will give quicker detection (on average) in every application.

Table 4.1: ATS and SSATS for CUSUM Charts with $n = 1$

	ATS			SSATS		
	T_k	$\ln(T_k)$	Z_k	T_k	$\ln(T_k)$	Z_k
	$\gamma = 1.46$	$\gamma = 0.93$	$\gamma = 0.42$			
$\frac{\sigma}{\sigma_0}$	$h = 12.165$	$h = 1.543$	$h = 5.039$			
1.1	138.51	182.48	156.06	134.90	181.45	152.02
1.2	59.22	85.59	70.26	56.70	84.73	67.39
1.3	33.35	47.86	40.10	31.40	47.09	37.84
1.4	22.17	30.34	26.65	20.56	29.63	24.76
1.5	16.32	21.08	19.56	14.93	20.41	17.91
1.6	12.82	15.68	15.35	11.59	15.04	13.87
1.7	10.53	12.28	12.62	9.41	11.66	11.26
1.8	8.92	10.00	10.72	7.89	9.40	9.47
1.9	7.75	8.40	9.34	6.79	7.81	8.16
2.0	6.85	7.23	8.30	5.94	6.65	7.18
3.0	3.35	3.20	4.18	2.68	2.56	3.35

Table 4.2: ATS and SSATS for CUSUM Charts with $n = 5$

	ATS			SSATS		
	T_k	$\ln(T_k)$	Z_k	T_k	$\ln(T_k)$	Z_k
	$\gamma = 7.30$	$\gamma = 0.40$	$\gamma = 0.78$			
$\frac{\sigma}{\sigma_0}$	$h = 15.186$	$h = 1.272$	$h = 2.968$			
1.1	74.13	81.67	75.02	72.76	80.41	73.59
1.2	22.59	25.48	23.19	21.59	24.55	22.16
1.3	10.97	12.08	11.25	10.14	11.28	10.40
1.4	6.88	7.37	7.04	6.14	6.65	6.28
1.5	4.95	5.22	5.08	4.27	4.55	4.38
1.6	3.87	4.06	4.00	3.23	3.41	3.33
1.7	3.19	3.34	3.31	2.57	2.72	2.67
1.8	2.73	2.87	2.85	2.13	2.26	2.23
1.9	2.39	2.53	2.52	1.81	1.94	1.91
2.0	2.14	2.28	2.27	1.57	1.69	1.67
3.0	1.25	1.32	1.31	0.73	0.80	0.78

4.5 EWMA Charts for Monitoring Process Variance

Three one-sided EWMA charts for detecting increases in process variability will be considered in this section.

1. An EWMA chart that is sensitive to increases in variance can be formed directly from T_k. Let $N_k = T_k - n\sigma_0^2$. The chart statistic can be found by substituting N_k for Q_k in (3.7) and letting $l = \theta_0 = 0$.

   Notice $E(N_k) = 0$ when the process is in control and $E(N_k) > 0$ if the process variance increases.

2. The EWMA chart described by Crowder and Hamilton (1992) can easily be extended to the case where the process mean is known. The chart statistic is given by substituting L_k for Q_k in (3.7) and letting $l = \theta_0 = E(L_k \mid \sigma = \sigma_0)$.

3. An EWMA chart based on Z_k can be used to detect increases in the variance. The chart statistic can be found by substituting Z_k for Q_k in (3.7) and letting $l = \theta_0 = 0$.

The EWMA charts based on L_k and Z_k offer significant computational advantages for small sample sizes. It is expected that the easier numerical computation comes at the cost of some loss in efficiency. A study of the three EWMA charts for $n = 1$ and $n = 5$ was performed to assess the costs of using the natural log and normal transformations.

All three charts were optimized to detect an increase in σ from σ_0 to $1.5\sigma_0$ by choosing a grid search to find the value of λ that minimizes the SSATS when $\sigma = 1.5\sigma_0$. Figure 4.4 is a plot of the SSATS when $\sigma = 1.5\sigma_0$ as a function of λ for an EWMA chart based on N_k with $n = 5$, $d = 1$, and an in-control ANSS of 500. The minimum steady state ATS occurs when $\lambda = 0.17$. The corresponding plots for EWMA charts based on $\ln(T_k)$ and Z_k are not reproduced here, but the curves show essentially the same behavior. The steady state ATS is a smooth function of λ and has a single minimum in all cases.

Table 4.3 gives the ATS and SSATS for the EWMA chart of each type that has been optimized for $\sigma = 1.5\sigma_0$ for $n = 1$, and 4.4 illustrates the same for $n = 5$. The ANSS for all charts is 500 when

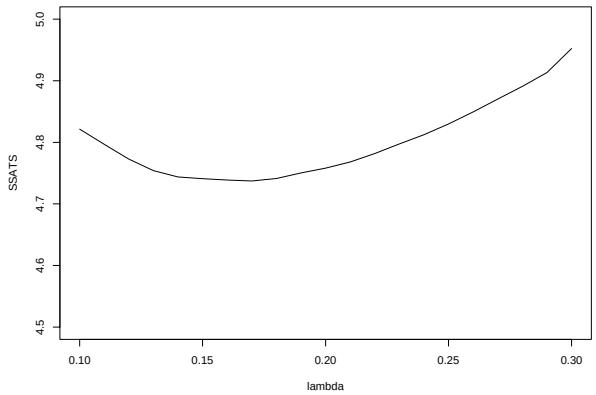

Figure 4.4: SSATS versus λ for an EWMA Chart of N_k with $n = 5$ and $\sigma = 1.5\sigma_0$

the process is in control and the sampling interval is $d = 1$. The optimal value of λ for detecting a 50% increase in the standard deviation for each EWMA chart and the control limit for each chart are given in the table headings.

The SSATS of the EWMA chart based on N_k is smallest for all values of σ. There is little difference between the SSATS of the charts that use $\ln(T_k)$ and Z_k when $n = 5$. The SSATS of both charts is about 10% greater than the SSATS of the chart based on N_k when $n = 5$.

When $n = 1$, the SSATS of the chart that uses $\ln(T_k)$ is between 20% and 50% greater than the SSATS of the chart that uses N_k. The difference is largest for small increases in σ. The chart based on Z_k performs slightly better than the chart based on $\ln(T_k)$. The steady state ATS of the chart that uses Z_k is about 25% larger than the steady state ATS of the chart that uses N_k. The normal transformation chart performs better than the natural log transformation chart for all values of σ except $\sigma > 1.8\sigma_0$ when $n = 1$.

The computational and design advantages of the charts that use L_k and Z_k are not sufficient reasons for recommending their use when $n = 5$. The numerical difficulties become more severe for the chart based on N_k when $n < 5$ but the performance gap between this chart and the charts that use L_k and Z_k becomes even wider.

The recommendation given above is based strictly on the performance of the three control charts for detecting increases in variability. The chart based on Z_k offers additional advantages when the

variance monitoring scheme is combined with an EWMA chart for the mean. This will be discussed in detail in Chapter 7.

Table 4.3: ATS and SSATS for EWMA Charts with $n = 1$

	ATS			SSATS		
	N_k	$\ln(T_k)$	Z_k	N_k	$\ln(T_k)$	Z_k
	$\lambda = 0.04$	$\lambda = 0.56$	$\lambda = 0.12$			
$\frac{\sigma}{\sigma_0}$	$h = 0.590$	$h = 0.939$	$h = 0.442$			
1.1	128.76	184.99	156.34	122.32	183.76	151.32
1.2	56.12	87.45	70.76	51.70	86.40	67.01
1.3	32.81	49.11	40.62	29.46	48.17	37.58
1.4	22.50	31.21	27.14	19.80	30.34	24.56
1.5	16.92	21.71	20.01	14.65	20.90	17.74
1.6	13.49	16.15	15.76	11.52	15.38	13.72
1.7	11.18	12.65	12.99	9.45	11.91	11.12
1.8	9.54	10.30	11.07	7.98	9.58	9.34
1.9	8.32	8.65	9.67	6.89	7.96	8.04
2.0	7.38	7.44	8.60	6.06	6.77	7.07
3.0	3.59	3.28	4.36	2.75	2.69	3.29

Table 4.4: ATS and SSATS for EWMA Charts with $n = 5$

	ATS			SSATS		
	N_k	$\ln(T_k)$	Z_k	N_k	$\ln(T_k)$	Z_k
	$\lambda = 0.17$	$\lambda = 0.29$	$\lambda = 0.28$			
$\frac{\sigma}{\sigma_0}$	$h = 0.670$	$h = 0.550$	$h = 1.175$			
1.1	67.23	77.90	73.19	65.05	76.16	71.12
1.2	21.28	24.57	23.13	19.74	23.28	21.62
1.3	10.87	11.98	11.52	9.64	10.90	10.28
1.4	7.04	7.51	7.35	5.99	6.55	6.26
1.5	5.16	5.43	5.37	4.24	4.55	4.39
1.6	4.08	4.29	4.26	3.23	3.46	3.35
1.7	3.38	3.58	3.56	2.59	2.79	2.70
1.8	2.90	3.10	3.07	2.16	2.34	2.26
1.9	2.54	2.76	2.72	1.84	2.02	1.94
2.0	2.28	2.50	2.45	1.60	1.78	1.70
3.0	1.30	1.45	1.40	0.74	0.86	0.80

Chapter 5

Variable Sample Size Control Charts for Monitoring Process Variance

5.1 Variable Sample Size Shewhart Chart

5.1.1 Definition

The VSS chart could be implemented with any number of possible sample sizes. The chart becomes very cumbersome in practice if more than two sample sizes are possible. Costa (1994) showed that a VSS Shewhart chart for the mean that uses two sample sizes performs much better than a FSS-FSI Shewhart chart for the mean. Based on this result and the need to maintain simplicity, the VSS chart for variance monitoring considered here will use two distinct sample sizes. Let n_1 be the smaller sample size and n_2 be the larger. The two sample sizes n_1 and n_2 should be considered chart parameters. Particular values can be chosen to provide protection against the expected magnitude of the shift in variance.

Let $n(k) =$ sample size used at time k. Since the distribution of the chart statistic T_k depends on $n(k)$, it is convenient to specify the control limit and the sample size limit in terms of probabilities. Let $M_{n(k)}$ be the distribution function of T_k when $\sigma = \sigma_0$. Then $n(k)$ is defined as

$$n(k) = \begin{cases} n_1 & 0 \leq M_{n(k-1)}(T_{k-1}) < g \\ n_2 & g \leq M_{n(k-1)}(T_{k-1}) < h. \end{cases} \tag{5.1}$$

The chart signals at time $k-1$ if $M_{n(k-1)}(T_{k-1}) \geq h$.

The constants g and h determine the ANSS and the average sample size when the process is in control. Figure 5.1 shows the correspondence between $n(k)$ and the plotted values on the control chart.

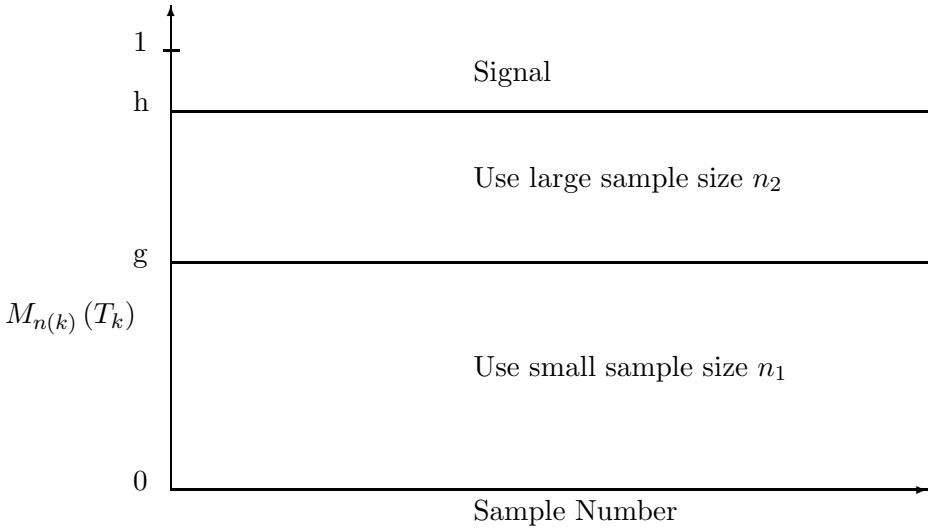

Figure 5.1: Control and Sample Size Limits for the VSS Shewhart Chart

5.1.2 Evaluation Methods

Costa (1994) used a simplification of the Markov chain method of Brook and Evans (1972) to

evaluate the properties of a VSS Shewhart chart for the mean. Prabhu et al. (1994) used a similar method to evaluate the properties of a combined VSS-VSI Shewhart chart for the mean. We will use a similar method to evaluate the properties of the VSS Shewhart chart for the variance.

The Markov chain has two transient states (use sample size n_1 on the next sample, use sample size n_2 on the next sample) and one absorbing state (signal). Let P = the matrix of transition probabilities for the Markov chain. The transition matrix can be written as

$$P = \begin{bmatrix} q_{11} & q_{12} & p_1 \\ q_{21} & q_{22} & p_2 \\ 0 & 0 & 1 \end{bmatrix} \tag{5.2}$$

and the matrix of transient states is

$$Q = \begin{bmatrix} q_{11} & q_{12} \\ q_{21} & q_{22} \end{bmatrix} \tag{5.3}$$

where

$$\begin{aligned} q_{11} &= P\left(0 \le T_k < M_{n_1}^{-1}(g) \,|n(k) = n_1\right) \\ q_{12} &= P\left(M_{n_1}^{-1}(g) \le T_k < M_{n_1}^{-1}(h) \,|n(k) = n_1\right) \\ q_{21} &= P\left(0 \le T_k < M_{n_2}^{-1}(g) \,|n(k) = n_2\right) \\ q_{22} &= P\left(M_{n_2}^{-1}(g) \le T_k < M_{n_2}^{-1}(h) \,|n(k) = n_2\right) \\ p_1 &= P\left(T_k \ge M_{n_1}^{-1}(h) \,|n(k) = n_1\right) \\ p_2 &= P\left(T_k \ge M_{n_2}^{-1}(h) \,|n(k) = n_2\right). \end{aligned}$$

As defined, the transition probabilities do not depend on the sample size for the current sample *when the process is in control*. Under this definition, it is clear that $q_{11} = q_{21} = g$, $q_{12} = q_{22} = h - g$, and $p_1 = p_2 = 1 - h$ when $\sigma = \sigma_0$.

5.1.3 Evaluation of Properties and Chart Design

Suppose the process variance is out of control at startup ($\sigma = \sigma_1 > \sigma_0$ at time $k = 0$). The ANSS depends on the sample size used for the initial sample. The expressions for the ANSS given below assume the initial sample size is either n_1 or n_2. The vector of ANSS values for the two possible initial sample sizes is

$$\mathbf{ANSS} = \begin{bmatrix} ANSS|n(0) = n_1 \\ ANSS|n(0) = n_2 \end{bmatrix} = [I - Q]^{-1} \begin{bmatrix} 1 \\ 1 \end{bmatrix}. \tag{5.4}$$

Since the Markov chain has only two transient states, it is possible to solve explicitly for the ANSS values in terms of the elements of Q. The explicit expressions are

$$\mathbf{ANSS} = \begin{bmatrix} ANSS\,|\,n(0) = n_1 \\ ANSS\,|\,n(0) = n_2 \end{bmatrix} = \begin{bmatrix} \frac{1-q_{22}+q_{12}}{1-q_{11}-q_{22}-q_{12}q_{21}+q_{11}q_{22}} \\ \frac{1-q_{11}+q_{21}}{1-q_{11}-q_{22}-q_{12}q_{21}+q_{11}q_{22}} \end{bmatrix}. \tag{5.5}$$

The ANOS also depends on the initial sample size. The ANOS is

$$\mathbf{ANOS} = \begin{bmatrix} ANOS\,|\,n(0) = n_1 \\ ANOS\,|\,n(0) = n_2 \end{bmatrix} = [I - Q]^{-1} \begin{bmatrix} n_1 \\ n_2 \end{bmatrix} = \begin{bmatrix} \frac{n_1(1-q_{22})+n_2q_{12}}{1-q_{11}-q_{22}-q_{12}q_{21}+q_{11}q_{22}} \\ \frac{n_2(1-q_{11})+n_1q_{21}}{1-q_{11}-q_{22}-q_{12}q_{21}+q_{11}q_{22}} \end{bmatrix}. \tag{5.6}$$

When the process is in control, (5.5) simplifies to

$$\mathbf{ANSS} = \begin{bmatrix} ANSS|n(0) = n_1 \\ ANSS|n(0) = n_2 \end{bmatrix} = \begin{bmatrix} \frac{1}{1-h} \\ \frac{1}{1-h} \end{bmatrix}. \tag{5.7}$$

If the sample size for the initial sample is the arbitrary value n_0, the ANSS is

$$\begin{aligned} [ANSS\,|\,n(0) = n_0] = 1 \;&+\; P\left(0 \le T_k < M_{n_0}^{-1}(g)\right) \cdot [ANSS\,|\,n(0) = n_1] \\ &+\; P\left(M_{n_0}^{-1}(g) \le T_k < M_{n_0}^{-1}(h)\right) \cdot [ANSS\,|\,n(0) = n_2] \end{aligned} \tag{5.8}$$

and the ANOS is

$$\begin{aligned}[ANOS \,|\, n(0) = n_0] = n_0 \quad &+ \quad P\left(0 \leq T_k < M_{n_0}^{-1}(g)\right) \cdot [ANOS \,|\, n(0) = n_1] \\ &+ \quad P\left(M_{n_0}^{-1}(g) \leq T_k < M_{n_0}^{-1}(h)\right) \cdot [ANOS \,|\, n(0) = n_2]. \end{aligned} \tag{5.9}$$

The VSS and FSS charts can be compared if the two charts have the same ANSS and ANOS when the process is in control. Let ANSS_0 be the desired ANSS for the two charts when the process is in control and suppose the FSS chart utilizes samples of size n.

Using (5.7), the control limit for the VSS chart should be

$$h = 1 - \frac{1}{\text{ANSS}_0}. \tag{5.10}$$

Notice this is the same control limit that would be used by a FSS chart that is standardized to a probability scale.

The two charts will have the same ANOS if the average sample size for the VSS chart equals the average sample size for the FSS chart when the process is in control (assuming the ANSS has already been matched). The average sample size for the VSS chart will be n if the sampling boundary for the VSS chart is chosen to be

$$g = \frac{n_2 - n}{n_2 - n_1} h. \tag{5.11}$$

Equations (5.10) and (5.11) provide a method for designing a VSS chart whose in control behavior is comparable to a FSS chart.

5.1.4 Steady State Properties

The Markov chain used to calculate the properties of the VSS chart is not ergodic since it contains an absorbing state. However, it is possible to calculate the steady state behavior of the chart conditional on no signals (false alarms) between startup and the time of the increase in the variance. Let π_i = the proportion of samples that are of size n_i when the process operates in control for

some long period of time and the chart has no signals. The vector $\underline{\pi} = [\pi_1, \pi_2]$ is the stationary distribution of the sample size conditional on no signals. It is possible to calculate the steady state sampling behavior analytically for the VSS Shewhart chart with two possible sample sizes. Expressions for the steady state properties are developed for the particular case of matching the VSS chart to an FSS chart for comparison purposes.

Suppose the VSS chart is to be matched with a FSS chart that utilizes samples of size n. This constraint leads to the system of equations

$$\begin{aligned} n_1\pi_1 + n_2\pi_2 &= n \\ \pi_1 + \pi_2 &= 1. \end{aligned} \tag{5.12}$$

These equations are easily solved to obtain

$$\pi_1 = \frac{n_2 - n}{n_2 - n_1} \quad \text{and} \quad \pi_2 = \frac{n - n_1}{n_2 - n_1}. \tag{5.13}$$

Notice the close relationship between (5.11) and (5.13). The proportion of time each sample size will be used if the probabilities are calculated conditional on no signal by the chart is given by (5.13). If the sample size probabilities are calculated assuming the chart can signal, then at any sampling time the probability another sample will be taken is h. The expression for g in (5.11) is simply the weighting of this probability by the appropriate proportion to ensure the average sample size will be n.

The steady state ANSS and ANOS of the VSS chart are given by

$$\begin{aligned} SSANSS &= \begin{bmatrix} \pi_1 & \pi_2 \end{bmatrix} [I - Q]^{-1} \begin{bmatrix} 1 \\ 1 \end{bmatrix} \\ &= \frac{\pi_1 \left(1 - q_{22} + q_{12} + \pi_2 \left(1 - q_{11} + q_{21}\right)\right)}{1 - q_{11} - q_{22} - q_{12}q_{21} + q_{11}q_{22}} \\ SSANOS &= \begin{bmatrix} \pi_1 & \pi_2 \end{bmatrix} [I - Q]^{-1} \begin{bmatrix} n_1 \\ n_2 \end{bmatrix} \end{aligned} \tag{5.14}$$

$$= \frac{n_1\pi_1(1-q_{22}+q_{12})+n_2\pi_2(1-q_{11}+q_{21})}{1-q_{11}-q_{22}-q_{12}q_{21}+q_{11}q_{22}}. \quad (5.15)$$

Following the outline given in Section 3.1, the SSATS of the VSS chart is

$$SSATS = ATS - \frac{d}{2} = d \cdot SSANSS - \frac{d}{2}.$$

5.1.5 Comparison with FSS Chart

It is expected that a VSS chart for detecting increases in variability will have smaller ANSS and ATS values than a comparable FSS chart. We calculated the ANSS, ATS, and ANOS for various values of n, n_1, and n_2 to evaluate this conjecture. The calculations were performed for $\sigma = \sigma_0, 1.1\sigma_0, 1.2\sigma_0 \ldots, 3\sigma_0$.

Table 5.1 shows what sample size combinations produced the smallest SSATS at each amount of increase in σ for the representative values $n = 5$, $ANSS_0 = 500$, and $d = 1$. The maximum value of n_2 considered in this study was $n_2 = 20$. In practice, if the comparable FSS chart uses subgroups of size $n = 5$, it is unlikely that samples larger than twenty are feasible for the VSS chart. The information in Table 5.1 gives some insight into the general behavior of the SSATS as a function of σ and the sample size pair (n_1, n_2) when comparing the VSS chart to a FSS chart with $n = 5$. Choosing n_1 as small and n_2 as large as possible gives the best performance when the increase in σ is small. For large increases in σ, the best VSS chart uses n_1 and n_2 near the sample size used for the corresponding FSS chart. This suggests the VSS feature is most effective when the increase in the process variability is small. Detecting a small increase in variability is quite difficult. The VSS chart can switch to the larger sample size and attain enough power to more quickly detect a small increase in σ.

Similar tables can easily be constructed for other values of n. Such tables would give practitioners the ability to design a VSS chart that is best for some particular amount of increase in σ, subject to any set of constraints on n_1 and n_2. This choice of the best chart should then be evaluated for a large set of possible changes in σ to ensure adequate performance across a wide range of possible process changes.

Table 5.1: Minimum SSATS for VSS Shewhart Charts with $n = 5$, $n_1 = 1 - 4$, and $n_2 = 6 - 20$

$\frac{\sigma}{\sigma_0}$	n_1	n_2	FSSATS	VSSATS	FSSANOS	VSSANOS
1.1	2	20	124.54	113.14	625.21	757.25
1.2	1	20	44.57	27.85	225.33	250.31
1.3	1	20	20.43	9.76	104.64	104.22
1.4	2	20	11.14	4.98	58.21	57.18
1.5	2	20	6.89	3.29	36.94	38.05
1.6	3	20	4.67	2.49	25.84	28.84
1.7	3	20	3.39	2.04	19.46	23.70
1.8	4	18	2.60	1.75	15.50	19.06
1.9	4	16	2.08	1.52	12.90	16.05
2.0	4	14	1.72	1.35	11.11	13.70
2.1	4	14	1.47	1.22	9.83	12.44
2.2	4	12	1.28	1.11	8.88	10.85
2.3	4	10	1.13	1.03	8.17	9.51
2.4	4	10	1.02	0.96	7.62	8.92
2.5	4	8	0.94	0.90	7.18	7.92
2.6	4	8	0.87	0.84	6.84	7.55
2.7	4	8	0.81	0.80	6.56	7.23
2.8	4	6	0.77	0.76	6.33	6.55
2.9	4	6	0.73	0.73	6.14	6.35
3.0	4	6	0.70	0.70	5.99	6.18

Table 5.2 contains SSATS and SSANOS values for FSS-FSI and VSS-FSI Shewhart charts at several values of σ. The table contains results for VSS charts with $n_1 \in \{1, 3\}$ and $n_2 \in \{7, 10, 15, 20\}$. The FSS chart utilizes samples of size $n = 5$. The sampling interval is $d = 1$ time unit for all charts, and all charts have an in control ANSS of 500 samples.

Table 5.2 shows the VSS chart offers substantially quicker detection of small to moderate ($<$ 80%) increases in the process standard deviation. The charts give essentially equivalent performance for large ($>$ 100%) shifts in the standard deviation.

It should be noted that the improved detection capabilities of the VSS chart come with slightly increased sampling costs when the process is not in control. For example, the VSS chart with $n_1 = 1$ and $n_2 = 20$ that has an average sample size of $n = 5$ when the process is in control will signal after 27.85 time periods on average (assuming steady state behavior) when the standard deviation increases by 20% versus about 44.57 time units for the FSS chart. However, the SSANOS

for the VSS chart is 250.31, which is slightly larger than the 225.33 observations required for the FSS chart. The SSANOS for the best VSS chart is usually a little larger than the SSANOS for the FSS chart, but this small increase in the SSANOS is outweighed by the large decreases in the SSATS. The increased sampling rate for the VSS chart is not unexpected since the VSS feature is specifically designed to increase the sampling rate when there is some evidence the process is not in control but not enough evidence for an out of control signal.

Table 5.2: SSATS and ANOS for VSS Shewhart Charts with $n = 5$

$\frac{\sigma}{\sigma_0}$	n_1	n_2	FSSATS	VSSATS	FSSANOS	VSSANOS
1.2	1	20	44.57	27.85	225.35	250.31
1.2	3	20	44.57	29.75	225.35	246.97
1.2	1	15	44.57	31.13	225.35	251.44
1.2	3	15	44.57	32.59	225.35	247.29
1.2	1	10	44.57	35.82	225.35	247.06
1.2	3	10	44.57	36.61	225.35	243.33
1.2	1	7	44.57	40.07	225.35	238.03
1.2	3	7	44.57	40.32	225.35	236.03
1.5	3	20	6.89	3.32	36.95	38.16
1.5	1	20	6.89	3.47	36.95	37.85
1.5	3	15	6.89	3.65	36.95	37.52
1.5	1	15	6.89	3.69	36.95	37.23
1.5	1	10	6.89	4.43	36.95	37.20
1.5	3	10	6.89	4.47	36.95	37.36
1.5	1	7	6.89	5.49	36.95	37.25
1.5	3	7	6.89	5.53	36.95	37.30
1.8	3	15	2.60	1.76	15.50	18.50
1.8	3	20	2.60	1.76	15.50	20.56
1.8	3	10	2.60	1.89	15.50	16.80
1.8	1	10	2.60	1.98	15.50	16.97
1.8	1	15	2.60	1.99	15.50	18.99
1.8	1	20	2.60	2.12	15.50	21.52
1.8	3	7	2.60	2.16	15.50	15.99
1.8	1	7	2.60	2.19	15.50	16.04
2.0	3	15	1.72	1.39	11.11	14.69
2.0	3	10	1.72	1.40	11.11	12.72
2.0	3	20	1.72	1.43	11.11	16.89
2.0	3	7	1.72	1.51	11.11	11.71
2.0	1	10	1.72	1.54	11.11	13.12
2.0	1	7	1.72	1.55	11.11	11.85
2.0	1	15	1.72	1.67	11.11	15.70
2.0	1	20	1.72	1.84	11.11	18.68

5.2 Variable Sample Size CUSUM Chart

5.2.1 Definition

Any of the three statistics considered in Section 4.4 could be used to define a VSS CUSUM chart for the variance. The FSS-FSI CUSUM chart based on T_k performed better than the CUSUM charts that are based on transformed statistics so the VSS CUSUM chart will use T_k.

Consider a CUSUM chart defined by

$$Y_k = \begin{cases} Y_k = max\{0, Y_{k-1}\} + T_k - \gamma_k & k \geq 1 \\ T_1 - \gamma_1 & k = 1 \end{cases}. \tag{5.16}$$

The reference value γ_k depends on the sample size that was used at time k and is defined by

$$\gamma_k = -\frac{r_1(k)}{r_2} = -\frac{n(k)\log\left(\frac{\sigma_0}{\sigma_1}\right)}{\frac{1}{2}\left(\frac{1}{\sigma_0^2} - \frac{1}{\sigma_1^2}\right)}.$$

The chart indicates an increase in the process variance at time k if $Y_k \geq h$.

Let $n(k)$ be the sample size at time k. Then for $k \geq 2$,

$$n(k) = \begin{cases} n_1 & Y_{k-1} < g \\ n_2 & g \leq Y_{k-1} < h \end{cases} \tag{5.17}$$

where the limits g and h determine the ANOS and ANSS.

The ANSS and ANOS of a VSS CUSUM or VSS EWMA chart depend on the initial sample size. The SSANOS and SSANSS also depend on the initial sample size since the control limit for a VSS chart that always uses a large initial sample size will be slightly larger than the control limit for a VSS chart that always uses a small initial sample size if the two charts have the same ANSS when the process is in control. Unless otherwise indicated, all results for VSS CUSUM and EWMA charts in this dissertation were calculated assuming that the average sample size when the process is in control was used for the initial sample.

5.2.2 Evaluation of Properties and Comparison with FSS CUSUM Chart

The distribution of T_k depends on the sample size that was used at time k. This makes evaluating the properties of the VSS CUSUM chart somewhat complicated. The unified integral equation-Markov chain method of Reynolds (1995) can still be used. Appendix B contains details of the evaluation methods.

The VSS charts will be compared to a FSS CUSUM chart that uses samples of size $n = 5$. The sampling boundary for the VSS charts was chosen to give an average sample size of $n = 5$. All charts have an in-control ANSS of 500 and use sampling interval $d = 1$. The procedure for finding g and h to give specified ANSS and ANOS values is discussed in Appendix B.

Table 5.3 gives the sample size combinations for the VSS CUSUM chart with the smallest SSATS at each value of σ. The results for a particular value of σ are for charts that are optimized for that value of σ. The minimum is taken over the sample size combinations of $n_1 = 1 - 4$ and $n_2 = 6 - 20$.

The behavior of the VSS CUSUM chart is generally similar to the VSS Shewhart chart. No particular sample size combination is best across a wide range of possible increases in σ. Choosing n_1 and n_2 far apart is best for detecting small and moderate increases in the variance. Choosing n_1 and n_2 somewhat closer together is best for detecting large increases. The optimal value of n_2 for a VSS CUSUM chart at a particular value of σ is somewhat larger than the best value of n_2 for a VSS Shewhart chart. The SSATS is much lower for the CUSUM charts than the Shewhart charts for small and moderate increases in the variance. The best VSS CUSUM chart has lower SSATS values than the best FSS CUSUM chart across all values of σ, but the difference is greatest for small and moderate increases. The SSANOS for the VSS chart is larger than the SSANOS for the FSS chart despite the smaller SSATS. As with the Shewhart chart, this increase in the SSANOS is due to the frequent use of the larger sample size when there is some evidence the process variability has increased but insufficient evidence to signal an increase.

The procedure used to construct Table 5.3 can be used to find the best VSS chart for any particular increase in σ subject to a set of constraints on n_1 and n_2. As noted in the previous chapter, the properties of the selected chart should be evaluated at other values of σ to ensure good

Table 5.3: Minimum SSATS for VSS CUSUM Charts with $n = 5$, $n_1 = 1 - 4$, and $n_2 = 6 - 20$

	FSS			VSS					
$\frac{\sigma_1}{\sigma_0}$	h	SSATS	SSANOS	n_1	n_2	g	h	SSATS	SSANOS
1.1	33.078	41.84	211.72	2	20	4.192	31.552	26.39	235.54
1.2	24.568	16.91	87.05	2	20	2.35	21.997	9.60	95.55
1.3	19.457	9.13	48.14	2	20	1.507	17.193	5.41	55.95
1.4	16.891	5.96	32.29	2	20	0.985	14.196	4.21	39.31
1.5	15.186	4.27	23.85	3	20	1.668	12.671	2.84	30.95
1.6	13.840	3.24	18.68	3	17	0.776	11.769	2.30	24.32
1.7	12.811	2.57	15.33	3	15	0.05	11.066	1.94	19.96
1.8	11.969	2.10	13.02	3	13	-0.714	10.558	1.69	16.65
1.9	11.259	1.77	11.36	4	13	0.312	10.282	1.49	14.50
2.0	10.642	1.52	10.12	4	12	-0.337	9.847	1.33	12.73
3.0	6.687	0.69	5.96	4	6	-7.62	6.682	0.69	6.16

performance in a wide range of situations.

Table 5.4 gives the SSATS and SSANOS for the sample size combinations $n_1 = 1, 3$ and $n_2 = 10, 15$, and 20. The differences among the various sample size combinations are not as pronounced for the VSS CUSUM chart as for the VSS Shewhart chart. It appears the sample sizes for the VSS CUSUM chart could even be chosen for convenience without seriously impacting the performance of the chart in most cases as long as the general rules about choosing n_1 and n_2 given above are followed. All of the VSS charts offer significantly quicker detection times than the FSS CUSUM chart.

Table 5.4: ATS, ANOS, SSATS, and SSANOS for VSS CUSUM Charts with $n = 5$

					ATS		ANOS		SSATS		SSANOS	
$\frac{\sigma}{\sigma_0}$	n_1	n_2	g	h	FSS	VSS	FSS	VSS	FSS	VSS	FSS	VSS
1.2	1	20	-0.036	11.514	22.59	14.75	112.95	118.47	21.59	14.45	110.45	118.67
1.2	3	20	1.667	12.671	22.59	15.14	112.95	123.07	21.59	14.54	110.45	122.02
1.2	1	15	-0.495	12.538	22.59	15.43	112.95	116.78	21.59	14.95	110.45	116.56
1.2	3	15	0.842	13.355	22.59	15.64	112.95	119.67	21.59	14.97	110.45	118.42
1.2	3	10	-0.467	14.172	22.59	17.08	112.95	116.84	21.59	16.31	110.45	115.28
1.2	1	10	-1.14	13.713	22.59	17.11	112.95	114.95	21.59	16.38	110.45	114.12
1.5	3	20	1.667	12.671	4.95	3.26	24.75	31.07	4.27	2.84	23.85	30.95
1.5	3	15	0.842	13.355	4.95	3.35	24.75	28.86	4.27	2.88	23.85	28.52
1.5	1	15	-0.495	12.538	4.95	3.28	24.75	28.08	4.27	2.96	23.85	28.20
1.5	1	20	-0.036	11.514	4.95	3.16	24.75	29.97	4.27	3.02	23.85	30.52
1.5	1	10	-1.14	13.713	4.95	3.66	24.75	26.34	4.27	3.11	23.85	26.11
1.5	3	10	-0.467	14.172	4.95	3.67	24.75	26.8	4.27	3.11	23.85	26.26
1.8	3	15	0.842	13.355	2.73	2.13	13.65	17.65	2.57	1.73	15.35	18.07
1.8	3	10	-0.467	14.172	2.73	2.23	13.65	15.55	2.57	1.75	15.35	15.51
1.8	3	20	1.667	12.671	2.73	2.11	13.65	19.84	2.57	1.77	15.35	20.78
1.8	1	10	-1.14	13.713	2.73	2.22	13.65	15.33	2.57	1.78	15.35	15.56
1.8	1	15	-0.495	12.538	2.73	2.10	13.65	17.28	2.57	1.90	15.35	18.36
1.8	1	20	-0.036	11.514	2.73	2.07	13.65	19.35	2.57	2.08	15.35	21.62
2.0	3	10	-0.467	14.172	2.14	1.85	10.70	12.49	1.57	1.41	10.35	12.75
2.0	3	15	0.842	13.355	2.14	1.80	10.70	14.43	1.57	1.44	10.35	15.37
2.0	1	10	-1.14	13.713	2.14	1.85	10.70	12.35	1.57	1.47	10.35	13.01
2.0	3	20	1.667	12.671	2.14	1.79	10.70	16.34	1.57	1.49	10.35	17.99
2.0	1	15	-0.495	12.538	2.14	1.78	10.70	14.19	1.57	1.66	10.35	16.22
2.0	1	20	-0.036	11.514	2.14	1.77	10.70	16.02	1.57	1.86	10.35	19.81

5.3 Variable Sample Size EWMA Chart

5.3.1 Definition

A VSS EWMA chart for detecting increases in process variability could be defined for any of the three statistics presented in Section 4.5. A VSS EWMA chart based on $N_k = T_k - n(k)\sigma_0^2$ will be defined here since the FSS-FSI chart based on N_k gave quicker detection of increases in σ than the charts based on the transformed statistics.

Define the chart statistic at time k by

$$Y_k = \begin{cases} \lambda\left(T_k - n(k)\sigma_0^2\right) + max\{0, (1-\lambda)Y_{k-1}\} & k \geq 1 \\ 0 & k = 0 \end{cases} . \tag{5.18}$$

For $k \geq 2$ the sample size at time k is

$$n(k) = \begin{cases} n_1 & Y_{k-1} < g \\ n_2 & g \leq Y_{k-1} < h \end{cases} .$$

The limits g and h are constants that determine the ANOS and ANSS.

5.3.2 Evaluation of Properties and Comparison with FSS EWMA Chart

The same method used to evaluate the properties of the VSS CUSUM chart can be used to evaluate the properties of the VSS EWMA chart. Appendix B contains details of the evaluation methods.

The VSS charts will be compared to an FSS EWMA chart that uses samples of size $n = 5$. The sampling boundary for the VSS charts was chosen to give an average sample size of $n = 5$. All charts have an in-control ANSS of 500 and use the sampling interval $d = 1$.

Table 5.5 gives the sample size pairs for the VSS EWMA chart with the smallest SSATS at each value of σ. The minimum is taken over the sample size combinations of $n_1 = 1 - 4$ and $n_2 = 6 - 20$ and over $\lambda \in \{0.10, 0.11, \ldots, 0.60\}$. The VSS EWMA chart exhibits the same general trends as the VSS Shewhart and VSS CUSUM charts. Choosing n_1 and n_2 far apart is best when the increase in σ is small and choosing n_1 and n_2 closer together is best when the increase in σ is large. The optimal value of λ for the VSS chart is much larger than the optimal value of λ for the

FSS chart at all values of σ. The true optimal value of λ is larger than the largest value considered when $\sigma > 1.4\sigma_0$. The optimal value of λ is one when $\sigma > 1.6\sigma_0$. The best VSS Shewhart chart in Table 5.1 has a smaller SSATS than any VSS EWMA chart considered in this comparison when $\sigma > 1.6\sigma_0$.

The SSATS of the best VSS EWMA chart is much lower than the SSATS of the FSS EWMA chart for small and moderate increases in σ and slightly smaller for large increases in σ. The SSANOS of the best VSS chart is slightly larger than the SSANOS of the FSS chart for all values of σ. The SSATS of the best VSS EWMA chart is much lower than the SSATS of the best VSS Shewhart chart for small values of σ. As noted above, the best VSS Shewhart chart performs better than the best VSS EWMA chart when $\sigma > 1.6\sigma_0$.

Table 5.5: Minimum SSATS for VSS EWMA Charts with $n = 5$, $n_1 = 1 - 4$, and $n_2 = 6 - 20$

	FSS				VSS						
$\frac{\sigma_1}{\sigma_0}$	λ	h	SSATS	SSANOS	λ	n_1	n_2	g	h	SSATS	SSANOS
1.1	0.02	0.2377	41.34	209.22	0.15	1	20	0.378	4.476	26.61	243.42
1.2	0.04	0.3836	16.11	83.05	0.28	2	20	0.983	6.837	9.85	97.48
1.3	0.08	0.6223	9.03	47.67	0.48	2	20	1.337	10.002	5.64	57.60
1.4	0.13	0.8749	5.92	32.09	0.6	3	19	2.277	11.174	3.89	40.16
1.5	0.17	1.0593	4.24	23.69	0.6	3	16	1.953	10.823	2.98	29.86
1.6	0.21	1.2347	3.22	18.62	0.6	3	14	1.686	10.558	2.43	23.63
1.7	0.25	1.4042	2.56	15.30	0.6	4	12	2.521	9.868	2.05	18.77
1.8	0.29	1.5698	2.10	13.01	0.6	4	11	2.297	9.764	1.77	15.91
1.9	0.33	1.7326	1.77	11.36	0.6	4	10	2.034	9.652	1.56	13.70
2.0	0.38	1.9335	1.53	10.13	0.6	4	9	1.717	9.53	1.39	11.94
3.0	0.6	2.7983	0.69	5.97	0.6	4	7	0.778	9.244	0.73	6.54

Table 5.6 contains the SSATS and SSANOS for the sample size combinations $n_1 = 1, 3$ and $n_2 = 10, 15,$ and 20. The ANSS of all charts is 500 when the process is in control. All charts use the value of λ that minimizes the SSATS when $\sigma = 1.5\sigma_0$.

Any VSS chart gives much quicker detection of small and moderate increases in the variance than the FSS EWMA chart. The differences among the VSS charts are substantial but still small relative to the difference between the FSS chart and the set of VSS charts.

Table 5.6: ATS, ANOS, SSATS, and SSANOS for VSS EWMA Charts with $n = 5$

				ATS		ANOS		SSATS		SSANOS	
$\frac{\sigma}{\sigma_0}$	λ	n_1	n_2	FSS	VSS	FSS	VSS	FSS	VSS	FSS	VSS
1.2	0.60	1	20	21.28	11.10	106.39	113.46	19.74	11.08	101.22	111.02
1.2	0.60	3	20	21.28	12.17	106.39	110.03	19.74	11.57	101.22	108.19
1.2	0.60	1	15	21.28	13.34	106.39	121.65	19.74	13.00	101.22	119.18
1.2	0.60	3	15	21.28	14.14	106.39	117.43	19.74	13.47	101.22	115.49
1.2	0.34	1	10	21.28	14.44	106.39	111.06	19.74	13.63	101.22	108.02
1.2	0.39	3	10	21.28	15.64	106.39	114.43	19.74	14.71	101.22	111.71
1.5	0.60	3	15	5.16	3.40	25.81	30.02	4.24	2.98	23.69	29.33
1.5	0.60	3	20	5.16	3.36	25.81	32.88	4.24	3.02	23.69	32.30
1.5	0.39	3	10	5.16	3.77	25.81	27.85	4.24	3.19	23.69	26.72
1.5	0.60	1	15	5.16	3.31	25.81	30.39	4.24	3.24	23.69	29.05
1.5	0.34	1	10	5.16	3.73	25.81	28.05	4.24	3.32	23.69	26.62
1.5	0.60	1	20	5.16	3.23	25.81	32.98	4.24	3.47	23.69	31.60
1.8	0.39	3	10	2.90	2.33	14.48	16.42	2.16	1.85	13.28	16.02
1.8	0.60	3	15	2.90	2.21	14.48	18.83	2.16	1.85	13.28	19.03
1.8	0.60	3	20	2.90	2.26	14.48	22.42	2.16	1.98	13.28	22.95
1.8	0.34	1	10	2.90	2.34	14.48	16.75	2.16	2.04	13.28	16.11
1.8	0.60	1	15	2.90	2.19	14.48	19.20	2.16	2.19	13.28	19.05
1.8	0.60	1	20	2.90	2.23	14.48	22.91	2.16	2.49	13.28	23.04
2.0	0.39	3	10	2.28	1.94	11.39	13.26	1.60	1.50	10.51	13.27
2.0	0.60	3	15	2.28	1.88	11.39	15.57	1.60	1.56	10.51	16.38
2.0	0.60	3	20	2.28	1.94	11.39	18.95	1.60	1.67	10.51	20.32
2.0	0.34	1	10	2.28	1.96	11.39	13.60	1.60	1.70	10.51	13.49
2.0	0.60	1	15	2.28	1.88	11.39	16.03	1.60	1.92	10.51	16.96
2.0	0.60	1	20	2.28	1.93	11.39	19.73	1.60	2.21	10.51	21.42

5.4 Comparison of All VSS Charts

The comparisons presented in the previous sections showed the advantages of VSS Shewhart, CUSUM, and EWMA charts compared with FSS analogues. This section compares the three types of VSS charts with one another. Table 5.7 contains the SSATS and SSANOS across a wide range of values of σ for the chart of each type that gives the quickest detection of a 50% increase in the process standard deviation. All charts have an average sample size of $n = 5$ and an ANSS of 500 when the process is in control.

The SSATS of the Shewhart chart is much greater than the SSATS of the CUSUM and EWMA charts when $\sigma < 1.4\sigma_0$. The EWMA chart has the smallest SSATS when the increase in the standard deviation is very small. The SSATS of all three charts are almost identical when $\sigma > 1.5\sigma_0$.

As expected, the SSANOS of all of the charts is large relative to the SSATS for all three charts when the process is not in control. The larger sample size may be used many times before a signal occurs. The EWMA chart has the smallest steady state ANOS in all cases.

Table 5.7: SSATS and ANOS for VSS Shewhart, CUSUM, and EWMA Charts

	Shewhart		CUSUM		EWMA	
	$n_1 = 2$	$n_2 = 20$	$n_1 = 2$	$n_2 = 20$	$n_1 = 3$	$n_2 = 16$
	$g = 0.8316$	$h = 0.998$	$g = 0.6332$	$h = 12.207$	$g = 1.953$	$h = 10.823$
$\frac{\sigma_1}{\sigma_0}$	SSATS	SSANOS	SSATS	SSANOS	SSATS	SSANOS
1.1	113.14	757.25	59.00	391.50	51.32	357.27
1.2	28.17	249.01	14.18	120.74	12.95	113.50
1.3	9.83	104.74	6.15	60.43	6.09	58.41
1.4	4.98	57.18	3.81	39.96	3.94	38.91
1.5	3.29	38.05	2.85	30.83	2.98	29.86
1.6	2.53	28.95	2.36	26.01	2.44	24.88
1.7	2.12	24.04	2.06	23.16	2.11	21.82
1.8	1.87	21.10	1.87	21.32	1.88	19.77
1.9	1.70	19.18	1.72	20.01	1.71	18.29
2.0	1.56	17.82	1.62	19.01	1.58	17.14
3.0	1.01	11.85	1.07	13.25	0.97	11.04

Chapter 6

Variable Sampling Interval Control Charts for Monitoring Process Variance

6.1 Variable Sampling Interval Shewhart Chart

6.1.1 Definition

It has previously been shown (see Reynolds et al. (1988)) that the use of two possible sampling intervals minimizes the ATS (but not necessarily the SSATS) of a VSI Shewhart chart for the mean of a normal distribution. Reynolds (1989) extended this result to VSI control charts for a general parameter for charts that can be represented with a Markov chain. A proof of the optimality of two sampling intervals for the special case of a VSI Shewhart chart for the variance is given in Appendix F.

Let d_1 be the longer time period and d_2 be the shorter. The choice of d_1 and d_2 in any particular application involves balancing the statistical concerns discussed here with the physical and economic limitations of the process and the sampling procedure.

For $k \geq 2$, let $d(k)$ be the time interval between sample $k-1$ and sample k and let $d(1)$ be

the time interval between the start of the process and the time the first sample is obtained. The initial sample could be taken after any arbitrary time period, but the chart is simplest if $d(1)$ is restricted to one of the two standard intervals (d_1 and d_2).

In a FSS VSI chart for monitoring variability, the distribution of T_k is the same at all sample times when σ is constant. Rescaling the observations to a probability scale is not strictly necessary, but we will do so to be consistent with the VSS charts presented earlier.

Intuitively, if the sample data observed at time $k-1$ indicate no evidence of an increase in the process variance, then it seems reasonable to wait longer before taking the next sample. Conversely, if the data at time $k-1$ provide some evidence of an increase in variability but insufficient evidence to signal, then perhaps the next sample should be taken after only a short time interval. Thus for $k \geq 2$ we define

$$d(k) = \begin{cases} d_1 & 0 < M_{n(k-1)}(T_{k-1}) < g \\ d_2 & g \leq M_{n(k-1)}(T_{k-1}) < h. \end{cases}$$

The chart signals at time $k-1$ if $M_{n(k-1)}(T_{k-1}) \geq h$.

The constants g and h determine the ATS for the VSI Shewhart chart. Figure 6.1 shows the correspondence between $d(k)$ and the plotted values on the control chart.

6.1.2 Evaluation Methods

The properties of the VSI Shewhart chart can be obtained from a simplification of the Markov chain method of Brook and Evans (1972). A direct derivation of the properties of the VSI Shewhart chart for the mean was given in Reynolds et al. (1988) and Runger and Pignatiello (1991). We will use a similar direct method to obtain the properties of the VSI Shewhart chart for the variance.

The distribution of $d(k)$ is conditional on $T_k < h$. Let $p = P(d(k) = d_1 \,|\, T_k < h)$ and let $q = P(d(k) = d_2 \,|\, T_k < h)$. Notice $p = \frac{g}{h}$ and $q = \frac{h-g}{h}$ when the process is in control. If $\sigma > \sigma_0$,

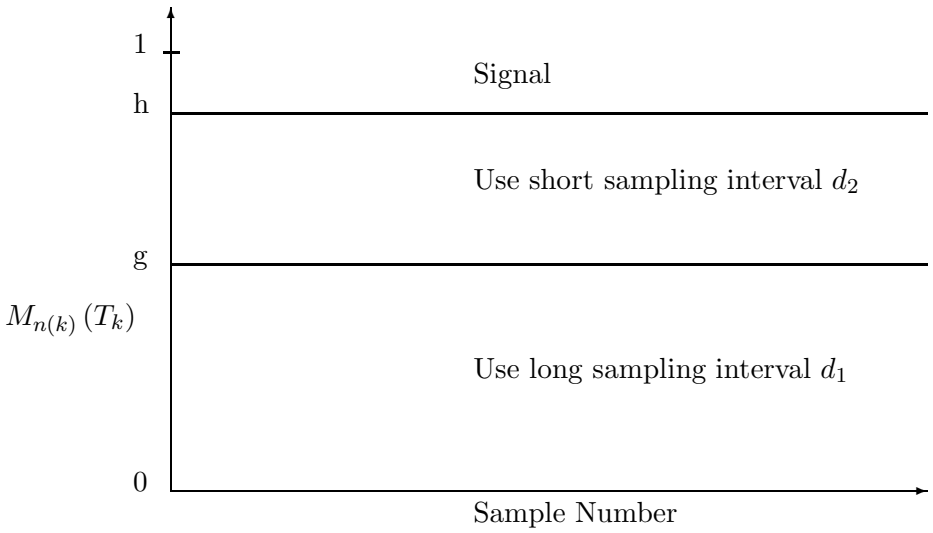

Figure 6.1: Control and Sampling Interval Limits for the VSI Shewhart Chart

$p < \frac{g}{h}$ and $q > \frac{h-g}{h}$. The chart responds to an increase in the process variance by using the shorter interval more often.

Let $N =$ the number of samples to signal. Then N has a geometric distribution with parameter $1 - p - q$ and

$$\text{ANSS} = E(N) = \frac{1}{1-p-q}. \tag{6.1}$$

Let $T =$ time to signal. Then

$$T = \begin{cases} d(1) & N = 1 \\ d(1) + \sum_{k=2}^{N} d(k) & N > 1 \end{cases}. \tag{6.2}$$

Using Wald's identity, the average time to signal is

$$\begin{aligned} \text{ATS} = E(T) &= d(1) + E(N-1)\, E(d(k) \mid T_k < h) && (6.3) \\ &= d(1) + \left(\frac{1}{1-p-q} - 1\right)\left(d_1 \frac{p}{p+q} + d_2 \frac{q}{p+q}\right) \\ &= d(1) + \left(\frac{1}{1-p-q}\right)(d_1 p + d_2 q). && (6.4) \end{aligned}$$

6.1.3 Choosing Chart Parameters

Suppose a VSI Shewhart chart is to be compared with a FSS-FSI Shewhart chart. Assume the sampling interval for the FSS-FSI chart is the unit time interval $d = 1$. We need to determine g and h such that the ATS and ANSS for the VSI chart is equivalent to the ATS and ANSS for the FSS-FSI chart.

Suppose the desired ANSS for the FSS-FSI chart is $ANSS_0$. The control limit should be set at $h = 1 - \frac{1}{ANSS_0}$ for both charts since the distribution of the chart statistic is the same in both cases.

The sampling interval limit g must be chosen so that the average time interval between samples is one time unit when the process is in control. The average time interval will be $d = 1$ if the sampling interval is

$$g = \frac{1 - d_2}{d_1 - d_2} h. \tag{6.5}$$

Since we assumed $d = 1$, the ATS of the FSS-FSI chart is $ANSS_0$ when the process is in control. The ATS of the VSI chart depends on the length of the initial sampling interval $d(1)$. For purposes of comparison with the FSS-FSI chart, we will assume the long interval d_1 is chosen with probability $\frac{g}{h}$ and the short interval d_2 is chosen with probability $\frac{h-g}{h}$. This implies the first interval is chosen randomly according to the same probabilities as all other intervals. Then the expected value of $d(1)$ is one, and the ATS of the VSI chart when the process is in control is

$$\begin{aligned} ATS &= 1 + \frac{d_1 g}{1-h} + \frac{d_2 (h-g)}{1-h} \\ &= 1 + \frac{d_1 \left(\frac{1-d_2}{d_1-d_2}\right) h}{1-h} + \frac{d_2 \left(h - \left(\frac{1-d_2}{d_1-d_2}\right) h\right)}{1-h} \\ &= 1 + \frac{h}{1-h} \\ &= ANSS_0. \end{aligned}$$

This establishes that choosing g and h as described above ensures the VSI chart has the same ATS and ANSS as the FSS-FSI chart when the process is in control.

6.1.4 Steady State Properties

Suppose the process operates with $\sigma = \sigma_0$ for some period of time and suppose the process variance increases to $\sigma_1 > \sigma_0$ at some random time. Under the assumptions in Section 3.1.2, the expected time of the change in the process is $\frac{d_i}{2}$ if the change occurs in an interval of length d_i.

Let T_0 = the interval between the increase in σ and the next sample. Then the steady state ATS is

$$SSATS = E(T_0) + \left(\frac{1}{1-p-q}\right)(d_1 p + d_2 q) \tag{6.6}$$

where p and q are the previously defined sampling interval probabilities. The SSATS is simply the expression for the ATS with the initial unit time interval replaced with the expected value of time interval between the increase in σ and the next sample.

The expected value of T_0 is calculated using the distribution of $d(k)$ when the process is in control. Conditional on no signal at the previous sampling time, $T_0 = \frac{d_1}{2}$ with probability $d_1 \frac{g}{h}$ and $T_0 = \frac{d_2}{2}$ with probability $d_2 \frac{h-g}{h}$. Then the expected time between the change in the process and the first sample is

$$\begin{aligned} E(T_0) &= d_1^2 \frac{g}{2h} + d_2^2 \left(\frac{h-g}{2h}\right) \\ &= \frac{d_1^2}{2}\left(\frac{1-d_2}{d_1-d_2}\right) + \frac{d_2^2}{2}\left(1 - \frac{1-d_2}{d_1-d_2}\right) \\ &= \frac{d_1 + d_2 - d_1 d_2}{2}. \end{aligned} \tag{6.7}$$

Substituting (6.7) into (6.6) gives

$$SSATS = \frac{d_1 + d_2 - d_1 d_2}{2} + \left(\frac{1}{1-p-q}\right)(d_1 p + d_2 q). \tag{6.8}$$

6.1.5 Comparison with FSS-FSI and VSS-FSI Charts

The VSI Shewhart chart should give much quicker detection of small increases in process variance than the FSS-FSI Shewhart chart. The ATS and SSATS of the VSI Shewhart chart were evaluated

for $d_1 \in \{1.05, 1.10, \ldots, 6.00\}$,$d_2 \in \{0.10, 0.20, \ldots, 0.90\}$, and for $\sigma \in \{\sigma_0, 1.1\sigma_0, 1.2\sigma_0 \ldots, 2\sigma_0, 3\sigma_0\}$.

Table 6.1 shows what sampling interval combinations gave the smallest SSATS at each value of σ. The best VSS-FSI chart is included to give a more complete comparison.

Table 6.1: Minimum SSATS for VSI Shewhart Charts with $n = 5$

	FSS-FSI	VSS-FSI			FSS-VSI		
$\frac{\sigma}{\sigma_0}$	SSATS	n_1	n_2	SSATS	d_1	d_2	SSATS
1.1	124.54	2	20	113.14	6.00	0.10	93.53
1.2	44.57	1	20	27.85	5.30	0.10	27.13
1.3	20.43	1	20	9.76	3.55	0.10	10.97
1.4	11.14	2	20	4.98	2.60	0.10	5.62
1.5	6.89	2	20	3.29	2.05	0.10	3.41
1.6	4.67	3	20	2.49	1.75	0.10	2.34
1.7	3.39	3	20	2.04	1.55	0.10	1.76
1.8	2.60	4	18	1.75	1.45	0.10	1.41
1.9	2.08	4	16	1.52	1.35	0.10	1.19
2.0	1.72	4	14	1.35	1.25	0.10	1.04
3.0	0.70	4	6	0.70	1.20	0.10	0.91

The SSATS of the best VSI chart is much lower than the SSATS of the FSS-FSI interval chart for all values of σ except $\sigma = 3\sigma_0$. The SSATS of the best VSS chart is slightly less than the SSATS of the best VSI chart when the increase in σ is small or moderate, but the relationship is reversed when the increase in σ is very large or very small. The differences between the best VSI chart and the best VSS chart are small in most instances.

The best value of d_2 is 0.10 (the smallest possible value) in all cases. Large values of d_1 are better for detecting small increases in the variance but small values of d_1 are better for detecting large increases. If a large value of d_1 is used and the variance increases during a long sampling interval, then a long period of time passes before the next sample is taken. Obviously, the increase in variance will not be detected during the period between the increase and the time of the next sample. A good compromise value is $d_1 = 1.9$. Choosing the interval lengths symmetrically about one means that each interval length will be used equally often when the process is in control.

Table 6.2 gives the ATS and SSATS for VSI Shewhart charts with $d_1 \in \{1.1, 1.5, 1.9, 2.0, 3.0, 5.0\}$ and $d_2 \in \{0.1, 0.5\}$ at several values of σ. The results at a particular value of σ are sorted by the

SSATS of the VSI charts. The ATS of a FSS-FSI chart is included for comparison. (The SSATS of the FSS-FSI chart can be found by subtracting one half from the ATS.) All of the charts use samples of $n = 5$ and have an in control ATS of 500.

The ATS of the VSI charts is lower than the ATS of the FSS-FSI chart for all values of d_1 and d_2 and all values of σ. The SSATS of the VSI charts is lower than the SSATS of the FSS-FSI chart except when the increase in σ is very large and the VSI uses a large value of d_2.

Table 6.2: ATS and SSATS for VSI Shewhart Charts with $n = 5$

			FSS-FSI	FSS-VSI	
$\frac{\sigma}{\sigma_0}$	d_1	d_2	SSATS	ATS	SSATS
1.2	5.0	0.1	44.57	25.39	27.69
1.2	3.0	0.1	44.57	27.06	28.46
1.2	2.0	0.1	44.57	29.24	30.19
1.2	1.9	0.1	44.57	29.61	30.52
1.2	1.5	0.1	44.57	31.86	32.58
1.2	5.0	0.5	44.57	33.56	35.06
1.2	3.0	0.5	44.57	34.26	35.26
1.2	2.0	0.5	44.57	35.23	35.98
1.2	1.9	0.5	44.57	35.40	36.12
1.2	1.5	0.5	44.57	36.48	37.10
1.2	1.1	0.1	44.57	38.11	38.65
1.2	1.1	0.5	44.57	40.01	40.53
1.5	2.0	0.1	6.89	2.85	3.80
1.5	1.9	0.1	6.89	2.91	3.82
1.5	3.0	0.1	6.89	2.51	3.91
1.5	1.5	0.1	6.89	3.31	4.03
1.5	5.0	0.1	6.89	2.27	4.57
1.5	1.1	0.1	6.89	4.69	5.24
1.5	2.0	0.5	6.89	4.70	5.45
1.5	1.9	0.5	6.89	4.73	5.45
1.5	1.5	0.5	6.89	4.90	5.53
1.5	3.0	0.5	6.89	4.56	5.56
1.5	5.0	0.5	6.89	4.47	5.97
1.5	1.1	0.5	6.89	5.59	6.12
1.8	1.5	0.1	2.60	1.02	1.74
1.8	1.9	0.1	2.60	0.88	1.79
1.8	2.0	0.1	2.60	0.86	1.81
1.8	1.1	0.1	2.60	1.57	2.11
1.8	3.0	0.1	2.60	0.75	2.15
1.8	1.5	0.5	2.60	1.87	2.49
1.8	1.9	0.5	2.60	1.81	2.54
1.8	2.0	0.5	2.60	1.80	2.55
1.8	1.1	0.5	2.60	2.12	2.65
1.8	3.0	0.5	2.60	1.76	2.76
1.8	5.0	0.1	2.60	0.68	2.98
1.8	5.0	0.5	2.60	1.73	3.23
2.0	1.5	0.1	1.72	0.63	1.36
2.0	1.9	0.1	1.72	0.55	1.45
2.0	2.0	0.1	1.72	0.53	1.48
2.0	1.1	0.1	1.72	1.00	1.55
2.0	3.0	0.1	1.72	0.47	1.87
2.0	1.5	0.5	1.72	1.29	1.92
2.0	1.9	0.5	1.72	1.26	1.98
2.0	1.1	0.5	1.72	1.46	1.98
2.0	2.0	0.5	1.72	1.25	2.00
2.0	3.0	0.5	1.72	1.23	2.23
2.0	5.0	0.5	1.72	1.21	2.71
2.0	5.0	0.1	1.72	0.42	2.72

6.2 Variable Sampling Interval CUSUM Chart

6.2.1 Definition

Any of the CUSUM charts considered in Section 4.4 can be modified to allow variable sampling intervals. A VSI CUSUM chart based on T_k will be considered here since it was shown in Section 4.4 that the FSS-FSI CUSUM chart based on T_k performs better than the CUSUM charts based on transformed statistics.

Consider a FSS CUSUM chart defined by $Y_k = max\{0, Y_{k-1}\} + T_k + \gamma$. Let $d(k)$ be the time interval between sample $k-1$ and sample k. Then for $k \geq 2$

$$d(k) = \begin{cases} d_1 & Y_{k-1} < g \\ d_2 & g \leq Y_{k-1} < h. \end{cases}$$

The chart signals at time $k-1$ if $Y_{k-1} \geq h$.

6.2.2 Evaluation of Properties and Comparison with FSI CUSUM Charts

The ANSS for a VSI CUSUM chart will be the same as the ANSS for a FSI CUSUM chart that uses the same sample size. The ATS for a VSI CUSUM chart will not, in general, be the same as the ATS for a corresponding FSI CUSUM chart. The Markov chain-integral equation method for calculating the ANSS for FSS-FSI CUSUM or EWMA charts that is outlined in Appendix A can be modified to calculate the ATS and steady state ATS for VSI CUSUM charts. The mathematical details of the evaluation methods are given in Appendix C.

The ATS of a VSI chart obviously depends on the length of time that is allowed to pass before the first sample is taken. The SSATS of a VSI CUSUM or EWMA chart also depends on the choice of the initial interval since the control limit for a chart that always uses the shorter interval initially will be slightly larger than the control limit for a chart that always uses the long sampling interval first if both charts are to have the same ATS when the process is in control. The differences in SSATS are usually extremely small. Unless otherwise noted, all results presented in this dissertation were calculated under the assumption that $d(0) = 1$.

A VSI CUSUM chart should give quicker detection of small and moderate increases in variability than a FSS-FSI CUSUM chart. The variable sampling rate charts will be compared to a FSS-FSI chart that uses samples of size $n = 5$ taken $d = 1$ time unit apart.

Table 6.3 shows what combination of sampling intervals minimizes the SSATS of the VSI CUSUM chart at each value of $\frac{\sigma}{\sigma_0}$. The SSATS was minimized over all combinations of $d_2 \in \{0.1, 0.5\}$ and $d_1 \in \{1.1, 1.5, 1.9, 2.0, 3.0, 5.0\}$. The control limits and sampling limits were chosen so that the ANSS and ATS of all charts is 500 when $\sigma = \sigma_0$. At a particular value of σ, all charts are optimized to detect an increase from σ_0 to σ. The best VSS CUSUM chart from Table 5.3 is included for comparison.

Table 6.3: Minimum SSATS for VSI CUSUM Charts with $n = 5$

	FSS-FSI	VSS			VSI				
$\frac{\sigma_1}{\sigma_0}$	SSATS	n_1	n_2	SSATS	d_1	d_2	g	h	SSATS
1.1	41.84	2	20	26.39	5.0	0.1	-1.2624	33.0684	21.93
1.2	16.91	2	20	9.60	3.0	0.1	-1.2963	23.9645	7.55
1.3	9.13	2	20	5.41	2.0	0.1	-0.8401	19.5992	4.07
1.4	5.96	2	20	4.21	1.9	0.1	-1.5088	16.9644	2.68
1.5	4.27	3	20	2.84	1.7	0.1	-1.5125	15.1678	2.03
1.6	3.24	3	17	2.30	1.5	0.1	-1.3942	13.8449	1.61
1.7	2.57	3	15	1.94	1.5	0.1	-1.9697	12.8123	1.35
1.8	2.10	3	13	1.69	1.3	0.1	-1.2551	11.9696	1.17
1.9	1.77	4	13	1.49	1.3	0.1	-1.7500	11.2582	1.04
2	1.52	4	12	1.33	1.3	0.1	-2.2107	10.6418	0.94
3	0.69	4	6	0.70	1.1	0.1	-3.0661	6.6874	0.61

The SSATS of the best VSI chart is much smaller than the SSATS of the FSS-FSI chart for all values of σ. The decrease in SSATS is about 50% when $1.1\sigma_0 \leq \sigma \leq 1.6\sigma_0$. The VSI CUSUM chart is significantly better than the VSS CUSUM chart at all values of σ.

In this example, the shorter interval should always be chosen at the smaller value of 0.1. A large value of the longer interval is best for detecting small increases in the variance and a small value of the longer interval is best for detecting large increases.

Table 6.4 gives the ATS and SSATS of all VSI charts used in the comparison above at several values of σ. The VSI charts have lower ATS and SSATS values than the FSS-FSI chart in most

cases, but there are large differences among the VSI charts. The combination $d_1 = 1.5$ and $d_2 = 0.1$ performs well in most cases.

The combination of $d_1 = 5.0$ and $d_2 = 0.1$ has the smallest ATS for all values of σ but not smallest SSATS for any value of σ. The same behavior was observed with VSI Shewhart charts. A large value of d_1 hurts the steady state performance of the chart, particularly when the increase in σ is large.

Table 6.4: ATS and SSATS for VSI CUSUM Charts with $n = 5$

$\frac{\sigma_1}{\sigma_0}$	d_1	d_2	g	h	ATS		SSATS	
					FSS-FSI	FSS-VSI	FSS-FSI	FSS-VSI
1.2	3.0	0.1	-3.6875	15.1668	10.04	22.59	21.59	10.40
1.2	5.0	0.1	-4.6875	15.1668	9.31	22.59	21.59	10.57
1.2	2.0	0.1	-2.3602	15.1668	11.08	22.59	21.59	10.98
1.2	1.9	0.1	-2.1289	15.1668	11.27	22.59	21.59	11.13
1.2	1.5	0.1	-0.7062	15.1668	12.45	22.59	21.59	12.13
1.2	3.0	0.5	-4.5547	15.1668	15.25	22.59	21.59	15.02
1.2	2.0	0.5	-3.5074	15.1668	15.68	22.59	21.59	15.20
1.2	5.0	0.5	-5.3166	15.1668	14.96	22.59	21.59	15.23
1.2	1.9	0.5	-3.3197	15.1668	15.76	22.59	21.59	15.25
1.2	1.5	0.5	-2.1285	15.1668	16.28	22.59	21.59	15.67
1.2	1.1	0.1	3.9384	15.1668	16.44	22.59	21.59	15.82
1.2	1.1	0.5	2.1700	15.1668	18.32	22.59	21.59	17.58
1.5	1.5	0.1	-0.7062	15.1668	2.33	4.95	4.27	2.04
1.5	1.9	0.1	-2.1289	15.1668	2.15	4.95	4.27	2.04
1.5	2.0	0.1	-2.3602	15.1668	2.13	4.95	4.27	2.06
1.5	3.0	0.1	-3.6875	15.1668	1.98	4.95	4.27	2.37
1.5	1.1	0.1	3.9384	15.1668	3.05	4.95	4.27	2.52
1.5	1.5	0.5	-2.1285	15.1668	3.40	4.95	4.27	2.94
1.5	1.9	0.5	-3.3197	15.1668	3.32	4.95	4.27	2.97
1.5	2.0	0.5	-3.5074	15.1668	3.31	4.95	4.27	2.99
1.5	1.1	0.5	2.1700	15.1668	3.73	4.95	4.27	3.16
1.5	5.0	0.1	-4.6875	15.1668	1.89	4.95	4.27	3.18
1.5	3.0	0.5	-4.5547	15.1668	3.26	4.95	4.27	3.19
1.5	5.0	0.5	-5.3166	15.1668	3.22	4.95	4.27	3.65
1.8	1.5	0.1	-0.7062	15.1668	1.49	2.73	2.13	1.21
1.8	1.1	0.1	3.9384	15.1668	1.79	2.73	2.13	1.30
1.8	1.9	0.1	-2.1289	15.1668	1.42	2.73	2.13	1.32
1.8	2.0	0.1	-2.3602	15.1668	1.41	2.73	2.13	1.36
1.8	1.5	0.5	-2.1285	15.1668	2.00	2.73	2.13	1.59
1.8	1.1	0.5	2.1700	15.1668	2.13	2.73	2.13	1.61
1.8	1.9	0.5	-3.3197	15.1668	1.97	2.73	2.13	1.66
1.8	2.0	0.5	-3.5074	15.1668	1.97	2.73	2.13	1.68
1.8	3.0	0.1	-3.6875	15.1668	1.36	2.73	2.13	1.75
1.8	3.0	0.5	-4.5547	15.1668	1.95	2.73	2.13	1.92
1.8	5.0	0.5	-5.3166	15.1668	1.94	2.73	2.13	2.40
1.8	5.0	0.1	-4.6875	15.1668	1.33	2.73	2.13	2.62
2.0	1.1	0.1	3.9384	15.1668	1.49	2.14	1.57	1.01
2.0	1.5	0.1	-0.7062	15.1668	1.30	2.14	1.57	1.02
2.0	1.9	0.1	-2.1289	15.1668	1.26	2.14	1.57	1.16
2.0	2.0	0.1	-2.3602	15.1668	1.25	2.14	1.57	1.20
2.0	1.1	0.5	2.1700	15.1668	1.74	2.14	1.57	1.23
2.0	1.5	0.5	-2.1285	15.1668	1.65	2.14	1.57	1.25
2.0	1.9	0.5	-3.3197	15.1668	1.63	2.14	1.57	1.34
2.0	2.0	0.5	-3.5074	15.1668	1.63	2.14	1.57	1.36
2.0	3.0	0.5	-4.5547	15.1668	1.62	2.14	1.57	1.60
2.0	3.0	0.1	-3.6875	15.1668	1.22	2.14	1.57	1.62
2.0	5.0	0.5	-5.3166	15.1668	1.61	2.14	1.57	2.09
2.0	5.0	0.1	-4.6875	15.1668	1.20	2.14	1.57	2.50

6.3 Variable Sampling Interval EWMA Chart

6.3.1 Definition

Variable sampling intervals can be added to any of the EWMA charts considered in Section 4.5. A VSI EWMA chart based on N_k will be defined here since the FSS-FSI EWMA chart based on N_k performs better than the EWMA charts that use transformed statistics.

Define the chart statistic at time k by

$$Y_k = \begin{cases} \lambda N_k + max\{0, (1-\lambda) Y_{k-1}\} & k \geq 1 \\ 0 & k = 0 \end{cases}.$$

Let $d(k)$ be the time interval between sample $k-1$ and sample k. Then for $k \geq 2$

$$d(k) = \begin{cases} d_1 & Y_{k-1} < g \\ d_2 & g \leq Y_{k-1} < h. \end{cases}$$

The chart signals at time $k-1$ if $Y_{k-1} \geq h$.

6.3.2 Evaluation of Properties and Comparison with FSI EWMA Charts

The ANSS of a VSI EWMA chart will be the same as the ANSS of a FSS-FSI EWMA chart with the same control limit. The ATS of a VSI EWMA chart is a function of d_1, d_2, and the sampling interval limit g. The evaluation methods used to find the ATS and SSATS are similar to the methods used for the VSI CUSUM chart. See Appendix C for details.

Like the VSI CUSUM chart, the ATS, and to a much lesser extent, the SSATS of the VSI EWMA chart depend on the initial sampling interval. The initial sampling interval was chosen to be the unit time interval $d = 1$ for all calculations reported in this dissertation.

It is expected that the VSI EWMA chart will detect small increases in σ much faster than the FSS-FSI EWMA chart. The VSI EWMA chart will be compared with an FSS-FSI EWMA chart that uses samples of size $n = 5$ that are taken $d = 1$ time unit apart.

Table 6.5 shows what combination of sampling intervals minimizes the SSATS of the VSI EWMA chart at each value of $\frac{\sigma}{\sigma_0}$. The SSATS was minimized over all combinations of $d_2 \in \{0.1, 0.5\}$ and $d_1 \in \{1.1, 1.5, 1.9, 2.0, 3.0, 5.0\}$ and for $\lambda \in \{0.10, 0.11, \ldots 0.60\}$. The control limits and sampling limits were chosen so that the ANSS and ATS of all charts is 500 when the process is in control. The best VSS EWMA chart from Table 5.5 is included for comparison.

Table 6.5: Minimum SSATS for VSI EWMA Charts with $n = 5$

	FSS-FSI		VSS				VSI					
$\frac{\sigma_1}{\sigma_0}$	λ	SSATS	λ	n_1	n_2	SSATS	λ	d_1	d_2	g	h	SSATS
1.1	0.02	41.34	0.15	1	20	26.61	0.10	5.0	0.1	-0.0992	2.3021	27.07
1.2	0.04	16.11	0.28	2	20	9.85	0.11	3.0	0.1	0.0437	2.4628	7.85
1.3	0.08	9.03	0.48	2	20	5.64	0.15	1.9	0.1	0.3128	3.0642	4.25
1.4	0.13	5.92	0.60	3	19	3.89	0.23	1.9	0.1	0.3096	4.1754	2.82
1.5	0.17	4.24	0.60	3	16	2.98	0.23	1.5	0.1	0.6959	4.7044	2.08
1.6	0.21	3.22	0.60	3	14	2.43	0.32	1.5	0.1	0.7224	5.3510	1.65
1.7	0.25	2.56	0.60	4	12	2.05	0.40	1.5	0.1	0.7430	6.3668	1.38
1.8	0.29	2.10	0.60	4	11	1.77	0.46	1.5	0.1	0.7460	7.1200	1.21
1.9	0.33	1.77	0.60	4	10	1.56	0.52	1.5	0.1	0.7401	7.8700	1.09
2.0	0.38	1.53	0.60	4	9	1.39	0.44	1.1	0.1	2.4941	6.8695	0.98
3.0	0.60	0.69	0.60	4	7	0.73	0.60	1.1	0.1	2.9923	8.8687	0.61

As expected, choosing d_1 and d_2 far apart is best when the increase in σ is small but the best combination of d_1 and d_2 is closer together when the increase in σ is large. The same general trend was observed with VSI Shewhart and VSI CUSUM charts.

At a particular value of σ, the optimal value of λ for a VSI EWMA chart is slightly larger than the best value of λ for a FSS-FSI chart but much smaller than the optimal value of λ for a VSS EWMA chart.

The best VSI EWMA chart is significantly better than the best VSS EWMA chart at all values of σ. Both VSR charts detect small to moderate increases in σ much quicker than the FSS-FSI EWMA chart. The SSATS of the best VSI EWMA chart is approximately 50% of the SSATS of the FSS-FSI chart when σ is between $1.2\sigma_0$ and $1.8\sigma_0$.

Table 6.6 contains the ATS and SSATS for several values of σ for the VSI charts used in the minimization above. All charts are optimized to detect a 50% increase in σ. The ATS and SSATS of

the VSI charts is smaller than the corresponding ATS and SSATS of the FSS-FSI chart in virtually all cases. The exceptions occur at large values of σ. The FSS-FSI chart is better at detecting very large increases in variability than a VSI chart with poorly chosen chart parameters.

Large differences exist among the various VSI charts. The combination $d_1 = 1.5$ and $d_2 = 0.1$ gives good performance in all cases.

Table 6.6: ATS and SSATS for VSI EWMA Charts with $n = 5$

$\frac{\sigma_1}{\sigma_0}$	d_1	d_2	λ	g	h	ATS		SSATS	
						FSS-FSI	FSS-VSI	FSS-FSI	FSS-VSI
1.2	1.5	0.1	0.23	0.6676	4.1754	21.28	11.89	19.74	11.37
1.2	3.0	0.1	0.33	-0.2704	5.4789	21.28	11.05	19.74	11.38
1.2	5.0	0.1	0.35	-0.6836	5.7343	21.28	10.38	19.74	11.61
1.2	2.0	0.1	0.30	0.2093	5.0938	21.28	11.84	19.74	11.70
1.2	1.9	0.1	0.30	0.2816	5.0938	21.28	12.10	19.74	11.91
1.2	1.1	0.1	0.16	1.4143	3.2088	21.28	14.49	19.74	13.27
1.2	1.9	0.5	0.19	0.0387	3.6312	21.28	14.59	19.74	13.79
1.2	3.0	0.5	0.21	-0.3000	3.9044	21.28	14.57	19.74	14.07
1.2	1.5	0.5	0.19	0.3147	3.6312	21.28	15.13	19.74	14.20
1.2	2.0	0.5	0.21	-0.0276	3.9044	21.28	15.00	19.74	14.27
1.2	5.0	0.5	0.21	-0.5039	3.9044	21.28	14.28	19.74	14.28
1.2	1.1	0.5	0.16	1.1120	3.2088	21.28	16.47	19.74	15.15
1.5	1.5	0.1	0.23	0.6676	4.1754	5.16	2.46	4.24	2.08
1.5	1.9	0.1	0.30	0.2816	5.0938	5.16	2.25	4.24	2.12
1.5	2.0	0.1	0.30	0.2093	5.0938	5.16	2.23	4.24	2.14
1.5	3.0	0.1	0.33	-0.2704	5.4789	5.16	2.08	4.24	2.46
1.5	1.1	0.1	0.16	1.4143	3.2088	5.16	3.27	4.24	2.49
1.5	1.5	0.5	0.19	0.3147	3.6312	5.16	3.58	4.24	3.00
1.5	1.9	0.5	0.19	0.0387	3.6312	5.16	3.51	4.24	3.05
1.5	2.0	0.5	0.21	-0.0276	3.9044	5.16	3.48	4.24	3.06
1.5	1.1	0.5	0.16	1.1120	3.2088	5.16	3.96	4.24	3.14
1.5	3.0	0.5	0.21	-0.3000	3.9044	5.16	3.43	4.24	3.26
1.5	5.0	0.1	0.35	-0.6836	5.7343	5.16	1.99	4.24	3.27
1.5	5.0	0.5	0.21	-0.5039	3.9044	5.16	3.39	4.24	3.72
1.8	1.5	0.1	0.23	0.6676	4.1754	2.90	1.59	2.16	1.26
1.8	1.1	0.1	0.16	1.4143	3.2088	2.90	1.98	2.16	1.35
1.8	1.9	0.1	0.30	0.2816	5.0938	2.90	1.48	2.16	1.37
1.8	2.0	0.1	0.30	0.2093	5.0938	2.90	1.47	2.16	1.40
1.8	1.5	0.5	0.19	0.3147	3.6312	2.90	2.13	2.16	1.65
1.8	1.1	0.5	0.16	1.1120	3.2088	2.90	2.32	2.16	1.66
1.8	1.9	0.5	0.19	0.0387	3.6312	2.90	2.10	2.16	1.73
1.8	2.0	0.5	0.21	-0.0276	3.9044	2.90	2.07	2.16	1.74
1.8	3.0	0.1	0.33	-0.2704	5.4789	2.90	1.41	2.16	1.80
1.8	3.0	0.5	0.21	-0.3000	3.9044	2.90	2.05	2.16	1.96
1.8	5.0	0.5	0.21	-0.5039	3.9044	2.90	2.04	2.16	2.45
1.8	5.0	0.1	0.35	-0.6836	5.7343	2.90	1.37	2.16	2.66
2.0	1.1	0.1	0.16	1.4143	3.2088	2.28	1.64	1.60	1.06
2.0	1.5	0.1	0.23	0.6676	4.1754	2.28	1.37	1.60	1.06
2.0	1.9	0.1	0.30	0.2816	5.0938	2.28	1.30	1.60	1.19
2.0	2.0	0.1	0.30	0.2093	5.0938	2.28	1.29	1.60	1.23
2.0	1.1	0.5	0.16	1.1120	3.2088	2.28	1.88	1.60	1.27
2.0	1.5	0.5	0.19	0.3147	3.6312.0	2.28	1.75	1.60	1.30
2.0	1.9	0.5	0.19	0.0387	3.6312.0	2.28	1.73	1.60	1.39
2.0	2.0	0.5	0.21	-0.0276	3.9044	2.28	1.71	1.60	1.40
2.0	3.0	0.5	0.21	-0.3000	3.9044	2.28	1.69	1.60	1.63
2.0	3.0	0.1	0.33	-0.2704	5.4789	2.28	1.25	1.60	1.64
2.0	5.0	0.5	0.21	-0.5039	3.9044	2.28	1.68	1.60	2.12
2.0	5.0	0.1	0.35	-0.6836	5.7343	2.28	1.23	1.60	2.52

6.4 Comparison of All VSI Charts

The three previous sections compared VSI Shewhart, CUSUM, and EWMA charts with the corresponding FSS-FSI charts. This section gives side by side comparisons of the three VSI charts. Table 6.4 gives the SSATS for several values of σ for the sampling interval combination that minimizes the SSATS when $\sigma = 1.5\sigma_0$. All charts have an average sampling interval of $d = 1$, an average sample size of $n = 5$, and an ATS of 500 when the process is in control.

The EWMA and CUSUM charts give much quicker detection of small increases in the process standard deviation. The VSI CUSUM chart is slightly better than the VSI EWMA chart at most values of σ, but the differences are very small in most cases. The choice between the VSI CUSUM chart and the VSI EWMA chart could be made simply by the preference of the user.

Table 6.7: SSATS for VSI Shewhart, CUSUM, and EWMA Charts

	Shewhart $d_1 = 2$ $d_2 = 0.1$ $g = 0.472737$ $h = 0.998$	CUSUM $d_1 = 1.7$ $d_2 = 0.1$ $g = -1.5470$ $h = 15.1668$	EWMA $d_1 = 1.5$ $d_2 = 0.1$ $g = 0.6959$ $h = 4.7044$ $\lambda = 0.23$
$\frac{\sigma_1}{\sigma_0}$	SSATS	SSATS	SSATS
1.1	101.26	52.06	55.78
1.2	30.19	11.51	12.45
1.3	12.12	4.70	4.98
1.4	6.17	2.79	2.91
1.5	3.80	2.02	2.08
1.6	2.70	1.63	1.66
1.7	2.13	1.41	1.41
1.8	1.81	1.26	1.24
1.9	1.61	1.16	1.13
2.0	1.48	1.09	1.05
3.0	1.16	0.86	0.78

Chapter 7

Simultaneous Monitoring of Process Mean and Variance

A control chart for monitoring the variance is used in conjunction with a separate control chart for monitoring the mean of the process in most applications. This combination of two charts is used to detect changes in the level or the consistency of the output of the process that lead to reduced quality. A signal of a change in the process is given at sample time k if either chart signals at time k. Dual process monitoring schemes are often used in practice without any explicit consideration of the joint properties of the two charts. For example, the simple scheme consisting of a FSS-FSI Shewhart $\bar{X}$-chart for the mean and a FSS-FSI Shewhart R-chart for the variance is widely used in industry. The charts are usually designed separately, and the true false alarm rate of the joint scheme is often not known by the user.

Some background information about control charts for monitoring the mean is given below. This is followed by some general comments about the nature of joint mean and variance monitoring schemes and a discussion of several possible methods. The remainder of this section is devoted to the application of variable sampling rate features to a joint monitoring procedure that uses a two-sided EWMA chart for the mean and a two-sided EWMA chart for the variance.

A two-sided Shewhart $\bar{X}$-chart is simply a plot of the standardized sample mean M_k defined by (1.3) versus the sample times or sample numbers. The chart signals a change in the mean if

$M_k < LCL$ or $M_k > UCL$ where LCL and UCL are the lower control limit and upper control limit of the chart, respectively. Traditionally, the control limits are defined by $LCL = \mu_0 - 3\frac{\sigma_0}{\sqrt{n}}$ and $UCL = \mu_0 + 3\frac{\sigma_0}{\sqrt{n}}$.

The usual two-sided EWMA chart for the mean is defined by substituting M_k for Q_k in (3.6). A one-sided CUSUM chart for detecting a change in the mean is defined by substituting M_k for Q_k in (3.1).

The standardized sample mean $M_k \sim N\left(\mu - \mu_0, \frac{\sigma}{\sigma_0}^2\right)$. In particular, M_k has a standard normal distribution when the process is in control ($\mu = \mu_0$ and $\sigma = \sigma_0$).

Simultaneous monitoring of mean and variance brings some new complications as listed below.

1. A change in one parameter may affect the performance of the chart for the other parameter. For example, the distribution of M_k depends on the true process variance.

2. Interpreting a signal is more difficult when two parameters are being monitored. This is related to the dependency discussed above. For example, if the variance increases, the chart for the mean may signal before the chart for the variance even if the mean remains constant.

3. Evaluating the joint properties of the two charts is much more difficult than evaluating the properties of the two separate charts. The joint behavior of the two charts can be approximated by a discrete Markov process by extending the techniques of Brook and Evans (1972). However, obtaining reasonable accuracy requires a very large number of states in the discrete Markov chain. This method is not practical with current computational capability. We will extend the method of Reynolds (1995) to evaluate the joint properties of the two charts.

4. Designing a dual monitoring scheme can be much more difficult than designing a chart for a single parameter. Ideally, a method for simultaneous monitoring of mean and variance should give quick detection of a wide range of changes in μ and σ. Obtaining such a chart may require adjusting many chart parameters. For example, a dual monitoring scheme that uses a two-sided FSS-FSI EWMA chart for the mean and a two-sided FSS-FSI EWMA chart for the variance has six chart parameters that must be specified by the user (λ, the UCL, and the LCL for each chart). The performance of each combination must then be evaluated.

As noted above, this is generally so computationally intensive that only a few cases can be evaluated. Gan (1995) recommended designing each chart separately and then evaluating the joint behavior. This method can be used to design dual monitoring schemes that perform fairly well, but determining the best choice of chart parameters is impossible using this procedure.

7.1 Dual Monitoring Schemes

In most applications, it is important to detect any type of change in the mean. All of the dual monitoring methods considered here employ a two-sided chart for the mean. Detection of increases in variability is generally considered to be more important than detection of decreases, and one-sided charts for detecting increases in variability are often employed. When the mean is also being monitored, it is important to note that a decrease in variability may adversely affect the performance of the control chart for the mean. Thus a two-sided chart for the variance is more attractive in the dual monitoring setting. An almost limitless number of dual monitoring control chart combinations are possible, but we will restrict this discussion to the schemes that are most logical and likely to be encountered in practice:

1. Two-sided Shewhart $\bar{X}$-chart and a Shewhart S-chart
2. Two one-sided CUSUM charts for the mean and one or two one-sided CUSUM charts for the variance
3. Two-sided EWMA chart for the mean and one or two one-sided EWMA charts for the variance
4. Two-sided EWMA chart for the mean and a two-sided EWMA chart for the variance, denoted by EE

Like Shewhart charts for a single parameter, Shewhart schemes for simultaneously monitoring the mean and variance will not quickly detect small changes in the parameters. We will use the Shewhart methods only as a basis for comparison with more efficient techniques.

Designing a dual monitoring method that uses two one-sided CUSUM charts for the mean and one or two one-sided CUSUM charts for the variance is quite complex since parameters for three

or four separate charts must be specified. A scheme that uses a two-sided EWMA chart for the mean and two one-sided EWMA charts for the variance also requires the design of three separate charts. The extra complication involved outweighs any other advantages offered by these methods.

It was noted above that a dual monitoring method that is not sensitive to decreases in variability can perform badly. In particular, such schemes perform poorly when there is a decrease in variability and a simultaneous small change in the mean (see Gan (1995)).

Method EE is relatively simple to implement and evaluate, and it is not adversely affected by decreases in variability. We will concentrate on methods that use two two-sided EWMA charts.

The EWMA chart for the mean will be based on M_k. A two-sided EWMA chart for the variance could be based on any of the statistics considered in Section 4.5, but the design and evaluation of the EE scheme is greatly simplified by using the statistic Z_k defined in (4.4). The control limits of a two-sided EWMA chart for the variance that uses Z_k are identical to the control limits of a two-sided EWMA chart for the mean based on M_k when the process is in control. Also, the control limits of both charts can be set symmetrically around zero since the in-control distribution of the test statistic is symmetric. Thus only four chart parameters must be specified:

$$\begin{aligned} \lambda_m &= \lambda \text{ for the mean chart} \\ \lambda_v &= \lambda \text{ for the variance chart} \\ h_m &= \text{UCL for the mean chart} \\ h_v &= \text{UCL for the variance chart.} \end{aligned}$$

We will choose $\lambda_m = \lambda_v = \lambda$ and $h_m = h_v$ to simplify the design process even further. With this assumption, a complete EE scheme for monitoring the variance can be designed by specifying only two chart parameters. It is possible to set a desired ANSS when the process is in control and find the value of λ that gives the quickest detection of a change in μ and σ of some specific magnitude. This is an enormous advantage over designing the charts separately and hoping for good joint performance.

7.2 FSS-FSI EE Chart

The FSS-FSI EE chart will be formally defined in this section. Let $\lambda = \lambda_m = \lambda_v$ be the weighting constant for the chart. Define the chart for the mean by

$$U_k = \begin{cases} \lambda M_k + (1-\lambda) U_{k-1} & k \geq 1 \\ 0 & k = 0 \end{cases}, \tag{7.1}$$

and define the chart for the variance by

$$V_k = \begin{cases} \lambda Z_k + (1-\lambda) V_{k-1} & k \geq 1 \\ 0 & k = 0 \end{cases}. \tag{7.2}$$

The chart signals if either chart signals.The statistic for the EE chart at sampling time k can be represented by the ordered pair $\underline{\mathbf{W}}_k = (U_k, V_k)$. This representation is useful when developing the properties of the chart, but it is better to plot the component statistics separately in practice to retain the time order of the observations. In terms of $\underline{\mathbf{W}}_k$, the chart signals if

$$\underline{\mathbf{W}}_k \notin (-h, h) \times (-h, h) \tag{7.3}$$

where h is the control limit of each chart.

The properties of the FSS-FSI EE chart can be evaluated by extending the methods of Reynolds (1995). Appendix E contains the mathematical details of the evaluation methods.

7.3 VSR EE Charts

A variable sampling rate feature that allows the sampling rate to increase when there is some evidence of a change in one or both parameters should improve the performance of any procedure for simultaneous monitoring of mean and variance. For simplicity, we will assume VSS charts use two sample sizes and VSI charts use two sampling intervals.

Let $n(u,v)$ be the sample size that will be used at sample time k given that $\underline{\mathbf{W}}_{k-1} = (u,v)$. Let $d(u,v)$ be the time interval between sample time $k-1$ and sample time k given that $\underline{\mathbf{W}}_{k-1} = (u,v)$. Notice that $n(u,v) \equiv n$ and $d(u,v) \equiv d$ for a FSS-FSI dual monitoring scheme that uses samples of size n taken d time units apart.

A variable sampling rate feature can be added to the EE chart in several ways. We will discuss issues related to defining rules for VSR charts in terms of the sample size function for VSS-FSI charts, but the same issues apply to defining the sampling interval function for FSS-VSI charts. Three possible choices for $n(u,v)$ are given below.

1. Use the larger sample size if the chart for the variance gives some evidence the variance may have changed. Define the sample size function by

$$n(u,v) = \begin{cases} n_1 & (u,v) \in (-h,h) \times (-g,g) \\ n_2 & (u,v) \in (-h,h) \times (-h,-g] \cup (-h,h) \times [g,h) \end{cases} \tag{7.4}$$

   where g is a constant with $0 < g < h$.

2. Use the larger sample size if the chart for the mean gives some evidence the mean may have changed. Define the sample size function by

$$n(u,v) = \begin{cases} n_1 & (u,v) \in (-g,g) \times (-h,h) \\ n_2 & (u,v) \in (-h,-g] \times (-h,h) \cup [g,h) \times (-h,h) \end{cases} \tag{7.5}$$

   where g is a constant with $0 < g < h$.

3. Use the larger sample size if either chart gives some indication of a change in a parameter. Define the sample size function by

$$n(u,v) = \begin{cases} n_1 & (u,v) \in (-g,g) \times (-g,g) \\ n_2 & (u,v) \in (-h,-g] \times (-h,h) \cup [g,h) \times (-h,h) \cup [-g,g] \times [g,h) \\ & \qquad \cup [-g,g] \times (-h,-g] \end{cases} \tag{7.6}$$

where g is a constant with $0 < g < h$.

Rule (1) has little intuitive appeal for most situations. Detecting changes in the variance is usually of less importance than detecting changes in the mean. Rule (2) should give quick detection of changes in the mean alone but much slower detection of changes in the variance alone or simultaneous changes in the mean and variance. Preliminary investigations show rule (2) performs poorly when a change in the mean is accompanied by a decrease in the variance. It is expected that rule (3) will have the best overall performance. The VSR charts presented in the following sections will allow the sampling rate to increase if either chart indicates a possible change in a parameter.

7.3.1 VSS-FSI EE Chart

Consider a VSS-FSI EE chart with $n(u, v)$ as defined in (7.6) and $d(u, v) \equiv d$. The use of the large sample size when there is some evidence of a change in either parameter but not enough evidence for a signal should lead to quicker detection of changes in the process.

The evaluation method given in Appendix E can be modified to evaluate the properties of VSS-FSI EE charts but implementing this method is not possible at this time. The ATS and SSATS of VSS-FSI charts were obtained via simulation.

7.3.2 FSS-VSI EE Chart

Let d_2 be the shorter sampling interval and let d_1 be the longer interval. The sampling interval function for a FSS-VSI chart is defined analogously to the sample size function given in (7.6). The sample size function for a FSS-VSI chart is $n(u, v) \equiv n$ and the sampling interval function is

$$d(u, v) = \begin{cases} d_1 & (u, v) \in (-g, g) \times (-g, g) \\ d_2 & (u, v) \in (-h, -g] \times (-h, h) \cup [g, h) \times (-h, h) \cup [-g, g] \times [g, h) \\ & \qquad \cup [-g, g] \times (-h, -g]. \end{cases} \tag{7.7}$$

The unified-integral equation method of Reynolds (1995) can be modified to evaluate the properties of FSS-VSI EE charts. See Appendix E for more details on the evaluation methods.

7.3.3 Performance of the VSR Charts

The FSS-FSI EE chart was compared with the VSS-FSI EE chart and FSS-VSI EE chart when $n = 5$. Without loss of generality, we assume $\mu_0 = 0$ and $\sigma_0^2 = 1$. The ATS for all charts is 250 time units when the process is in control. The sampling interval limit for the FSS-VSI charts was chosen to give an average sample interval length of one time unit when the process is in control. Similarly, the average sample size for the VSS-FSI charts is five when the process is in control. The FSS-VSI charts all use an initial sampling interval of $d = 1$ and the VSS-FSI charts all use an initial sample size of $n = 5$ to give a fair basis of comparison.

Table 7.1 gives the value of λ that minimizes the ATS of the FSS-FSI chart, the values of λ, n_1, and n_2 that minimize the ATS of the VSS-FSI chart, and the values of λ, d_1, and d_2 that minimize the ATS of the FSS-VSI chart for several values of μ and σ. The minimization was taken over $\lambda \in \{0.1, 0.11, \ldots, 0.60\}$. For the FSS-VSI charts, minimization was taken over $d_2 \in \{0.1, 0.5\}$ and $d_1 \in \{1.1, 1.5, 1.9, 2.0, 3.0\}$. For VSS-FSI charts, the minimum ATS was taken over $n_1 \in \{2, 3, 4\}$ and $n_2 \in \{10, 15, 20\}$. The true mean of the observations is $\mu = \pm\delta \cdot \frac{1}{\sqrt{5}}$ and the true variance is σ^2. The ATS of the VSS-FSI charts was obtained via simulation using $r = 1000$ runs. The standard error of the simulation mean is included for the VSS-FSI charts to show the estimated simulation error. The error is roughly proportional to the ATS.

The ATS was used as the criterion instead of the SSATS because the SSATS of the FSS-VSI and VSS-FSI charts must be obtained by simulation. Using simulation to calculate the SSATS for so many cases is not computationally feasible.

The value of λ that minimizes the ATS of the FSS-FSI EE chart is surprisingly large. For example, $\lambda = 0.39$ is best for detecting a change in the mean of $\delta = 0.5$ standardized units and a 50% increase in σ. The best value of λ for the FSS-VSI chart is slightly larger than the optimal value of λ for the FSS-VSI chart at most combinations of δ and σ, and the corresponding value of λ for the VSS-FSI is even larger still.

The best sampling interval pair for the FSS-VSI chart is $d_1 = 3.0$ and $d_2 = 0.1$ for every value of μ and σ. This sampling interval pair is furthest apart among those considered. This agrees with earlier results for monitoring the mean alone or the variance alone (see Reynolds (1995)).

The best sample size pair for the VSS-FSI chart is $n_1 = 2$ and $n_2 = 20$ for all values of μ and σ. The smallest possible value of n_1 is $n_1 = 2$ since S_k is the observed statistic for the variance. Choosing n_1 as small as possible was found to be best for monitoring the variance alone in Section 5.3.

The ATS of the FSS-FSI chart is uniformly larger than the ATS of either VSR chart. The FSS-VSI has the smallest ATS at all values of the parameters, which is consistent with the results observed for monitoring the variance alone. The VSS-FSI chart performs especially poorly when σ decreases.

Table 7.1: ATS for Optimal FSS-FSI, FSS-VSI, and VSS-FSI EE Charts with $n = 5$

		FSS-FSI		FSS-VSI				VSS-FSI				
δ	σ	λ	ATS	λ	d_2	d_1	ATS	λ	n_1	n_2	ATS	SE(ATS)
0	0.50	0.21	5.41	0.35	3	0.1	2.64	0.43	2	20	6.3	0.16
0	0.75	0.10	18.51	0.12	3	0.1	11.59	0.25	2	20	17.9	0.44
0	1.00	.	250.00	.	.	.	250.00	.	.	.	250.0	.
0	1.25	0.13	17.56	0.16	3	0.1	9.74	0.42	2	20	11.9	0.30
0	1.50	0.37	6.23	0.36	3	0.1	2.94	0.60	2	20	4.0	0.09
0.5	0.50	0.21	5.42	0.37	3	0.1	2.34	0.48	2	20	6.2	0.17
0.5	0.75	0.10	16.47	0.16	3	0.1	7.88	0.27	2	20	13.6	0.27
0.5	1.00	0.10	30.09	0.10	3	0.1	18.61	0.15	2	20	22.4	0.50
0.5	1.25	0.16	13.54	0.20	3	0.1	6.96	0.39	2	20	8.6	0.20
0.5	1.50	0.39	5.78	0.38	3	0.1	2.71	0.58	2	20	3.8	0.08
1	0.50	0.20	5.30	0.38	3	0.1	1.88	0.46	2	20	5.2	0.11
1	0.75	0.13	9.52	0.26	3	0.1	3.80	0.50	2	20	7.2	0.14
1	1.00	0.14	10.13	0.22	3	0.1	5.15	0.40	2	20	7.3	0.15
1	1.25	0.24	8.03	0.29	3	0.1	3.80	0.44	2	20	5.3	0.11
1	1.50	0.44	4.75	0.43	3	0.1	2.23	0.55	2	20	3.3	0.06
1.5	0.50	0.26	4.51	0.37	3	0.1	1.49	0.49	2	20	3.5	0.06
1.5	0.75	0.22	5.40	0.38	3	0.1	2.02	0.50	2	20	4.0	0.07
1.5	1.00	0.24	5.44	0.36	3	0.1	2.45	0.53	2	20	4.0	0.08
1.5	1.25	0.33	4.96	0.39	3	0.1	2.29	0.52	2	20	3.5	0.07
1.5	1.50	0.51	3.69	0.49	3	0.1	1.78	0.57	2	20	2.7	0.05
2	0.50	0.36	3.27	0.39	3	0.1	1.24	0.60	2	20	2.4	0.03
2	0.75	0.34	3.47	0.47	3	0.1	1.39	0.58	2	20	2.7	0.04
2	1.00	0.37	3.51	0.48	3	0.1	1.58	0.58	2	20	2.8	0.05
2	1.25	0.45	3.37	0.49	3	0.1	1.62	0.60	2	20	2.6	0.05
2	1.50	0.58	2.84	0.56	3	0.1	1.47	0.60	2	20	2.3	0.04

A chart that is optimal at some particular combination of μ and σ could perform poorly at other values of the parameters. A chart that performs well across a wide range of parameter values is better in practice than a chart that is optimal at some particular parameter values but lousy at other values. This issue is especially important here since the best value of λ is so large. EWMA charts that use a large value of λ generally are not good at detecting small changes in the parameters.

Table 7.2 contains the SSATS for several charts that should perform well based on the results observed in Table 7.1. The chart of each type from Table 7.1 that is optimal when $\delta = 0.5$ and $\sigma = 1.25$ is included in Table 7.2.

The best FSS-VSI EE chart in Table 7.1 uses $d_1 = 3.0$ and $d_2 = 0.1$. It was shown in Chapter 6 that a large value of d_1 hurts the steady state performance of an FSS-VSI EWMA chart for the variance. Reynolds (1995) observed similar behavior in FSS-VSI EWMA charts for the mean. An FSS-VSI EE chart with $d_1 = 1.5$ and $d_2 = 0.1$ that is optimized when $\delta = 0.5$ and $\sigma = 1.25$ is included in Table 7.2. The best VSS-FSI EE chart in Table 7.1 uses $n_1 = 2$ and $n_2 = 20$. It was shown in Chapter 5 that a small value of n_1 and a large value of n_2 hurts the steady state performance of a VSS-FSI EWMA chart for the variance. Table 7.2 also contains a VSS-FSI chart with $n_1 = 4$ and $n_2 = 10$ that is optimized when $\delta = 0.5$ and $\sigma = 1.25$. A chart that uses a FSS-FSI Shewhart $\bar{X}$-chart for the mean and a FSS-FSI Shewhart chart based on Z_k for the variance is also included. All charts have an average sampling interval of $d = 1$ and an average sample size of $n = 5$ when the process is in control. The chart parameters are given in the table headings.

The SSATS values for the FSS-FSI chart can be calculated analytically using the methods given in Appendix E. The SSATS values for the VSS-FSI and FSS-VSI charts were obtained from a simulation using $r = 10000$ runs. The simulated SSATS can be considered accurate to the first decimal place except when the SSATS is greater than ten.

The Shewhart scheme is competitive only for very large changes in the mean that are accompanied by large increases in the variance. The SSATS of the Shewhart chart is larger than the in-control ATS of 250 if the mean stays constant or changes slightly and the variance decreases. The SSATS of the Shewhart chart is significantly larger than the SSATS of the FSS-FSI EE chart at almost all parameter values. The Shewhart chart is slightly better when $\delta = 2.0$ and $\sigma = 1.5$.

The SSATS of all VSR EE charts is generally much less than the SSATS of the FSS-FSI EE chart when the changes in the parameters are small. The SSATS of the VSR EE charts is usually slightly smaller than the SSATS of the FSS-FSI EE chart when the changes in the parameters are large.

The SSATS of the FSS-VSI chart with $d_1 = 3.0$ and $d_2 = 0.1$ differs little from the SSATS of the FSS-VSI chart with $d_1 = 1.5$ and $d_2 = 0.1$ in most cases. The chart with $d_1 = 3.0$ is slightly better when the δ is small and slightly worse when δ is large. The differences are not significant in most cases. The SSATS of the VSS-FSI chart with $n_1 = 2$ and $n_2 = 20$ is significantly larger than the SSATS of the VSS-FSI chart with $n_1 = 4$ and $n_2 = 10$ when there is a large change in the variance. The VSS-FSI chart with $n_1 = 2$ and $n_2 = 20$ is slightly better than the VSS-FSI chart with $n_1 = 4$ and $n_2 = 10$ when $\delta \leq 1.0$ and the variance remains constant.

The SSATS of the FSS-VSI charts is significantly lower than the SSATS of the VSS-FSI charts when $\delta \leq 1.0$ and $\sigma \leq 1$. The VSS-FSI charts are slightly better when $\delta \geq 1.5$ and $\sigma \geq 1$. The FSS-VSI chart with $d_1 = 3.0$ and $d_2 = 0.1$ gives the quickest detection of small changes in the parameters, and the VSS-FSI chart with $n_1 = 4$ and $n_2 = 10$ gives the quickest detection of large changes in the parameters.

Table 7.2: SSATS for FSS-FSI Shewhart, FSS-FSI, FSS-VSI, and VSS-FSI EE Charts with $n = 5$

		SSATS					
		Shewhart	FSS-FSI EE	FSS-VSI EE		VSS-FSI EE	
		$h = 3.090$	$\lambda = 0.16$	$\lambda = 0.20$	$\lambda = 0.17$	$\lambda = 0.39$	$\lambda = 0.34$
			$h = 0.860$	$h = 0.986$	$h = 0.893$	$h = 1.501$	$h = 1.374$
				$g = 0.383$	$g = 0.251$	$g = 0.831$	$g = 0.763$
				$d_1 = 3.0$	$d_1 = 1.5$	$n_1 = 2$	$n_1 = 4$
δ	σ			$d_2 = 0.1$	$d_2 = 0.1$	$n_2 = 20$	$n_2 = 10$
0	0.5	67.82	4.96	3.88	3.66	7.3	3.7
0	0.75	319.04	20.62	11.91	12.50	20.0	20.4
0	1	250	250	250	250	250.0	250.0
0	1.25	30.41	16.48	10.79	11.39	12.5	14.0
0	1.5	7.79	5.97	4.45	4.42	4.7	4.4
0.5	0.5	67.82	4.83	3.86	3.51	7.1	3.7
0.5	0.75	296.36	17.86	8.00	8.76	14.5	16.3
0.5	1	143.24	33.62	24.21	24.56	31.5	39.6
0.5	1.25	24.53	12.48	7.83	8.25	9.0	10.5
0.5	1.5	7.15	5.59	4.28	4.14	4.4	4.1
1	0.5	67.75	4.74	3.57	3.29	5.8	3.5
1	0.75	173.51	8.76	4.81	4.79	7.6	7.2
1	1	48.76	9.41	5.93	6.04	7.6	8.1
1	1.25	14.64	7.37	5.01	4.99	5.7	5.9
1	1.5	5.66	4.70	3.82	3.61	3.8	3.5
1.5	0.5	64.59	3.88	3.22	2.91	4.2	3.0
1.5	0.75	49.39	4.84	3.69	3.43	4.5	3.7
1.5	1	16.80	4.99	3.98	3.73	4.3	3.9
1.5	1.25	7.90	4.67	3.83	3.57	4.0	3.5
1.5	1.5	4.09	3.74	3.43	3.12	3.3	2.8
2	0.5	33.91	2.99	2.97	2.59	3.2	2.3
2	0.75	12.67	3.25	3.17	2.83	3.3	2.4
2	1	6.66	3.34	3.32	2.95	3.3	2.5
2	1.25	4.33	3.29	3.28	2.89	3.2	2.5
2	1.5	2.85	2.95	3.12	2.73	2.8	2.2

Chapter 8

Conclusions and Future Research

The results presented in Chapter 5 and Chapter 6 show that VSR procedures give much quicker detection of increases in variability on average than corresponding fixed sampling rate control charts. The VSR charts for simultaneous monitoring of mean and variance that are defined in Chapter 7 are easy to design and detect changes in the process parameters much more quickly than traditional methods. The extension of the evaluation methods developed by Reynolds (1995) to the two parameter case gives an efficient and accurate method for evaluating the properties of FSS simultaneous control charts for mean and variance.

8.1 Guidelines on Chart Design

Control charts for the variance that use a natural log transformation or normal probability transformation to simplify calculations do not perform as well as charts that are based on the natural likelihood ratio statistic T_k. The penalty incurred by using the transformations is most severe when the sample size is small. The ATS of a chart that uses a transformed statistic may be as much as 40% greater than the ATS of the chart that uses T_k. The properties of the chart that uses T_k can now be accurately (if not easily) evaluated due to technological advances so there is no longer any compelling reason to use transformed statistics when monitoring the variance alone.

The chart parameters for the VSS charts have a significant impact on the performance of the charts. If ATS is used as the criterion, it is generally best to choose n_1 as small as possible and n_2

as large as possible (within reason) when using a VSS chart. If SSATS is used as the criterion, the choice of the sample size pair depends on the magnitude of the increase in the standard deviation that is important to detect. Very large values of n_2 should be avoided if detecting a shift in σ of 100% or more is important.

Obtaining large samples even occasionally may be impossible in some situations. VSS charts with $n_1 = 1$ or $n_1 = 2$ and $n_2 = 10$ or $n_2 = 20$ perform well for many values of σ. These charts may be feasible alternatives to the traditional FSS-FSI chart with $n = 5$.

VSI charts for monitoring the variance are also sensitive to the choice of chart parameters. It is always best to choose d_1 and d_2 as far apart as possible if the goal is to minimize the ATS. We do not recommend this strategy in practice. Large values of the long interval d_1 hurt the steady state performance of the chart. Very long sampling intervals are also intuitively unappealing to practitioners. It is usually best to choose d_2 as small as possible and use the expected level of change in σ to guide the selection of d_1. Large values of d_1 are best for detecting small increases in σ, and small values of d_1 are best for detecting large increases in σ. The sampling interval pair $d_2 = 0.1$ and $d_1 = 1.5$ is a good compromise in most instances.

The guidelines for selecting sample size pairs and sampling interval pairs given above apply to Shewhart, EWMA, and CUSUM charts. As with FSS-FSI charts, the performance of VSR EWMA charts also depends on the choice of λ and the performance of VSR CUSUM charts depends on the choice of γ. The same rules for the choice of λ and γ that apply to FSS-FSI charts also apply to the VSR charts. It is possible to design a chart that is optimal for detecting a change in σ of some particular amount, but the chart should also perform well for many values of σ. In most cases, a chart that is optimized to detect a 50% increase in σ is a good compromise.

The VSR EE charts for simultaneous monitoring of mean and variance behave similarly to the charts for variance alone in most respects. However, the optimal value of λ for detecting a change in the parameters of some specified level is larger than expected. The chart should be optimized to detect small changes in the mean and variance (perhaps $\delta = 0.5$ and $\sigma = 1.25$) if good overall performance is desired. The sampling intervals for the VSI chart should be chosen as far apart as possible to minimize the ATS. A very large value of d_1 hurts the steady state performance of the chart when the changes in the parameters are large. Thus d_1 should not be taken excessively

large if detecting small changes in the parameters is considered important. Like VSS charts for the variance alone, n_1 should be small and n_2 should be large if the emphasis is on detecting small changes in the mean and variance. Choosing n_1 and n_2 closer together is better if quick detection of large changes in the parameters is important.

8.2 Future Research

8.2.1 Control Charts for the Variance

We assumed that the observations are independent and normally distributed and that the target values for the mean and variance are known. It is well known that control charts for the mean can be greatly affected by non-normal observations or autocorrelated observations. Control charts for the variance will likely also be affected if the observations do not come from a normal distribution or are autocorrelated. Chang and Gan (1995) showed that the false alarm rate for a CUSUM chart for the variance may be much larger than expected if the data come from a distribution with heavy tails. Chang and Gan (1995) also found that positive autocorrelation increases the ATS of CUSUM charts for the variance. The effects of autocorrelation and heavy tailed distributions on VSR control charts for the variance is unknown.

We also assumed a step increase in the process standard deviation, i.e., the standard deviation remains at the target value of σ_0 for some period of time and then suddenly increases to some value $\sigma_1 > \sigma_0$ and remains at the new value until the change is detected. A drift in the standard deviation over time is more realistic in circumstances where the change is caused by part wear or machine operator fatigue.

The VSS and VSI features can be combined to form a VSS-VSI chart that increases the sample size and decreases the sampling interval when there is evidence the standard deviation has increased. Prabhu et al. (1994) developed a Shewhart VSS-VSI chart for the mean and showed that it worked better than a VSS or VSI chart alone. We have developed a VSS-VSI Shewhart chart for the variance, but VSS-VSI CUSUM and EWMA charts have not been evaluated.

8.2.2 Control Charts for the Mean and Variance

The steady state properties of the VSR EE schemes were approximated using simulation. It is theoretically possible to calculate steady state properties of the EE charts using the methods in Appendix E, but implementing this method is not feasible with current computational capability. A more efficient algorithm for calculating steady state results would help with the design of VSR EE charts.

A VSS-VSI EE chart that simultaneously increases the sample size and decreases the sampling interval when there is evidence of a change in the process should give quicker detection of changes in the parameters than a VSS-FSI EE chart or a FSS-VSI EE chart. We have developed methods for designing such charts but have not yet evaluated the performance of VSS-VSI charts.

Gan (1997) considered a dual mean and variance scheme with an elliptical acceptance region and suggested a VSR version of the chart without giving any details. A VSR version of this chart should be competitive with the VSR EE charts.

Appendix A

Evaluation of Properties for One-Sided FSS-FSI CUSUM and EWMA Charts

Suppose a sample of n observations is taken at time points that are d time units apart. Let $Q(k)$ be the statistic observed at sample k and let Y_k be the control statistic at sample k. We will assume $Q(k)$ has a continuous distribution. Properties of the chart may be found using the combined integral equation-Markov chain method outlined in Reynolds (1987) and Reynolds (1995).

Suppose the chart signals at time k if $Y_k > h$ and resets to l if $Y_k \leq l$ where h is the control limit of the chart and l is the lower reflecting boundary. In most applications, $l = 0$ and we assume $l = 0$ in the derivations that follow.

Let $L(u) = \text{ANSS given} Y_0 = u$ where Y_0 is the initial value of the chart statistic. Then $L(u)$ satisfies

$$L(u) = 1 + P(Y_1 \leq 0|u) L(0) + \int_0^h L(y) f(y|u) dy \tag{A.1}$$

where $f(y|u)$ is a transition density that depends on the distribution of $Q(k)$.

The integral may be approximated with Gaussian quadrature. Suppose $\{y_1, y_2, \ldots, y_r\}$ is a set

of quadrature points for $[0,h]$ and $\{w_1, w_2, \ldots, w_r\}$ is the corresponding set of quadrature weights. See, for example, Abramowitz and Stegun (1965) for tables of quadrature points and weights. Let $\tilde{L}(u) = 1 + P(Y_1 \leq 0|u)\,\tilde{L}(0) + \sum_{i=1}^{r} w_i \tilde{L}(y_i)\, f(y_i|u)$ be the approximation for $L(u)$.

Apply this approximation at the points $\{0, y_1, y_2, ..., y_r\}$ to obtain

$$\begin{bmatrix} \tilde{L}(0) \\ \tilde{L}(y_1) \\ . \\ . \\ \tilde{L}(y_r) \end{bmatrix} = \begin{bmatrix} 1 \\ 1 \\ . \\ . \\ 1 \end{bmatrix} + \begin{bmatrix} P(Y_1 \leq 0|0)\, L(0) \\ P(Y_1 \leq 0|y_1)\, L(0) \\ . \\ . \\ P(Y_1 \leq 0|y_r)\, L(0) \end{bmatrix}$$
$$+ \begin{bmatrix} w_1 \tilde{L}(y_1) f(y_1|0) & . & . & w_r \tilde{L}(y_r) f(y_r|0) \\ w_1 \tilde{L}(y_1) f(y_1|y_1) & . & . & w_r \tilde{L}(y_r) f(y_r|y_1) \\ . & . & . & . \\ . & . & . & . \\ w_1 \tilde{L}(y_1) f(y_1|y_r) & . & . & w_r \tilde{L}(y_r) f(y_r|y_r) \end{bmatrix}. \tag{A.2}$$

This may be expressed as the system of linear equations

$$\underline{\tilde{\mathbf{L}}} = \underline{\mathbf{1}} + Q\underline{\tilde{\mathbf{L}}} \tag{A.3}$$

where

$$Q = \begin{bmatrix} P(Y_1 \leq 0|0) & w_1 f(y_1|0) & . & . & w_r f(y_r|0) \\ P(Y_1 \leq 0|y_1) & w_1 f(y_1|y_1) & . & . & w_r f(y_r|y_1) \\ . & . & . & . & . \\ . & . & . & . & . \\ P(Y_1 \leq 0|y_r) & w_1 f(y_1|y_r) & . & . & w_r f(y_r|y_r) \end{bmatrix}. \tag{A.4}$$

This system of equations is easily solved to give

$$\underline{\tilde{\mathbf{L}}} = (I - Q)^{-1} \underline{\mathbf{1}}.$$

The vector $\underline{\tilde{\mathbf{L}}}$ gives the ANSS for initial starting values of $Y_0 = 0$ or $Y_0 = y_k$ for the set of quadrature points $\{y_1, y_2, \ldots, y_r\}$. The ANSS for some arbitrary starting value $Y_0 = u$ is given by

$$L(u) = (\text{ANSS}|Y_0 = u) = 1 + \underline{\mathbf{q}}(u)(I - Q)^{-1} \underline{\mathbf{1}} \tag{A.5}$$

where $\underline{\mathbf{q}}(u)$ is the row vector of transition probabilities given by

$$\underline{\mathbf{q}}(u) = [P(Y_1 \leq 0|u), w_1 f(y_1|u), \ldots, w_r f(y_r|u)]. \tag{A.6}$$

The ANOS given that $Y_0 = u$ is $N(u) = nL(u)$. The appropriate approximation is clearly $\tilde{N}(u) = n\tilde{L}(u)$.

An approximation to the conditional steady state distribution was given by Reynolds (1987). The conditional steady state ANSS is given by

$$SSANSS = \underline{\pi} \cdot (I - Q)^{-1} \underline{\mathbf{1}}$$

where $(I - Q)^{-1} \underline{\mathbf{1}}$ is the vector of ANSS values for $\{0, y_1, \ldots, y_r\}$ for a one-sided chart and the vector of ANSS values for $\{y_1, \ldots, y_r\}$ for a two-sided chart and $\underline{\pi}$ is the standardized left eigenvector associated with the largest eigenvalue of the Q matrix. All steady state calculations were performed using this approximation.

The upper control limit for the chart is usually chosen to achieve some desired value of the ANSS when the process is in control. Determining the control limit that will give a particular value of the ANSS requires the use of some iterative procedure. The secant method was used to determine the control limits for the FSS-FSI CUSUM and EWMA charts. An easy to implement algorithm is given in Burden and Faires (1989).

Appendix B

Evaluation of Properties for One-Sided VSS CUSUM and EWMA Charts

The method outlined in Appendix A can be modified to evaluate the properties of the VSS charts. The properties of the chart will show some slight dependence on the choice of the initial sample size. Expressions for the ANOS and ANSS of will be given for arbitrary values of $n(1)$. Define $L(u,m) = \text{ANSS given} Y_0 = u \text{ and } n(1) = m$. Denote the distribution function and density function of Q_k by $F_{n(k)}$ and $f_{n(k)}$, respectively. Suppose the sample size function at sample time k is

$$n(k) = \begin{cases} n_1 & Y_{k-1} < g \\ n_2 & g \leq Y_{k-1} < h \end{cases}$$

when $k \geq 2$.

Case 1: Suppose $g > 0$. Let $\{y_1, y_2, \ldots, y_r\}$ be a set of quadrature points for $[0, g]$ and $\{w_1, w_2, \ldots, w_r\}$ be the corresponding set of quadrature weights. Similarly, let $\{s_1, s_2, \ldots, s_p\}$ be a set of quadrature points for $[g, h]$ and $\{v_1, v_2, \ldots, v_p\}$ be a set of weights for $[g, h]$.

Let $\underline{\mathbf{L}}'$ be the $1 \times (1 + r + p)$ row vector defined by

$$\underline{\mathbf{L}}' = [L(0,n_1), L(y_1,n_1), \ldots, L(y_r,n_1), L(s_1,n_2), \ldots, L(s_p,n_2)].$$

Then the elements of $\underline{\mathbf{L}}$ satisfy the equations

$$\begin{aligned}
L(0,n_1) &= 1 + P(Y_1 \leq 0|0,n_1) L(0,n_1) + \int_0^g L(y,n_1) f_{n_1}(y|0)\, dy + \int_g^h L(y,n_2) f_{n_2}(y|0)\, dy \\
L(y_i,n_1) &= 1 + P(Y_1 \leq 0|y_i,n_1) L(0,n_1) + \int_0^g L(y,n_1) f_{n_1}(y|y_i)\, dy + \int_g^h L(y,n_2) f_{n_1}(y|y_i)\, dy \\
L(s_j,n_2) &= 1 + P(Y_1 \leq 0|s_j,n_2) L(0,n_1) + \int_0^g L(y,n_1) f_{n_2}(y|s_j)\, dy + \int_g^h L(y,n_2) f_{n_2}(y|s_j)\, dy
\end{aligned}$$

where y_i is any quadrature point in $[0,g]$ and s_j is any quadrature point in $[g,h]$.

The approximate solution to the integral equation at zero and the quadrature points is given by

$$\underline{\tilde{\mathbf{L}}} = (I - Q)^{-1} \underline{\mathbf{1}}$$

where

$$Q = \begin{bmatrix}
F_{n_1}(0) & w_1 f_{n_1}(y_1|0) & \cdots & w_r f_{n_1}(y_r|0) & v_1 f_{n_1}(s_1|0) & \cdots & v_r f_{n_1}(s_r|0) \\
F_{n_1}(-y_1) & w_1 f_{n_1}(y_1|y_1) & \cdots & w_r f_{n_1}(y_r|y_1) & v_1 f_{n_1}(s_1|y_1) & \cdots & v_r f_{n_1}(s_r|y_1) \\
\vdots & \vdots & \cdots & \vdots & \vdots & \cdots & \vdots \\
\vdots & \vdots & \cdots & \vdots & \vdots & \cdots & \vdots \\
F_{n_1}(-y_r) & w_1 f_{n_1}(y_1|y_r) & \cdots & w_r f_{n_1}(y_r|y_r) & v_1 f_{n_1}(s_1|y_r) & \cdots & v_r f_{n_1}(s_r|y_r) \\
F_{n_2}(-s_1) & w_1 f_{n_2}(y_1|s_1) & \cdots & w_r f_{n_2}(y_r|s_1) & v_1 f_{n_2}(s_1|s_1) & \cdots & v_r f_{n_2}(s_r|s_1) \\
\vdots & \vdots & \cdots & \vdots & \vdots & \cdots & \vdots \\
\vdots & \vdots & \cdots & \vdots & \vdots & \cdots & \vdots \\
F_{n_2}(-s_r) & w_1 f_{n_2}(y_1|s_r) & \cdots & w_r f_{n_2}(y_r|s_r) & v_1 f_{n_2}(s_1|s_r) & \cdots & v_r f_{n_2}(s_r|s_r)
\end{bmatrix},$$

I is an $(1+r+p)\times(1+r+p)$ identity matrix, and $\underline{\mathbf{1}}'$ is the $1\times(1+r+p)$ vector

$$\underline{\mathbf{1}}' = [1, \ldots, 1].$$

Then $L(u, m)$ for arbitrary starting values $Y_0 = u$ and $n(1) = m$ satisfies the integral equation

$$L(u, m) = 1 + F_m(-u) \cdot L(0, n_1) + \int_0^g L(y, n_1) f_m(y|u)\, dy + \int_g^h L(y, n_2) f_m(y|u)\, dy, \quad \text{(B.1)}$$

and the quadrature approximation is

$$\begin{aligned} \tilde{L}(u, m) &= 1 + \underline{\mathbf{q}}(u, m)(I - Q)^{-1} \underline{\mathbf{1}} \\ &= 1 + \underline{\mathbf{q}}(u, m) \underline{\tilde{\mathbf{L}}} \end{aligned} \quad \text{(B.2)}$$

where

$$\begin{aligned} \underline{\mathbf{q}}(u, m) &= [P(Y_1 \leq 0|u, m), w_1 f_m(y_1|u), \ldots, w_r f_m(y_r|u)\, v_1 f_m(s_1|u), \ldots, v_r f_m(s_r|u)] \\ &= [F_m(-u), w_1 f_m(y_1|u), \ldots, w_r f_m(y_r|u)\, v_1 f_m(s_1|u), \ldots, v_r f_m(s_r|u)]. \end{aligned} \quad \text{(B.3)}$$

The ANOS given that $Y_0 = u$ must also be found by the integral equation method in this case. The derivation of the ANOS is essentially similar to the work for the ANSS given above. Let $N(u, m) = \text{ANOS given} Y_0 = u$ and $n(1) = m$. The integral equation approximation for $N(u, m)$ is given by

$$\tilde{N}(u, m) = m + \underline{\mathbf{q}}(u, m)(I - Q)^{-1} \underline{\mathbf{n}} \quad \text{(B.4)}$$

where $\underline{\mathbf{q}}(u, m)$, Q, and I are defined above and $\underline{\mathbf{n}}'$ is the $1 \times (1 + r + p)$ row vector defined by

$$\underline{\mathbf{n}}' = [n_1, n_1, \ldots, n_1, n_2, \ldots, n_2].$$

Case 2 : Suppose $g < 0$. Let $\{y_1, y_2, \ldots, y_r\}$ be a set of quadrature points for $[0, h]$ and $\{w_1, w_2, \ldots, w_r\}$ be the corresponding set of weights. Let $\underline{\mathbf{L}}'$ be the $1 \times (2 + r)$ row vector defined by

$$\underline{\mathbf{L}}' = \left[L(0, n_1), L(0, n_2), L(y_1, n_2), \ldots, L(y_r, n_2) \right].$$

Then the elements of $\underline{\mathbf{L}}$ satisfy the equations

$$\begin{aligned}
L(0, n_1) &= 1 + P(Y_1 \leq g | 0, n_1) L(0, n_1) + P(g < Y_1 \leq 0 | 0, n_1) L(0, n_2) + \int_0^h L(y, n_2) F_{n_1}(y|0)\, dy \\
L(0, n_2) &= 1 + P(Y_1 \leq g | 0, n_2) L(0, n_1) + P(g < Y_1 \leq 0 | 0, n_2) L(0, n_2) + \int_0^h L(y, n_2) F_{n_2}(y|0)\, dy \\
L(y_i, n_2) &= 1 + P(Y_1 \leq g | y_i, n_2) L(0, n_1) + P(g < Y_1 \leq 0 | y_i, n_2) L(0, n_2) + \int_0^h L(y, n_2) F_{n_2}(y|y_i)\, dy
\end{aligned}$$

where y_i is a quadrature point in $[0, h]$.

Let $\underline{\tilde{\mathbf{L}}}$ be the approximation obtained by Gaussian quadrature at the points $\{0, y_1, \ldots, y_r\}$. Then $\underline{\tilde{\mathbf{L}}}$ satisfies the system of equations

$$\begin{aligned}
\underline{\tilde{\mathbf{L}}} = \begin{bmatrix} \tilde{L}(0, n_1) \\ \tilde{L}(0, n_2) \\ \tilde{L}(y_1, n_2) \\ \cdot \\ \cdot \\ \tilde{L}(y_r, n_2) \end{bmatrix} &= \begin{bmatrix} 1 \\ 1 \\ 1 \\ \cdot \\ \cdot \\ 1 \end{bmatrix} + \begin{bmatrix} P(Y_1 \leq g | 0, n_1) \tilde{L}(0, n_1) \\ P(Y_1 \leq g | 0, n_2) \tilde{L}(0, n_1) \\ P(Y_1 \leq g | y_1, n_1) \tilde{L}(0, n_1) \\ \cdot \\ \cdot \\ P(Y_1 \leq g | y_r, n_1) \tilde{L}(0, n_1) \end{bmatrix} + \begin{bmatrix} P(g < Y_1 \leq 0 | 0, n_1) \tilde{L}(0, n_2) \\ P(g < Y_1 \leq 0 | 0, n_2) \tilde{L}(0, n_2) \\ P(g < y_1 \leq 0 | y_1, n_2) \tilde{L}(0, n_2) \\ \cdot \\ \cdot \\ P(g < Y_1 \leq 0 | y_r, n_2) \tilde{L}(0, n_2) \end{bmatrix} \\
&+ \begin{bmatrix} w_1 \tilde{L}(y_1, n_2) F_{n_1}(y_1|0) & . & . & w_r \tilde{L}(y_r, n_2) F_{n_1}(y_r|0) \\ w_1 \tilde{L}(y_1, n_2) F_{n_2}(y_1|0) & . & . & w_r \tilde{L}(y_r, n_2) F_{n_2}(y_r|0) \\ w_1 \tilde{L}(y_1, n_2) F_{n_2}(y_1|y_1) & . & . & w_r \tilde{L}(y_r, n_2) F_{n_2}(y_r|y_1) \\ \cdot & & . & \cdot \\ \cdot & & . & \cdot \\ w_1 \tilde{L}(y_1, n_2) F_{n_2}(y_1|y_r) & . & . & w_r \tilde{L}(y_r, n_2) F_{n_2}(y_r|y_r) \end{bmatrix}. \qquad \text{(B.5)}
\end{aligned}$$

As before, this system of equations has solution

$$\underline{\tilde{\mathbf{L}}} = (I - Q)^{-1} \underline{\mathbf{1}}$$

where

$$\begin{aligned} Q &= \begin{bmatrix} P(Y_1 \leq g|0,n_1) & P(g < Y_1 \leq 0|0,n_1) & w_1 F_{n_1}(y_1|0) & . & . & w_r F_{n_1}(y_r|0) \\ P(Y_1 \leq g|0,n_2) & P(g < Y_1 \leq 0|0,n_2) & w_1 F_{n_2}(y_1|0) & . & . & w_r F_{n_2}(y_r|0) \\ P(Y_1 \leq g|y_1,n_2) & P(g < y_1 \leq 0|y_1,n_2) & w_1 F_{n_2}(y_1|y_1) & . & . & w_r F_{n_2}(y_r|y_1) \\ . & . & . & . & . & . \\ . & . & . & . & . & . \\ P(Y_1 \leq g|y_r,n_2) & P(g < Y_1 \leq 0|y_r,n_2) & w_1 F_{n_2}(y_1|y_r) & . & . & w_r F_{n_2}(y_r|y_r) \end{bmatrix} \\ &= \begin{bmatrix} F_1(-g) & F_1(0) - F_1(-g) & w_1 F_{n_1}(y_1|0) & . & . & w_r F_{n_1}(y_r|0) \\ F_2(-g) & F_2(0) - F_2(-g) & w_1 F_{n_2}(y_1|0) & . & . & w_r F_{n_2}(y_r|0) \\ F_2(-g-y_1) & F_2(-y_1) - F_2(-g-y_1) & w_1 F_{n_2}(y_1|y_1) & . & . & w_r F_{n_2}(y_r|y_1) \\ . & . & . & . & . & . \\ . & . & . & . & . & . \\ F_2(-g-y_r) & F_2(-y_r) - F_2(-g-y_r) & w_1 F_{n_2}(y_1|y_r) & . & . & w_r F_{n_2}(y_r|y_r) \end{bmatrix}, \end{aligned} \quad \text{(B.6)}$$

I is a $(2+r) \times (2+r)$ identity matrix, and $\underline{\mathbf{1}}'$ is the $1 \times (2+r)$ row vector defined by

$$\underline{\mathbf{1}}' = [1, \ldots, 1].$$

The approximate ANSS given $Y_0 = u$ and $n(1) = m$ for arbitrary u and m is given by

$$L(u,m) = 1 + \underline{\mathbf{q}}(u,m) \cdot \underline{\tilde{\mathbf{L}}}$$

where

$$\begin{aligned} \underline{\mathbf{q}}(u,m) &= [P(Y_1 \leq g|u,m) \quad P(g < Y_1 \leq 0|u,m) \quad w_1 f^*(y_1|u) \quad \ldots \quad w_r f_m(y_r|u)] \\ &= [F_m(-u-g) \quad F_m(-u) - F_m(-u-g) \quad w_1 f_m(y_1|u) \quad \ldots \quad w_r f_m(y_r|u)]. \end{aligned} \quad \text{(B.7)}$$

The integral equation approximation for the ANOS is given by

$$\tilde{N}(u,m) = (\text{ANOS}|Y_0 = u \,\text{and}\, n(1) = m) = m + \underline{\mathbf{q}}(u,m)(I-Q)^{-1}\underline{\mathbf{n}}$$

where $\underline{\mathbf{q}}$, Q, and I are defined above and $\underline{\mathbf{n}}'$ is the $1 \times (2+r)$ vector

$$\underline{\mathbf{n}}' = [n_1, n_2, n_2, \ldots, n_2].$$

Determining the values of g and h that will give specified values of the ANSS and ANOS when the process is in control is more difficult than simply finding the upper control limit h for a one-sided FSS-FSI control chart. This is a root finding problem for a two dimensional function of two variables. The Broyden algorithm given in Burden and Faires (1989) was used to find g and h. The algorithm usually converged in five to ten iterations if reasonable initial guesses were used. The algorithm can fail to converge if the initial guesses are chosen poorly.

Appendix C

Evaluation of Properties for One-Sided VSI CUSUM and EWMA Charts

The ANSS of a VSI chart is identical to the ANSS of a FSI chart with the same control limit. The ATS can be found by methods similar to those used to find the ANSS of one-sided VSS charts. Let Q_k be the statistic observed at sample time k and Y_k be the chart statistic at sample time k. Suppose the sampling interval function at sample time k is

$$d(k) = \begin{cases} d_1 & Y_{k-1} < g \\ d_2 & g \leq Y_{k-1} < h. \end{cases}$$

Case 1: Suppose $g > 0$. Let $\{x_1, \ldots, x_r\}$ be a set of quadrature points for $(0, g)$ and let $\{y_1, \ldots, y_r\}$ be a set of quadrature points for (g, h). Let $\{a_1, \ldots, a_r\}$ and $\{b_1, \ldots, b_r\}$ be the corresponding quadrature weights. Let $\underline{\mathbf{v}} = \{x_1, \ldots, x_r, y_1, \ldots, y_r\}$ and let $\underline{\mathbf{w}} = \{a_1, \ldots, a_r, b_1, \ldots, b_r\}$.

Let $T(u, d)$ be the ATS given $Y_0 = u$ and $d(1) = d$. Then $T(u, d)$ satisfies the equation

$$T(u,d) = d + P(Y_1 \leq 0 \mid u, d)\, T(0, d_1) + \int_0^g T(y, d_1)\, f(y \mid u)\, dy + \int_g^h T(y, d_2)\, f(y \mid u)\, dy. \quad \text{(C.1)}$$

The quadrature approximation is

$$\tilde{T}(u,d) \;=\; d + \underline{\mathbf{q}}(u)\,(I-Q)^{-1}\,\underline{\mathbf{d}} \tag{C.2}$$

where

$\underline{\mathbf{q}}(u)$ is the row vector of transition probabilities given by

$$\underline{\mathbf{q}}(u) = \left[P(Y_1 \le 0 \,|\, u), w_1 f(v_1|u), \ldots w_{2r} f(v_{2r}|u)\right], \tag{C.3}$$

I is a $(1+2r)\,\mathrm{x}\,(1+2r)$ identity matrix,

$$Q \;=\; \begin{bmatrix} P(Y_1 \le 0 \,|\, 0) & w_1 f(v_1|0) & . & . & . & w_{2r} f(v_{2r}|0) \\ P(Y_1 \le 0 \,|\, v_1) & w_1 f(v_1|v_1) & . & . & . & w_{2r} f(v_{2r}|v_1) \\ . & . & . & . & . & . \\ . & . & . & . & . & . \\ P(Y_1 \le 0 \,|\, v_{2r}) & w_1 f(v_1|v_{2r}) & . & . & . & w_{2r} f(v_{2r}|v_{2r}) \end{bmatrix}, \tag{C.4}$$

and $\underline{\mathbf{d}}'$ is the $1\,\mathrm{x}\,(1+2r)$ vector

$$\underline{\mathbf{d}}' = [d_1, d_1, \ldots, d_1, d_2, \ldots, d_2].$$

Case 2 : Suppose $g < 0$. Let $v_1, \ldots, v_r$ be a set of quadrature points for $(0,h)$ and let $w_1, \ldots, w_r$ be the corresponding set of quadrature weights.

Then the ATS satisfies the equation

$$\begin{aligned} T(u,d) = d \;&+\; P(Y_1 \le g \,|\, u,d)\,T(0,d_2) + P(g < Y_1 \le 0 \,|\, u,d)\,T(0,d_2) \\ &+\; \int_0^h T(y,d_2)\, f(y \,|\, u)\, dy. \end{aligned} \tag{C.5}$$

The quadrature approximation is

$$\tilde{T}(u,d) \;=\; d + \underline{\mathbf{q}}(u)\,(I-Q)^{-1}\,\underline{\mathbf{d}} \tag{C.6}$$

where $\underline{\mathbf{q}}(u)$ is the row vector of transition probabilities given by

$$\underline{\mathbf{q}}(u) = \left[P(Y_1 \le g \,|\, u), P(g < Y_1 \le 0 \,|\, u), w_1 f(v_1|u), \ldots w_{2r} f(v_{2r}|u)\right], \tag{C.7}$$

I is a $(2+r)\times(2+r)$ identity matrix,

$$Q \;=\; \begin{bmatrix} P(Y_1 \le g \,|\, 0) & P(g < Y_1 \le 0 \,|\, 0) & w_1 f(v_1|0) & . & . & . & w_{2r} f(v_{2r}|0) \\ P(Y_1 \le g \,|\, 0) & P(g < Y_1 \le 0 \,|\, 0) & w_1 f(v_1|0) & . & . & . & w_{2r} f(v_{2r}|0) \\ P(Y_1 \le g \,|\, v_1) & P(g < Y_1 \le 0 \,|\, v_1) & w_1 f(v_1|v_1) & . & . & . & w_{2r} f(v_{2r}|v_1) \\ . & . & . & . & . & . & . \\ . & . & . & . & . & . & . \\ P(Y_1 \le g \,|\, v_{2r}) & P(g < Y_1 \le 0 \,|\, v_{2r}) & w_1 f(v_1|v_{2r}) & . & . & . & w_{2r} f(v_{2r}|v_{2r}) \end{bmatrix}, \tag{C.8}$$

and $\underline{\mathbf{d}}'$ is the $1\times(2+r)$ vector

$$\underline{\mathbf{d}}' = [d_1, d_2, d_2, \ldots, d_2].$$

Steady state calculations for VSI charts are slightly more complicated than for FSI charts. Let $\pi(y)$ be the density of the stationary distribution of the control statistic conditional on no false alarms. The approximate conditional stationary distribution at the set of quadrature points $\{v_1, \ldots, v_r\}$ (see Reynolds (1995)) is given by $\underline{\pi} = [\pi_1, \ldots, \pi_r]$ where $\underline{\pi}$ is the normalized left eigenvector of Q.

Let $\alpha(y)$ be the density of the control statistic at the sample time immediately before the change in the variance. Like Reynolds et al. (1990) and Reynolds (1995), we will assume $\alpha(y)$ is proportional to the product of the sampling interval function and the stationary distribution of the control statistic. We will also assume that the time of the change is uniformly distributed over the

interval in which it occurs. Suppose the change in the variance occurs between samples k and $k+1$. Under these assumptions,

$$\alpha(y) = \frac{\pi(y)\, d(k)}{\int_0^h \pi(y)\, d(k)} \tag{C.9}$$

and the approximation at the set of quadrature points is

$$\underline{\alpha} \;=\; [\alpha_1, \ldots, \alpha_r] = \frac{\underline{\pi} \cdot \underline{\mathbf{d}}}{\underline{\pi \mathbf{d}}} \tag{C.10}$$

where $\cdot$ represents elementwise vector multiplication.

The steady state time to signal can be written as $T^* = T_0 + T$ where T_0 is the time interval between the change in the variance and the first sample after the change and T is the time between the first sample after the change and a signal. Let $A(y) = E(T \mid Y_k = y)$. Notice that $A(v_i)$ is the i^{th} element of $(I - Q)^{-1} \underline{\mathbf{d}}$ if v_i is a quadrature point.

Then

$$\begin{aligned} E(T^* \mid Y_k = y) &= E(T_0 \mid Y_k = y) + E(T \mid Y_k = y) && \text{(C.11)} \\ &= \frac{d(k)}{2} + \int_0^h A(u)\, f(u \mid y)\, du && \text{(C.12)} \end{aligned}$$

and

$$E(T^*) = E_Y \left(\frac{d(k)}{2} + \int_0^h A(u)\, f(u \mid y)\, du \right). \tag{C.13}$$

Applying the quadrature approximations to (C.12) gives

$$E(T^* \mid Y_k = y) \approx \frac{d(k)}{2} + \sum_{i=1}^{r} w_i A(v_i)\, f(v_i \mid y). \tag{C.14}$$

Then if the expectation in (C.13) is taken with respect to the approximate steady state distribution of Y_k in (C.10), the SSATS is

$$\begin{aligned} SSATS &= \sum_{k=1}^{r} \alpha_k \frac{d(k)}{2} + \sum_{k=1}^{r} \sum_{i=1}^{r} \alpha_k w_i f(v_i \mid v_k) A(v_i) \\ &= \frac{\underline{\alpha} \cdot \underline{\mathbf{d}}}{2} + \underline{\alpha} Q (I - Q)^{-1} \underline{\mathbf{d}}. \end{aligned} \tag{C.15}$$

Appendix D

Markov Chain Method for Evaluating Properties of Control Charts

The Markov chain method of Brook and Evans (1972) uses a discrete state Markov chain with m transient states to approximate the behavior of a continuous chart statistic. An application to a one-sided VSI chart will be outlined here, but the method can easily be generalized to other situations.

Suppose the interval $[0, h]$ is the continuation region of the chart. The m transient states of the Markov chain correspond to the division of $[0, h]$ into m subintervals. Suppose g is the sampling control limit of the chart. We will use p transient states for the interval $[0, g)$ and q transient states to represent the interval $[g, h)$ so that $p + q = m$. There are many ways to select p and q. We will choose p such that $\frac{p}{m}$ is approximately equal to $\frac{g}{h}$ so that the subintervals are roughly the same width.

Let $p = [\frac{g}{h}m]$ be the greatest integer less than or equal to $\frac{g}{h}m$ and let $q = m - p$. Divide the interval $(0, g)$ into p subintervals $\left(0, \frac{g}{p}\right)$, $\left(\frac{g}{p}, 2\frac{g}{p}\right)$, ... , $\left((p-1)\frac{g}{p}, g\right)$ and divide the interval (g, h) into q subintervals $\left(g, \frac{h-g}{q}\right)$, $\left(g + \frac{h-g}{q}, g + 2\frac{h-g}{q}\right)$, ... , $\left(g + (q-1)\frac{h-g}{q}, h\right)$. Let $\{z_1, \ldots, z_m\} = \{\frac{g}{p}{2}, \ldots, g - \frac{\frac{g}{p}}{2}, g + \frac{\frac{h-g}{q}}{2}, \ldots, h - \frac{\frac{h-g}{q}}{2}\}$ be the set of midpoints of the intervals. Then $\{0, z_1, \ldots, z_r\}$ represents the set of transient states of the Markov chain.

Let Z_k be the discretized version of the chart statistic Y_k at sampling point k. Define Z_k as

$$Z_k = \begin{matrix} 0 & Y_k \leq 0 \\ z_j & Y_k \in I_j \end{matrix} \tag{D.1}$$

where I_j is the subinterval containing z_j.

The transition probabilities for the states other than the state corresponding to zero are calculated by allowing each interval midpoint to correspond to the continuous subinterval to which it belongs. Let $p_{ij} = P\left(Z_k = z_i \,|\, Z_{k-1} = z_j\right)$ be the transition probability from state i to state j. Then

$$p_{ij} = P\left(z_j + S\left(k\right) \in I\right) = F\left(u - z_j\right) - F\left(l - z_j\right) \tag{D.2}$$

where F is the cumulative distribution function of $S\left(k\right)$, u is the upper boundary of subinterval I_j and l is the lower boundary of subinterval I_j.

Transition probabilities involving the state corresponding to zero are defined in a similar manner. Let $p_{0j} = P\left(Z_k = z_i \,|\, Z_{k-1} = 0\right)$ be the transition probability from state 0 to state j. This probability can be written is terms of $S\left(k\right)$ as

$$p_{0j} = P\left(S\left(k\right) \in I\right) = F\left(u\right) - F\left(l\right). \tag{D.3}$$

Let $p_{i0} = P\left(Z_k = 0 \,|\, Z_{k-1} = Z_i\right)$ be the transition probability from state i to state 0. This probability can be expressed as

$$p_{i0} = P\left(z_i + S\left(k\right) \leq 0\right) = F\left(-z_i\right). \tag{D.4}$$

The ANSS given $Y_0 = u$ is

$$L\left(u\right) = 1 + q\left(u\right)\left(I - Q\right)^{-1}\underline{\mathbf{1}} \tag{D.5}$$

where Q is the $1+p+q \times 1+p+q$ matrix of transition probabilities for the transient states, I is the $1+p+q \times 1+p+q$ identity matrix , $\underline{\mathbf{1}}$ is an $1+p+q \times 1$ vector of ones, and

$$q(u) = \left[P(Y_1 \leq 0 \mid u), P\left(0 < Y_1 < \frac{g}{p} \mid u\right), \ldots, P\left((q-1)\frac{h-g}{q} < Y_1 < h \mid u\right) \right].$$

The ATS given $Y_0 = u$ and $d(1) = d$ is

$$T(u,d) = d + q(u)(I-Q)^{-1}\underline{\mathbf{d}} \tag{D.6}$$

where Q and $q(u)$ are defined above and $\underline{\mathbf{d}}'$ is the $1 \times (1+p+q)$ vector

$$\underline{\mathbf{d}}' = [d_1, d_1, \ldots, d_1, d_2, \ldots, d_2].$$

Appendix E

Evaluation of Properties for Dual Mean and Variance Charts

The properties of the VSI EE charts can be evaluated by extending the method in Reynolds (1995) to two dimensions. Assume the joint distribution of $\mathbf{W}_1, \mathbf{W}_2, \ldots$ does not depend on the sampling times $t_1, t_2, \ldots$ when $\theta = (\mu, \sigma)$ is constant. Let $C = (-h, h) \times (-h, h)$ be the continuation region of the chart and define the function $F_i(u, v \mid x, y)$ by

$$F_i(u, v \mid x, y) = P(W_{1i} \leq u, W_{2i} \leq v \text{ and } \mathbf{W}_1, \ldots \mathbf{W}_{i-1} \in C \mid \mathbf{W}_0 = (x, y)). \tag{E.1}$$

Define $M(u, v \mid x, y)$ by

$$M(u, v \mid x, y) = \sum_{i=1}^{\infty} F_i(u, v \mid x, y). \tag{E.2}$$

The function $M(u, v \mid x, y)$ is analogous to a cumulative distribution function, but $M(\infty, \infty \mid x, y)$ may be greater than one. For the EE chart, $M(u, v \mid x, y)$ can be expressed in terms of continuous functions $m(u, v \mid x, y)$ that are analogous to density functions. We will develop expressions for approximating $m(u, v \mid x, y)$ and show that the ATS of the EE chart can be expressed in terms of the $m(u, v \mid x, y)$.

Suppose $F_i(u, v \mid x, y)$ can be represented as

$$F_i(u, v \mid x, y) = \int_{-\infty}^{u} \int_{-\infty}^{v} f_i(r, s \mid x, y)\, dr ds \tag{E.3}$$

for some continuous function $f_i(r, s \mid x, y)$.

Define $m(u, v \mid x, y)$ by

$$m(u, v \mid x, y) = \sum_{i=1}^{\infty} f_i(u, v \mid x, y). \tag{E.4}$$

Then $M(u, v \mid x, y)$ can be written as

$$M(u, v \mid x, y) = \int_{-\infty}^{u} \int_{-\infty}^{v} m(u, v \mid x, y). \tag{E.5}$$

Many important properties of the EE chart can be expressed through an integral equation involving $m(u, v \mid x, y)$. Let $N =$ the number of samples to signal. Then the ANSS is

$$\begin{aligned} E(N \mid \mathbf{W}_0 = (x, y)) &= 1 + \sum_{i=1}^{\infty} P(N > i \mid \mathbf{W}_0 = (x, y)) \\ &= 1 + \sum_{i=1}^{\infty} \int_C dF_i(u, v \mid x, y) \\ &= 1 + \int_C dM(u, v \mid x, y) \\ &= 1 + \int_{-h}^{h} \int_{-h}^{h} m(r, s \mid x, y)\, dr ds. \end{aligned} \tag{E.6}$$

Let $T =$ the time to signal and let $d(u, v)$ be the sampling interval function. The ATS given that $\mathbf{W}_0 = (x, y)$ is

$$\begin{aligned} E(T \mid \mathbf{W}_0 = (x, y)) &= t_1 + \sum_{i=1}^{\infty} \int_C d(u, v)\, dF_i(u, v \mid x, y) \\ &= t_1 + \int_C d(u, v)\, dM(u, v \mid x, y) \\ &= t_1 + \int_{-h}^{h} \int_{-h}^{h} d(u, v)\, m(u, v \mid x, y)\, dr ds. \end{aligned} \tag{E.7}$$

An approximation to $m(u, v \mid x, y)$ can be found by numerical quadrature. Let $\{r_1, \ldots r_r\}$ be a set of quadrature points for $(-h, h)$ and let $\{\alpha_1, \ldots, \alpha_r\}$ be the corresponding set of weights. Define the matrix $Q_{r^2 \times r^2}$ by

$$Q_{r^2 \times r^2} = [q_{ij}] = [\alpha_k \alpha_l f(r_k, r_l \mid r_l, r_k)] \tag{E.8}$$

where $k = 1$ if $1 \leq i \leq r$, $k = 2$ if $r + 1 \leq i \leq 2r$, ... and $l = 1$ if $1 \leq j \leq r$, $l = 2$ if $r + 1 \leq j \leq 2r$, ...

Let $m^*(u, v \mid x, y)$ be the approximation for $m(u, v \mid x, y)$ obtained by using numerical quadrature. Then $m^*(u, v \mid x, y)$ is given by

$$m^*(u, v \mid x, y) = f(u, v \mid x, y) + \underline{\mathbf{q}}'(x, y)(I - Q)^{-1} \underline{\mathbf{f}}(u, v) \tag{E.9}$$

where $\underline{\mathbf{q}}'(x, y)$ is the $1 \times r^2$ row vector whose i-th element is

$$\underline{\mathbf{q}}'(x, y)[i] = [\alpha_k \alpha_l f(r_k, r_l \mid x, y)], \tag{E.10}$$

$\underline{\mathbf{f}}(u, v)$ is the $r^2 \times 1$ column vector whose i-th element is

$$\underline{\mathbf{f}}(u, v)[i] = [f(u, v \mid r_k, r_l)], \tag{E.11}$$

and I is the $r^2 \times r^2$ identity matrix.

Approximations to the ANSS and ATS can be obtained by substituting (E.9) in (E.6) and (E.7). The integrals in (E.6) and (E.7) must be evaluated numerically using quadrature techniques. The final approximation for the ANSS conditional on the starting value $\mathbf{W}_0 = (x, y)$ is

$$ANSS = 1 + \sum_{p=1}^{r} \sum_{q=1}^{r} \alpha_p \alpha_q m^*(r_p, r_q \mid x, y). \tag{E.12}$$

The expression for the ATS is slightly more complicated since $d(u,v)$ is not continuous. A separate application of numerical quadrature is necessary for each region on which $d(u,v)$ is continuous. The integral must be split into five pieces for the sampling interval function defined in (7.7).

Let $\{x_1,\ldots,x_r\}$ be a set of quadrature points for $(-h,-g]$, let $\{y_1,\ldots,y_r\}$ be a set of quadrature points for $(-g,g)$, and let $\{z_1,\ldots,z_r\}$ be a set of quadrature points for $[g,h)$. Let $\{\beta_1,\ldots,\beta_r\}$, $\{\gamma_1,\ldots,\gamma_r\}$, and $\{\delta_1,\ldots,\delta_r\}$ be the corresponding sets of quadrature weights. Then the ATS is given by

$$\begin{aligned} ATS = t_1 \quad &+ \quad \sum_{p=1}^{r}\sum_{q=1}^{r} \beta_p \alpha_q d\left(x_p, r_q\right) m^*\left(x_p, r_q \,|\, x, y\right) + \sum_{p=1}^{r}\sum_{q=1}^{r} \delta_p \alpha_q d\left(z_p, r_q\right) m^*\left(z_p, r_q \,|\, x, y\right) \\ &+ \quad \sum_{p=1}^{r}\sum_{q=1}^{r} \gamma_p \gamma_q d\left(y_p, y_q\right) m^*\left(y_p, y_q \,|\, x, y\right) + \sum_{p=1}^{r}\sum_{q=1}^{r} \gamma_p \delta_q d\left(y_p, z_q\right) m^*\left(y_p, z_q \,|\, x, y\right) \\ &+ \quad \sum_{p=1}^{r}\sum_{q=1}^{r} \gamma_p \beta_q d\left(y_p, x_q\right) m^*\left(y_p, x_q \,|\, x, y\right). \end{aligned} \tag{E.13}$$

Obtaining the approximations to the ANSS and ATS is numerically intensive but not prohibitively so. The numerical results reported in this dissertation were obtained using $r = 16$ quadrature points. The greatest numerical penalty is incurred while inverting the $r^2 \times r^2$ matrix $I - Q$. This need only be done once for each set of chart parameters. Evaluating m^* on the grid of quadrature points requires a large number of functional evaluations and matrix-vector multiplications, but these calculations are easily handled.

Appendix F

Optimality of Two Sampling Intervals

Reynolds (1989) showed that using two sampling intervals that are spaced as far apart as possible minimizes the ATS of a VSI control chart for a general parameter under certain restrictions. A modified version of this proof for the special case of a Shewhart chart for the variance is given for completeness. Let d_1 be the largest possible sampling interval and let d_2 be the smallest possible sampling interval. Let h be the upper control limit of the chart. Define the sampling interval function by

$$d(k) = \begin{cases} d_1 & 0 < M_{n(k-1)}(T_{k-1}) < g \\ d_2 & g \leq M_{n(k-1)}(T_{k-1}) < h \end{cases}$$

where g is a constant such that $E(d(k) \mid T < h) = 1$ when the process is in control.

Let $s(k)$ be a sampling interval function such that $d_2 \leq s(k) \leq d_1$ and $E(s(k) \mid T < h) = 1$ when the process is in control. Using (6.3), it is sufficient to show that $E(d(k) \mid T < h) \leq E(s(k) \mid T < h)$ when $\sigma > \sigma_0$.

Let f_0 be the density of T when $\sigma = \sigma_0$ and let f_1 be the density of T when $\sigma > \sigma_0$. Since the distribution of T has the monotone likelihood ratio property, $T < g$ if and only if $f_1 < cf_0$ for some constant c. Then

$$E(d(k) - s(k) \mid T < h) - 0 = \int (d(k) - s(k)) f_1 - \int (d(k) - s(k)) cf_0$$

$$
\begin{aligned}
&= \int (d(k) - s(k))(f_1 - cf_0) \\
&= \int_{\{T<g\}} (d(k) - s(k))(f_1 - cf_0) + \int_{\{T\geq g\}} (d(k) - s(k))(f_1 - cf_0) \\
&= \int_{f_1<cf_0} (d_1 - s(k))(f_1 - cf_0) + \int_{f_1\geq cf_0} (d_2 - s(k))(f_1 - cf_0) \\
&\leq 0.
\end{aligned}
$$

Therefore $E(d(k) \mid T < h) - E(s(k) \mid T < h) \leq 0$ and $d(k)$ minimizes the ATS.

Bibliography

Abramowitz, M., and Stegun, I. (1965). *Handbook of Mathematical Functions*. Dover, New York.

Acosta-Mejia, C. A. (1998). "Monitoring Reduction in Variability with the Range," *IIE Transactions*. **30**, 515–523.

Brook, D., and Evans, D. (1972). "An Approach to the Probability Distribution of CUSUM Run Length," *Biometrika*. **59**, 539–549.

Burden, R., and Faires, J. (1989). *Numerical Analyis*. PWS-Kent, Boston.

Chang, T., and Gan, F. (1994). "Optimal Designs of One-Sided EWMA Charts for Monitoring a Process Variance," *Journal of Statistical Computation and Simulation*. **49**, 33–48.

Chang, T., and Gan, F. (1995). "A Cumulative Sum Control Chart for Monitoring Process Variance," *Journal of Quality Technology*. **27**, 109–119.

Chengular-Smith, I., Arnold, J., and Reynolds, M. (1989). "Variable Sampling Intervals for Multiparameter Shewhart Charts," *Communications in Statistics-Theory and Methods*. **18**, 1769–1792.

Costa, A. (1994). "Xbar Charts with Variable Sample Size," *Journal of Quality Technology*. **26**, 12–22.

Crowder, S., and Hamilton, M. (1992). "An EWMA for Monitoring a Process Standard Deviation," *Journal of Quality Technology*. **20**, 155–163.

Domangue, R., and Patch, S. (1991). "Some Omnibus Exponentially Weighted Moving Average Statistical Process Monitoring Schemes," *Technometrics*. **33**, 299–313.

Gan, F. (1989). "Combined Cumulative Sum and Shewhart Variance Charts," *Journal of Statistical Computation and Simulation*. **32**, 149–163.

Gan, F. (1995). "Joint Monitoring of Process Mean and Variance Using Exponentially Weighted Moving Average Statistical Process Monitoring Schemes," *Technometrics*. **37**, 446–453.

Gan, F. (1997) "Joint Monitoring of Process Mean and Variance," *Proceedings of the Second World Congress of Nonlinear Analysts*.

Hawkins, D. (1981). "A CUSUM for a Scale Parameter," *Journal of Quality Technology*. **13**, 228–231.

Hawkins, D. (1987). "Self Starting CUSUM Charts for Location and Scale," *The Statistician*. **36**, 299–316.

Hawkins, D. (1992). "Evaluation of Average Run Lengths of Cumulative Sum Charts for an Arbitrary Data Distribution," *Communications in Statistics-Simulation and Computation*. **21**, 1001–1020.

Hawkins, D., and Olwell, D. (1998). *Cumulative Sum Charts and Charting for Quality Improvement*. Springer, New York.

Howell, D. (1987). "A CUSUM Scheme for the Control of Process Variance," presented at the 1987 Joint Statistical Meetings.

Lowry, C., Champ, C., and Woodall, W. (1995). "The Performance of Control Charts for Monitoring Process Variation," *Communications in Statistics and Simulation*. **24**, 400–437.

Lucas, J., and Crosier, R. (1990). "Fast Initial Response for CUSUM Quality Control Schemes," *Technometrics*. **24**, 199–205.

MacGregor, J., and Harris, T. (1993). "The Exponentially Weighted Moving Variance," *Journal of Quality Technology*. **25**, 106–118.

Nelson, L. (1990). "Monitoring Reduction in Variation with a Range Chart," *Journal of Quality Technology*. **22**, 163–165.

Page, E. (1963). "Controlling the Standard Devation by CUSUMs and Warning Limits," *Technometrics*. **5**, 307–315.

Prabhu, S. S., Montgomery, D. C., and Runger, G. C. (1994). "A Combined Adaptive Sample Size and Sampling Interval $\bar{X}$ Control Scheme," *Journal of Quality Technology*. **26**, 164–176.

Quesenberrry, C. (1995). "On Properties of Q Charts for Variables," *Journal of Quality Technology*. **27**, 184–203.

Reynolds, M. R. (1987) "The Markov Chain and Integral Equation Methods for Evaluating Properties of Control Charts," *Proceedings of the Joint Statistical Meetings*. 95–100.

Reynolds, M. R. (1989). "Optimal Variable Sampling Interval Control Charts," *Sequential Analysis*. **8**, 361–379.

Reynolds, M. R. (1995). "Evaluating Properties of Variable Sampling Interval Control Charts," *Sequential Analysis*. **14**, 59–97.

Reynolds, M. R. (1996)a. "Shewhart and EWMA Variable Sampling Interval Control Charts with Sampling at Fixed Times," *Journal of Quality Technology*. **28**, 199–212.

Reynolds, M. R. (1996)b. "Variable-Sampling-Interval Control Charts with Sampling at Fixed Times," *IIE Transactions*. **28**, 497–510.

Reynolds, M. R., Amin, R., Arnold, J., and Nachlas, J. (1988). "X-bar Charts with Variable Sampling Intervals," *Technometrics*. **30**, 181–192.

Reynolds, M. R., Arnold, J., and Amin, R. (1990). "CUSUM Charts with Variable Sampling Intervals," *Technometrics*. **32**, 371–384.

Runger, G. C., and Pignatiello, J. J. (1991). "Adaptive Sampling for Process Control," *Journal of Quality Technology*. **23**, 135–155.

Saccucci, M., Amin, R., and Lucas, J. (1992). "Exponentially Weighted Moving Average Control Schemes with Variable Sampling Intervals," *Communications in Statistics-Simulation and Computation*. **21**, 627–657.

Stoumbos, Z. G., and Reynolds, M. R. (1997)a. "Control Charts Applying a General Sequential Test at Each Sampling Point," *Sequential Analysis*. **15**, 159–183.

Stoumbos, Z. G., and Reynolds, M. R. (1997)b. "Control Charts Applying a Sequential Test at Fixed Sampling Intervals," *Journal of Quality Technology*. **29**, 21–40.

Tagares, G. (1998). "A Survey of Recent Developments in the Design of Adaptive Control Charts," *Journal of Quality Technology*. **30**, 212–231.

Tuprah, K., and Ncube, M. (1987). "A Comparison of Dispersion Quality Control Charts," *Sequential Analysis*. **6**, 155–163.

van Dobben de Bruyn, C. (1968). *Cumulative Sum Tests*. Hafner, New York.

Wald, A. (1947). *Sequential Analysis*. Wiley, New York.

Western Electric Company. (1956). *Statistical Quality Control Handbook*.

Vitae

Dr. Christopher S. Hughes was born in September 1969 in rural western North Carolina and was raised by his mother and maternal grandparents.

From his ancestors, who practiced subsistence-farming, Dr. Hughes has inherited a love for gardening and has a special fondness for grafting and growing antique varieties of apple trees. Other hobbies include meteorology, fly-fishing, and weight-training.

After completing high school in 1987, Dr. Hughes was named a National Merit Scholar. He attended Virginia Tech and was awarded a Hatcher Math Scholarship. Dr. Hughes earned his B.S. in Mathematics in December 1990. Dr. Hughes then returned to western North Carolina and obtained his M.A. in Mathematics from Appalachian State University in 1993. The fall of 1994 found Dr. Hughes back at Virginia Tech to pursue his M.S. (1995) and Ph.D. (1999) in Statistics.

Dr. Hughes is applying his research in quality control at 3M in St. Paul, Minnesota.

Dr. Hughes lives with his wife, Lori, and their Great Dane, Grendel, in White Bear Lake, Minnesota.